PHD

A biophysical study of the thermostability of citrate synthase

Kanu, Aminata Yanda

Award date:
2002

Awarding institution:
University of Bath

A BIOPHYSICAL STUDY OF THE THERMOSTABILITY OF CITRATE SYNTHASE

Submitted by Aminata Yanda Kanu

for the degree of PhD

of the

University of Bath 2002

ProQuest LLC
789 East Eisenhower Parkway
P.O. Box 1346
Ann Arbor, MI 48106-1346

For Mama and Papa

Acknowledgements

"There is no such thing as a 'self-made' man. We are made up of thousands of others. Everyone who has ever done a kind deed for us, or spoken one word of encouragement to us, has entered into the make-up of our character and of our thoughts, as well as our success." --- George Burton Adams

We succeed in life because of our hard work and the help, support and trust of other people. During my journey to this place, a number of people have made a difference in my life.

I must firstly express my gratitude to my supervisors Michael Danson and David Hough for their patience, for stimulating discussions about science as well as about life and for their critical reading of this manuscript. If this thesis is readable, they are due most of the credit. I especially want to thank David for all his help with the equations and for not giving up on my unfolding problems and me. Thank you also for supporting me through hard times and illnesses. I am also grateful to Susan Crennell for the production of all the structure figures and for all the interesting structure/function discussions over the three years.

I have also had great help from collaborators including Alan Cooper, Sharon Kelly, Olwyn Byron and Gordon Campbell at the University of Glasgow, John Ladbury and Simon Bergqvist at University College London.

Financial support for this work was received from the EPSRC and is gratefully acknowledged.

Apart from help and support with lab work, the need for a friendly atmosphere is a prerequisite for surviving the ups and downs of PhD student life. To this end, I am grateful to the members of labs 1.33 and 1.28, past and present including: Carlos Carlito II, to whom I am so grateful for all his help, expertise and friendship, Mikki Poo who made me realise that 'Care in the community' doesn't work and who lifted me with her humour through the hard times, Becky for perhaps the greatest ever citrate

synthase partnership, Dina who is possibly the sweetest person I have ever met, Tina, Major Mullet, Tree, Nathalie, Ursula, Hans, Harry, Mick, Hannah, Tracey, Andrea and many others who passed through these labs.

Outside the lab, some people have come to mean a lot to me. I had the marvellous privilege of meeting Bunmi, Legs, Stalky, Rachel, Shalin, James, Hong, Li and Zen. You have all made my time in Bath so much more enjoyable.

Having an aunt and a sister with whom you can share life's pleasures and sorrows without judgement is a delight and for this Agatha and Abigail, I thank you.

Without my parents Elizabeth and Ahmed, I would not have been the person I am today. You taught me that sense of humour is the best characteristic to get me through life. Thank you for your love, encouragement, and confidence, for always standing by my side and for always being proud of me. I will always love you and will forever be indebted to you.

Finally, I want to thank God for being with me throughout my time in Bath. Without my belief in God, I probably would not have made it to where I am today.

CONTENTS

ABBREVIATIONS

AcCoA	Acetyl coenzyme A
APS	Ammonium persulphate
Asn	Asparagine
BSA	Bovine serum albumin
CD	Circular dichroism
C_p	Heat capacity
CS	Citrate synthase
Cys	Cysteine
DS CS	*Arthrobacter* citrate synthase
DSC	Differential scanning calorimetry
DTNB	5,5'-dithiobis-2-nitrobenzoic acid
EDTA	Ethylenediamine tetraacetate
GdnHCl	Guanidine hydrochloride
Gln	Glutamine
Ile	Isoleucine
kDa	Kilodalton
LB	Luria-Bertani medium
Met	Methionine
OAA	Oxaloacetate
Pf CS (– 2)	*Pyrococcus furiosus* –2 C-terminal amino acid deletion mutant citrate synthase
Pf CS (–13)	*Pyrococcus furiosus* –13 C-terminal amino acid deletion mutant citrate synthase
Pf CS wt	*Pyrococcus furiosus* wild-type citrate synthase
PfCS (D113A)	*Pyrococcus furiosus* Asp133Ala ionic network mutant citrate synthase

PfCS (D113S)	*Pyrococcus furiosus* Asp133Ser ionic network mutant citrate synthase
Phe	Phenylalanine
PigCS	Pig heart citrate synthase
SDS	Sodium dodecyl sulfate/sodium lauryl sulfate
Ss CS	*Sulfolobus solfataricus* wild-type enzyme
Ta CS	*Thermoplasma acidophilum* wild-type enzyme
TB	Terrific Broth
TEMED	Tetramethylethylenediamine
Trp	Tryptophan
Tyr	Tyrosine
ΔG	Gibbs free energy
ΔH	Change in enthalpy
ΔS	Change in entropy

ABSTRACT

The dissociation and unfolding of the dimeric enzyme citrate synthase from *Pyrococcus furiosus* by guanidine hydrochloride have been investigated at equilibrium. The overall process was reversible, as judged by the almost complete recovery of enzymic activity and tertiary structure after dilution. Dissociation and unfolding were monitored by fluorescence spectroscopy and enzyme activity and occurred in two separate phases. The dissociation of the enzyme at 2.4M GdnHCl coincided with a loss of activity, whereas the unfolding of the enzyme coincided with a decrease in the fluorescence of the protein.

P. furiosus citrate synthase is a highly interesting candidate for thermodynamic studies not only because of its dimeric state but also because it is a hyperthermophilic protein. Proteins from hyperthermophiles must remain folded and fully functional at such extreme temperatures (>80°C) with the requisite stability and flexibility. Hyperthermophilic proteins are therefore expected to provide unique insights into the features responsible for protein thermostability and thermoactivity. There have been few quantitative studies of the thermodynamics of hyperthermophilic and oligomeric proteins, and thermostability is normally reported as the half-life of a protein at a certain high temperature, a measure of the kinetic stability of the protein.

In this work, the first thermodynamic characterisation of the enzyme citrate synthase from the hyperthermophile *Pyrococcus furiosus* is reported. It has been observed that GdnHCl-induced unfolding of the enzyme proceeds via a three-state mechanism of:

$$N_2 \rightleftharpoons 2N \rightleftharpoons 2U.$$

The unfolding data were fitted to this mechanism using a non-linear least squares method and ΔG values for the unfolding of the enzyme were determined at several temperatures. C-terminal and ionic networks mutants have also been investigated in the same way and the thermodynamic parameters for each of these proteins at a range of temperatures have been determined using the linear extrapolation model.

It has been observed from these parameters that these mutants exhibit similar stability to the wild type enzyme. This observation differs from that obtained from thermal inactivation studies carried out at pH 7 which suggest all these mutants are less stable than the wild-type enzyme.

A sequential activation and inactivation accompanies the unfolding of *P. furiosus* citrate synthase by increasing concentrations of denaturants. It is subsequently proposed that the active site of the enzyme is more easily perturbed by denaturants than the bulk of the protein; therefore the activated enzyme may have a more open and flexible conformation at the active site, which may be required for the full expression of the catalytic power of the enzyme.

1. CHAPTER ONE

PROTEIN STABILITY

1.1. Extremophiles and extremozymes

Extremophiles are defined as organisms that grow optimally in environments hostile to man. 'Extremes' include temperature, pressure, salinity, and pH. Depending on their optimal growth conditions, extremophiles can be classified as psychrophiles, thermophiles, hyperthermophiles, acidophilies, alkalophiles, halophiles and piezophiles, respectively (**Table 1**). They are found in all three domains of life – Archaea, Prokarya and Eucarya. Although hyperthermophiles are Archaea or bacteria, extremophiles include multicellular organisms and there are some psychrophilic vertebrates such as the Arctic and Atlantic cod. Certain extremophiles are polyextremophilic ie they thrive in more than one extreme. An example would be *Sulfolobus acidocaldarius*, an Archaeon that could be classified as both an acidophile and a hyperthermophile as it flourishes at pH 3 and 80°C.

Table 1.1: Classification and examples of extremophiles and their environments (adapted from Hough & Danson, 1999 and Rothschild & Mancinelli, 2001).

Environmental parameter	Phenotype	Definition	Typical genera
Temperature	Psychrophile	Growth < 15°C	*Psychrobacter**, *Alteromonas**
	Thermophile	Growth 55-80°C	*Methanobacterium*, *Synechococcus*, *Thermoplasma*, *Thermus**, some *Bacillus** species
	Hyperthermophile	Growth> 80°C	*Aquifex**, *Archaeoglobus*, *Hydrogenobacter**, *Methanothermus*, *Pyrococcus*, *Pyrolobus*, *Sulfolobus*, *Thermococcus*, *Thermotoga**
pH	Acidophile	pH < 4	*Acidianus*, *Desulfurolobus*, *Ferroplasma*, *Sulfolobus*, *Thiobacillus**
	Alkaliphile	pH > 9	*Natronobacterium*, *Natronococcus*, *Spirulina*, some *Bacillus** species
Salinity	Halophile	2-5M NaCl	*Haloarcula*, *Halobacterium*, *Haloferax*, *Halorubrum*
Desiccation	Xerophile	Anhydrobiotic	*Artemia*[#]
Pressure	Pieozophile		*Photobacterium*

* Genera of the domain Bacteria: all others are Archaea; [#]Athropod

Extremophiles are adapted to hostile environments by their physiological and nutritional requirements (Stetter, 1999). As a consequence, cell components like proteins, nucleic acids etc. must be stable and able to function at such extremes. Extremophilic organisms are, therefore, a valuable resource for exploitation in novel biotechnological processes and can be used as unique models for investigations of how biomolecules are stabilized when subjected to extreme conditions (Aguilar, 1996). They are a unique source of enzymes with interesting biological properties. These enzymes have a potential not only for use by themselves but also as a source of ideas to modify the stability of mesophilic enzymes.

1.1.1. Importance of extremozymes

Enzymes are being used as biocatalysts in industrial applications. The majority of enzymes used to date, however, have been obtained from mesophilic organisms, and their application is restricted because of their limited stability to certain environmental factors (Hough & Danson, 1999). Recent developments show that extremophiles are a good source of novel enzymes of biotechnological importance. Some of these enzymes have been isolated and their genes cloned and expressed in mesophilic hosts. Thus, hydrolytic enzymes such as amylases, xylanases, cellulases, pullulanases and proteinases from thermophiles and hyperthermophiles have been studied.

The most significant example of an extremozyme in biotechnology is *Taq* polymerase, the enzyme at the heart of the Polymerase Chain Reaction (PCR), the basis of a 300 million dollar industry. *Taq* polymerase was isolated from the thermophilic bacterium *Thermus aquaticus*. (Saiki *et al*, 1988).

The commercial potential of extremophiles and their metabolites has been recognized but is far from being realised. Rapid development of this area of

research guarantees important and widespread implications. Extremozymes have the potential to become a billion dollar industry.

Table 1.2 shows some of the current uses of metabolites from extremophiles in industrial applications

Table 1.2: Biotechnological and industrial applications of extremophiles and their metabolites. Adapted from Rothschild & Mancinelli (2001) and Aguilar (1996)

Phenotype	Biomolecule	Applications	Advantages
Psychrophiles	Neutral proteases	Cheese maturation, dairy production	Stable at low temperatures
	Proteases, amylases, lipases	In detergents - degradation of polymers	Improved cleaning performance at low temperatures
Thermophiles	Amylases	Hydrolysis of starch to produce dextrins, maltodextrins and corn syrups	High stability
	Xylanases	Paper bleaching	Decrease amount of bleach used
	Proteases	Food processing, baking, brewing, detergents, amino acid production	Stable at high temperatures
Acidophiles	Sulphur oxidation	Desulphurication of coal	Stable in the acidic environment that results from sulphur degradation
Alkaliphiles	Proteases, cellulases, lipases, amylases,	In detergents -degradation of polymers	Stable at high pH

1.1.2. Structural basis of thermostability

The conformation of a protein is generally only marginally stable under physiological conditions. The conformational stability of a protein arises from a delicate balance between opposing energetic forces (of the folded and unfolded states), and this balance needs to be maintained to prevent the denaturation of the protein (Price, 2000). The folded/native structures of proteins can easily be disrupted by small environmental changes such as a rise in temperature, a change in pH or the addition of chemical denaturants.

Proteins from thermophilic organisms have proven to be stable at a variety of conditions, and comparative structural analyses of thermophilic and mesophilic proteins have revealed structural features that may be responsible for enhancing thermostability. There appear to be multiple strategies via which a protein can be stabilised, including a decrease in the size of the surface loops of thermophilic proteins and the presence of disulphide bonds, salt bridges and metal binding sites. The oligomerization state of thermophilic proteins may also be greater than that of mesophilic proteins (Shima *et al*, 1998; Thoma *et al*, 2000).

The structural basis of protein thermostability is a major objective in protein engineering. If we understand the structural basis of stability, it might be possible to introduce appropriate changes by protein engineering in order to enhance the stability of the target protein. Each of the features implicated in protein stability will be considered.

1.1.2.1. Intrinsic features

Ion pairs

Of all the trends commonly associated with increased thermostability, an increase in the number of ion pairs (salt bridges), especially in networks, appears to be the most frequently observed stabilizing factor (Petsko, 2001). Salt bridges often occur between groups distant in the protein sequence, forming cross-links that stabilize the tertiary structure (Karshikoff & Ladenstein, 2001). Proteins from hyperthermophilic organisms are often characterised by an increased number of ion pairs with respect to their mesophilic counterparts.

Cambillau & Claverie (2000) analysed 150 proteins by using comparative analysis of 30 complete genome sequences from Bacteria, Eukarya and Archaea. They compared the amino acid compositions of proteins from twenty-two mesophiles and seven hyperthermophiles. Their analysis of a large number of the three dimensional structures of these proteins found an increase in charged residues located in the solvent accessible regions at the surface of the hyperthermophilic proteins.

One of the best examples to support this hypothesis was found by a structural comparison of the icosahedral lumazine synthase capsids from *Bacillus subtilis* (mesophile) and *Aquifex aeolicus* (hyperthermophile) (Zhang *et al*, 2001). Specifically, the number of ion pairs in the protein from *A. aeolicus* is increased by > 90% and, compared to other lumazine synthases, the *Aquifex* enzyme had the largest accessible surface area formed by charged residues and the smallest formed by hydrophobic residues. Charged residues in the enzyme from *Aquifex* replace most of the polar residues in the *B. subtilis* enzyme. The corresponding difference in the melting temperature was 27°C. Other studies indicating the importance of ionic interactions in thermostable proteins based on the structural

comparison of proteins from hyperthermophiles and mesophiles include glutamate dehydrogenase (Knapp *et al*, 1997) and citrate synthase (Russell *et al*, 1997).

Ionic networks are thought to be more favourable than pairwise ionic interactions. It has been suggested that the energy of a single ion pair contributes very little to the stability of a protein at mesophilic temperatures. This is due to the fact that the entropic cost of desolvating and immobilising a charged residue is likely to be similar to the favourable electrostatic energy gained from the charge-charge interaction (Matthews, 1993; Honig & Nicholls, 1995). At higher temperatures, stabilisation due to ionic interactions increases due to the lower dielectric constant of water (Elcock, 1998).

Although it would seem that ion pairs could be engineered almost anywhere in a protein to increase stability, this may not be the case. A number of site-directed mutagenesis studies have questioned the importance of ion pair networks to thermostability. For example, Lebbink and coworkers tried to enlarge an existing ionic network in *T. maritima* glutamate dehydrogenase and found that this decreased the thermal stability of the protein (Lebbink *et al*, 1999). In another case, the replacement by mutagenesis of three charged residues that form part of a small ion pair network in the Arc repressor by three hydrophobic residues resulted in an increase in stability (Waldburger *et al*, 1995).

Hydrophobic effect

The hydrophobic effect is considered to be the major driving force for the folding of globular proteins (Darby & Creighton, 1993). The thermodynamic factors, that give rise to the hydrophobic effect are complex and still incompletely understood (Vieille & Zeikus, 2001). The contribution of the hydrophobic effect to globular protein

stability has been estimated empirically both by measuring the thermodynamics of transfer of model compounds (e.g. blocked amino acids) from organic solvents to water, and by site directed mutagenesis. Pace (1992), in a study of 72 side-chain aliphatic mutations in four enzymes, calculated that each buried CH_2 group contributed on average 5 $kJmol^{-1}$ to the conformational stability of the protein.

A number of hyperthermostable proteins including *Thermotoga maritima* lactate dehydrogenase (Auerbach *et al*, 1998) and *Thermococcus litoralis* pyrrolidone carboxyl peptidase (Singleton *et al*, 1999) show a significant increase in the number of hydrophobic residues, especially in the core of the structure or at the subunit interfaces. The increase in stability of a chimera constructed between the *Methanococcus voltae* (mesophile) and *M. jannaschii* (thermophile) adenylate kinases also indicated that a larger and more hydrophobic core might be responsible for the stability of the *M. jannaschii* adenylate kinase (Haney *et al*, 1999).

Although there are a few examples to suggest the potential role of hydrophobic interactions in thermostability, not much direct experimental evidence is available to confirm the stabilizing role of hydrophobic interactions in hyperthermophilic proteins. Some hyperthermophilic proteins show no increase in hydrophobic residues, infact a few, have more polar water molecules in the core instead. β-glycosidase from *Thermosphaera aggregans* is one such example (Chi *et al*, 1999).

Aromatic clusters

Closely packed aromatic ring-ring interactions in proteins represent a type of hydrophobic effect and aromatic interactions are thought to be important in the stabilization of proteins (Burley & Petsko, 1985). Burley & Petsko analysed 272 aromatic pairs in 34 high-resolution structures of mesophilic proteins and found that

about 80% are energetically favourable. A pair of aromatic interactions contributes between 2 and 8 $kJmol^{-1}$ to the stability of a protein (Burley & Petsko, 1985). Georis *et al* (2000) demonstrated that introducing aromatic interactions present in a family 11 xylanase from the thermophile *Thermomonospora fusca* into the mesophilic enzyme from *Streptomyces* sp. improved its thermostability. The hyperthermophilic α-amylase from *Pyrococcus furiosus* contains 5% more aromatic residues than its mesophilic homologue from *Bacillus licheniformis*, but it is not known whether these residues are involved in stabilizing interactions (Dong *et al*, 1997). Other examples include thermitase from *Thermoactinomyces vulgaris*. This serine proteinase contains 10 aromatic pairs whereas the mesophilic homologue, *Bacillus amyloliquefaciens* subtilisin BPN, contains only 6 aromatic pairs (Teplyakov *et al*, 1990). Two aromatic clusters are found in RNAse H from *Thermus* that are not found in the *E. coli* enzyme (Ishikawa *et al*, 1993).

Petsko (2001) concludes that the increased content of hydrophobic residues is a major factor in thermostability. One might expect to see a significant increase in the number of aromatic residues in the core, because they bury more hydrophobic surface area than aliphatic residues and have the opportunity for stabilization through aromatic-aromatic interactions.

Disulphide bonds

A disulphide bond is formed when the sulphydryl groups of two cysteine residues are oxidised to produce a cystine residue. Disulphide bonds stabilize a protein via a reduction in the conformational entropy of the unfolded state without an effect on the folded state. Analysis of natural disulphide bridges has indicated that they can contribute up to 20 $kJmol^{-1}$ per disulphide bridge to the stability of the protein (Pace *et al*, 1988).

Attempts to stabilize proteins by introducing disulphide bridges have resulted in mixed successes. A number of groups have demonstrated an increase in stability by engineering in cysteine residues to form disulphide bridges. Examples include the introduction of a disulphide bridge in a thermolysin-like protease from *Bacillus stearothermophilus* (Van den Burg *et al*, 1998) and T4-lysozyme (Matsumura *et al*, 1989). However, in some other cases, the introduction of disulphide bridges has decreased the stability of the protein e.g. dihydrofolate-reductase (Villafranca *et al*, 1987) and T4-lysozyme (Wetzel *et al*, 1988).

Thus it can be said that the effect of introducing disulphide bridges to increase thermostability varies from protein to protein.

Hydrogen bonding

An estimation of the contribution of hydrogen bonding to protein stability has been made by a combination of experiments with model compounds and site-directed mutagenesis studies. From these experiments, it is thought that hydrogen bonding contributes around 5-10 $kJmol^{-1}$ to the stability of the protein by the formation of a buried intramolecular uncharged hydrogen bond (Pace *et al*, 1996; Fersht, 1997). There is also evidence that hydrogen bonding contributes to the stability of hyperthermophilic proteins.

A comparison of glyceraldehyde-3-phosphate dehydrogenase (GAPDH) from four organisms with a range of thermostabilities and more than 50% sequence identity found that the strongest correlation to thermostability was with the number of buried charged residues hydrogen-bonded to neutral residues (Tanner *et al*, 1996). Also Shirley and co workers carried out thermal denaturation and unfolding studies on 12 mutants of ribonuclease T1 (with disrupted H-bonds) and found that the H-bonds made a significant contribution to the protein's conformational stability (Shirley *et al*, 1992). An average decrease in stability of 5 $kJmol^{-1}$ was found per hydrogen bond destroyed. Vogt *et al* (1997), in their comparison of the mesophilic and thermophilic structures of proteins from 16 families found that in 80% of the proteins there was an average increase of 11.7 bonds per chain per 10°C rise in thermal stability.

Packing density

The role of packing density in the thermostability of hyperthermophilic proteins is widely discussed in the literature. The evidence of its role is mixed. Britton *et al* (1995) suggested that the strong increase in isoleucine content in *P. furiosus* glucose dehydrogenase was consistent with a general increase in packing when compared to the mesophilic *Clostridium symbiosum* GDH. With the ability of Ile to adopt more conformations than Leu in proteins, it is better able to fill various voids in the protein core. This increase in Ile content is also seen in a comparison of citrate synthase, as is discussed in **Section 1.3.4**.

Better core packing (i.e. a decrease in the number of internal cavities) is often linked to increased hydrophobicity and therefore an increased protein thermostability. However, the comparisons including isopropylmalate dehydrogenase from *Thermus thermophilus* (Wallon *et al*, 1997), glyceraldehyde-3-phosphate dehydrogenase (GAPDH) from *Sulfolobus solfataricus* (Isupov *et al*, 1999) and the superstable superoxide dimutase from *Sulfolobus acidocaldarius* (Knapp *et al*, 1999) have found no decrease in the number of internal cavities in the thermophilic enzymes. In the *T. thermophilus* isopropylmalate dehydrogenase case, a mutation was made that created a new cavity of 32Å in volume in the interior of the protein, but no decrease in thermostability was observed (Wallon *et al*, 1997). Karshikoff & Ladenstein (1998) also compared the partial specific volumes, voids and cavity volume in a set of 80 mesophilic, 20 thermophilic and 4 hyperthermophilic proteins. They concluded that none of these factors could be considered to decrease with increasing thermostability.

Reduction in loop size

Loop regions have a tendency towards higher mobility in a protein structure. They are likely to unfold first during thermal denaturation (Dagget & Levitt, 1993). Two loop-stabilizing trends have been observed in thermophilic proteins. Firstly, a reduction in the length of loops has been observed in some thermophilic proteins (Russell *et al*, 1997; Thompson & Eisenberg, 1999; Vieille & Zeikus, 2001). Secondly, the loops have also been observed to be better anchored to the rest of the protein and this is achieved through ion pairing, hydrogen bonding or hydrophobic interactions (Vieille & Zeikus, 2001).

The shortening of loop regions between areas of secondary structure and anchoring of loops has been observed in thermophilic citrate synthases (Russell *et al*, 1994 & 1997), lactate dehydrogenase from *Thermotoga maritima* (Auerbach *et al*, 1998) and ferrodoxin from *T. maritima* (Macedo-Ribeiro *et al*, 2001).

There are, however, some dramatic exceptions. In the case of two-subtilisin-like proteases from *P. furiosus* and *Thermococcus stetteri* (Voorhorst *et al*, 1997), the thermostable proteases actually have several extra surface loops compared with their mesophilic counterparts.

Rigidity

Proteins isolated from thermophilic microorganisms often display enhanced rigidity at mesophilic temperatures with respect to that of their mesophilic counterparts. A growing body of experimental data supports this hypothesis. Evidence of protein rigidity can be obtained from hydrogen exchange measurements (Wrba *et al*, 1990; Rehaber & Jaenicke, 1992), fluorescence quenching (Varley & Pain, 1991) and

theoretical calculations (Vihinen, 1987) and molecular dynamics simulations (Lazaridis *et al*, 1997). In his protein flexibility study, Vihinen (1987) showed that flexibility decreased as thermostability increased, although the analysis did not include hyperthermophilic proteins.

Lazaridis *et al* (1997) argue that there is no single measure of flexibility and that there is no fundamental reason for stability and rigidity to be correlated. One factor that suggests that there may be a relationship between stability and rigidity is the increased number of proline residues found in hyperthermophilic protein sequences (Tahirov *et al*, 1998; Wallon *et al*, 1997). Proline has been implicated in reducing the flexibility of the polypeptide chain.

While most comparisons of mesophilic and hyperthermophilic proteins support this hypothesis that hyperthermophilic proteins are more rigid enzymes, the recent study of Hernandez *et al* (2000), does not support this conclusion. Using amide hydrogen exchange data, this group concluded that *Pyrococcus furiosus* rubredoxin at 28°C shows a degree of conformational flexibility comparable to that of mesophilic proteins.

Increased rigidity has been proposed as an explanation of why hyperthermophilic enzymes are often inactive at low temperatures. A few hyperthermophilic enzymes have, however, been characterised that are more active than their mesophilic counterparts even at 37°C (Meng *et al*, 1991; Sterner *et al*, 1996 and Ichikawa & Clarke, 1998). The existence of such enzymes suggests that thermostability is not incompatible with high activity at low temperatures.

Amino acid preferences

Another feature of thermophilic and hyperthermophilic proteins thought to be correlated with thermostability is amino acid composition. Statistical analyses comparing amino acid compositions from thermophilic proteins with their mesophilic counterparts indicate a few minor trends.

A general reduction in the number of thermolabile residues with increase in thermostability has been observed in some proteins (Menendez-Arias & Argos, 1989; Russell & Taylor, 1995). Cysteine and methionine residues are avoided due to the possibility of oxidation at high temperatures and also asparagine and glutamine due to possible deamidation (Daniel *et al*, 1996).

The comparison of residue contents of proteins from hyperthermophilic organisms and mesophilic organisms based on the genome sequence of seven hyperthermophiles and eight mesophiles showed a few trends (Vieille & Zeikus, 2001). More charged residues are found in hyperthermophilic proteins, and they also contain slightly more hydrophobic and aromatic residues than mesophilic proteins. However, the authors insist that 'the data obtained from genome sequencing cannot be generalised since large variations exist among hyperthermophilic genomes themselves'.

Probably, more relevant to the thermostability of the protein is the distribution of the residues and their interactions in the protein. For example, Teplyakov *et al* (1990) found when comparing two homologous proteases from *Bacillus amyloliquefaciens* subtilisin BPN with *Thermoactinomyces vulgaris* thermitase that both proteins contain the same number of charged residues, but the thermophilic enzyme contains eight more ion pairs.

Oligomerization

The vast majority of enzymes (approximately 80%) exist as oligomers, in most cases with active sites situated between the subunits. An increasing number of hyperthermophilic proteins are found to have a higher oligomerization state than their mesophilic counterparts (Vielle & Zeikus, 2001), and there has been some experimental evidence to support the hypothesis that oligomerization increases the thermostability of proteins. Thoma and coworkers engineered monomeric variants of *T. maritima* phosphoribosylathranilate isomerase by site directed mutagenesis. These monomeric enzymes remained as active as the wild-type enzyme, but their kinetic stability at 85°C decreased by factors of 60 to 100 (Thoma *et al*, 2000). Other solid experimental evidence includes the trimerization of *Methanopyrus kandleri* methyl H4MPT cyclohydrolase (MkCH) that led to an increase in enzyme stability (Grabarse *et al*, 1999).

1.1.2.2. Extrinsic factors

Although most extremophilic proteins are intrinsically stable, some hyperthermophilic proteins gain at least part of their stability *in vivo* from external factors such as the presence of additives (salts, compatible solutes, substrates, activators, coenzymes), high protein concentration, or other environmental factors such as pressure.

Many commercially available enzymes contain compounds such as glycerol or some other stabilizing additive to prevent inactivation. The presence of 'inert' molecules is another method via which a protein may be stabilized *in vitro.* A wide range of compounds such as salts, sugars, substrates and cofactors have been identified as potential protein stabilizers (Fagain, 1995).

Volkin and Klibanov (1989) have classified stabilizing additives as specific (substrates and ligands) and non-specific (sugars, salts etc).

Stabilization by salts Inorganic salts stabilize proteins in two ways, either by specific binding or by preferential exclusion. The first effect involves the metal ion such as Ca, Zn, Mo, Fe interacting with the protein in a conformational manner. These metal ions are normally required for catalytic function or maintenance of tertiary structure, or in some cases for both. For example, glucose dehydrogenase from *Thermoplasma acidophilum* requires one catalytic and one structural Zn^{+} per subunit (John *et al*, 1994). The second salt stabilizing effect is a general salt effect, which mainly reduces the water activity.

Stabilization by substrates A number of studies have reported enhanced stability in the presence of substrates, products, inhibitors etc. The binding of these molecules to the enzyme's active site is usually quite strong and induces a slight conformational change in the protein backbone. The protein adopts a more tightly folded conformation and becomes less prone to unfolding and proteolysis (Volkin & Klibanov, 1989).

Pressure effects Many high temperature environments are also high-pressure environments. Therefore, cell components of organisms that live in these environments have to be adapted to these pressures. Thus, it is not surprising to find hyperthermophiles that are also barophilic such as *Thermococcus barophilus*, and to find enzymes that are stabilized to the effects of temperature by high pressures (Vieille & Zeikus, 2001). Examples of enzymes stabilized by high pressure are protease and hydrogenase from *M. jannaschii* (Miller *et al*, 1989; Michels & Clark, 1997). Stabilization by pressure is thought to occur because pressure favours the structure with the smallest volume (Vieille & Zeikus, 2001).

1.2. Conformational stability of proteins

All proteins exhibit a specific native conformation, that is required for their biological function. Maintenance of this conformation under the influence of various deleterious conditions is referred to as the stability of the protein (Andersson, 1999).

Before entering into a discussion about the stability of proteins, one must define the meaning of the word 'stability'. Stability means different things to different people. The stability of proteins is taken to mean the maintenance of their function *in vitro* (Fagain & O'Kennedy, 1991). Protein stability may also be understood as the resistance of a protein against unfolding (Darby & Creighton, 1993).

Stability can be defined in terms of thermodynamic stability or kinetic stability. Thermodynamic stability is used to describe a protein that unfolds and refolds reversibly and cooperatively. The kinetic stability on the other hand describes the rate of unfolding of a protein and usually relates to an irreversible process.
The schematic in **Figure 1.1** illustrates the thermodynamic and kinetic stability of a protein.

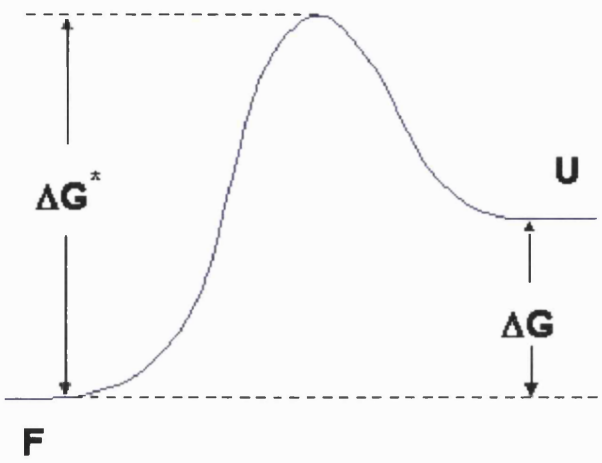

Figure 1.1: A free energy profile describing the unfolding of a protein. F is the folded state, U is the unfolded state and ΔG is a measure of the thermodynamic stability. The activation energy or ΔG* determines the kinetic stability of the protein.

1.2.1. Thermodynamic stability

Thermodynamic stability refers to the reversible unfolding of a protein.

$$F \underset{k_F}{\overset{k_U}{\rightleftharpoons}} U$$

where k_U and k_F are the rate constants for unfolding and (re)folding respectively. Thus K_{eq} (the equilibrium constant) = [U]/[F] = k_U / k_F, and ΔG (the free energy difference between folded and unfolded forms) is given by:

$$\Delta G^0 = -RT \ln K_{eq}$$

where **R** is the gas constant and **T** is the absolute temperature.

Thus, ΔG is a measure of the thermodynamic stability of the protein and is essentially the difference in free energy between the folded and the unfolded states.

$$\Delta G = G_U - G_F$$

ΔG values are generally determined by analysis of protein unfolding induced by denaturants such as urea or guanidine hydrochloride, and in some cases heat.

The only factors affecting the conformational stability of the protein are the relative free energies of the folded and the unfolded states. The larger and more positive the value of ΔG, the more stable the protein is to denaturation. The free energy difference of a protein is typically small, of the order of 20-60 kJ/mol for a monomeric protein, and is equivalent to a few non-covalent interactions (Pace, 1990). However, even though ΔG is small in magnitude, it is in fact the combination of two large opposing contributions from the enthalpic (ΔH) and entropic (ΔS) changes between F and U:

$$\Delta G = \Delta H - T\Delta S$$

1.2.2. Kinetic stability

Most protein scientists are concerned with whether a protein is stable enough to function under harsh conditions of temperature or solvent. Whilst the answer to this question may lie in the thermodynamic stability of the protein, for irreversible or slowly unfolding proteins, it may lie in the kinetic stability.

Kinetic stability is a measure of the rate at which a protein unfolds. It is particularly important for proteins that unfold very slowly or denature irreversibly. Irreversible loss of protein structure is represented by:

$$\text{Folded} \underset{k_2}{\overset{k_1}{\rightleftharpoons}} \text{Unfolded} \xrightarrow{k_3} \text{Irreversibly-inactivated}$$

Where where k_1 and k_2 are the rate constants for unfolding and (re)folding, respectively and k_3 is the rate constant of the formation of I. If the steady-state assumption is made, at least over the period of experimental observation, [U] is constant, and then:

$$k_1[F] = (k_2 + k_3)[U]$$

$$[U] = \frac{k_1[F]}{(k_2 + k_3)}$$

$$\text{Rate of thermal inactivation} = \frac{dx}{dt} = k_3[U] = \frac{k_1 k_3 [F]}{(k_2 + k_3)}$$

According to this model, the upper limit of k_{obs} is set by k_1 as only U will undergo irreversible inactivation.

The kinetic stability is determined by the free energy difference between the folded and the transition states (activation energy). The magnitude of this difference dictates the rate of inactivation of the protein and, therefore the factors affecting stability are the relative free energies of the folded and the transition states.

1.3. Protein unfolding and denaturation

There are a number of techniques available to follow the denaturation of proteins, and they are based on the physical changes that occur when a protein is unfolded. The property used to study the denaturation of a protein depends on the sensitivity of the method to the protein conformation and the precision of the method, because denaturation experiments are carried out at low protein concentrations to minimise aggregation of the protein and also because the amount of protein available normally is limited. In general, the greater the change in the physical property when the protein unfolds, the better the technique for following protein unfolding.

The most often used techniques to follow the folding and unfolding reactions of protein are fluorescence, circular dichroism, NMR, catalytic activity and differential scanning calorimetry. The techniques chosen for use in this study are fluorescence, differential scanning calorimetry and catalytic activity.

Chemical denaturation is the most widely used method via which the conformational stability of proteins is studied.

Effect of chemical denaturants

Urea and guanidine hydrochloride are well known denaturants of proteins. It is known that proteins unfold upon the addition of these denaturants, but the mechanism(s) by which they do so is still a mystery. Numerous experimental studies have attempted to explain the mechanism of unfolding of proteins in aqueous urea solutions. Most of these studies are based on untested assumptions.

There are two models used to describe denaturant-induced protein unfolding: the denaturant molecules may act (a) directly, by binding to peptide groups, thereby weakening internal hydrogen bonds or (b) indirectly, by causing a change in the structure of the water's hydrogen bond network around hydrophobic groups in proteins, thereby increasing their solubility and weakening the hydrophobic effect. It is also possible that both mechanisms are operating or that protein unfolding occurs by a different mechanism not yet described.

Urea Guanidinium

Figure 1.2: Molecular structures of urea and guanidinium with charge distributions.

Demonstrating that chemical denaturants unfold proteins through their effect on water structure and thus on the strength of the hydrophobic effect has proved elusive. Wallqvist *et al* (1998) dispute this mechanism, and suggest that the ability of urea to dissolve in water is a consequence of the minimum disruption of the overall hydrogen bonding of the aqueous solution. Moreover, Vanzi *et al* (1998) have shown that the hydrogen bond network of water is maintained in urea and even enhanced surrounding the amine groups.

Another possible explanation for denaturation is that urea preferentially saturates the hydrophobic residues and leads to an effective reduction of the hydrophobic interaction, which in turn destabilises the native state. This claim has also been contradicted by calculations carried out by Wallqvist *et al* (1998) of the potential mean force (POMF – the effect of the denaturant on hydrophobic interactions), which suggest that for their model system (methane molecules) urea appears to enhance the hydrophobic interactions and acts as a renaturant.

Wallqvist and co-workers suggest a third method via which the chemical denaturation of globular proteins occurs (Wallqvist *et al*, 1998). The urea is adsorbed onto the charged hydrophilic residues on the surface of the protein. This adsorption leads to repulsion between the residues on the protein surface and this in turn gives rise to the swelling of the protein. Swelling of the protein exposes the hydrophobic residues and the entry of water into the interior leads to the destabilization of the native state resulting in denaturation. Large amounts of denaturant reduce the driving force of the compact structure formation, which is believed to be a subtle balance between hydrophobic interactions and interfacial free energies (Thirumalai *et al*, 1997). It also follows that, because urea dissolves readily in water without disrupting the water structure, an excess amount of urea is required before adsorption onto the surface residues of proteins becomes effective.

Guanidine is isosteric to urea but differs by the replacement of the oxygen with an amino group (see **Figure 1.2**), which enables it to support more positive charge. Guanidine is thought to share some of urea's non-polar-like effect on water structure (Vanzi *et al*, 1998). It is thought that both guanidine and urea have both polar and non-polar characteristics that could be important in their denaturing action.

Monera *et al* (1993, 1994) have shown that guanidine cannot discern the contributions of electrostatic interactions but the effects of electrostatic interactions are effectively monitored in urea. GdnHCl has ionic properties that are absent in urea. GdnHCl is a salt and is, therefore, expected to ionise in water. At low concentrations, $GdnH^+$ and Cl^- ions are presumed to mask the positively and negatively charged amino acid side chains, thereby reducing or even totally eliminating electrostatic interactions.

Monera and his colleagues also suggest that these differential effects of GdnHCl and urea on the electrostatic interactions may enable us to monitor selectively the contribution of a particular type of interaction that is hydrophobic or electrostatic. If the effects of the changes in electrostatic interactions are to be assessed, or if the overall stability of the protein is of interest, urea or temperature denaturation becomes the obvious choice. However, GdnHCl is more appropriate in determining the specific contributions of hydrophobic or non-ionic interactions on protein stability.

It is worth remembering that the majority of experiments simulating chemical denaturation of proteins use methane molecules as models. The model of two methane molecules is not an appropriate approximation of the exposed hydrophobic groups of proteins where such groups might correspond to large hydrophobic molecules (Ikeguchi *et al*, 2001). Therefore, simulation experiments using a model of the hydrophobic core that is more realistic than methane molecules are needed.

1.3.1. Monitoring unfolding and refolding

1.3.1.1. Fluorescence

All molecules absorb light but only a small number of molecular species emit light as a result of absorption of light from other sources. Fluorescence is the emission of light from a molecule in an electronically excited singlet state (Schmid, 1998). The emission of light is usually in the ultraviolet to the visible portion of the spectrum. Molecules that fluoresce tend to be conjugated polyaromatic hydrocarbons or heterocyclics (Lakowicz, 1999). Of the 20 amino acids usually found in proteins, the aromatic residues phenylalanine, tyrosine and tryptophan are the only ones of sufficient fluorescence intensity to be measured directly in solution. This makes fluorescence a highly specific and sensitive method for studying protein structure and conformation. Fluorescence is probably the most simple yet the most sensitive method for following the folding and unfolding of proteins. A prerequisite for the use of fluorescence is that the protein must contain aromatic residues i.e. tryptophan, tyrosine and phenylalanine. The residue that fluoresces depends on the excitation wavelength used.

At ambient temperature most molecules occupy the lowest vibrational level of the electronic ground state, and on absorption of radiant energy they are elevated to produce excited states. Fluorescence is observed after an electron is promoted from the ground state to an excited state and a photon (light molecule) is emitted when the molecule returns to the ground state (Schmid, 1998). Fluorescence is closely related to UV/Visible absorption spectroscopy, although it has significant advantages of selectivity and higher sensitivity for those materials that fluoresce. One similarity is that fluorescence intensity is generally directly proportional to concentration, provided that some basic ground rules are obeyed. The main difference is that fluorescence is an emission rather than an absorption technique, and this means that the results are relative rather than absolute.

Changes in the conformation of the protein, such as unfolding, often lead to large changes in the fluorescence emission. In proteins that contain aromatic residues, both shifts in wavelength and changes in intensity are generally observed upon unfolding. The tryptophan emission of a native protein can be greater or smaller than the emission of free tryptophan in aqueous solution. Consequently, both increases and decreases in fluorescence can occur upon protein unfolding.

One of the aims of this project is to unfold proteins using temperature and guanidine hydrochloride. Fluorescence is significantly affected by increases in temperature (Schmid, 1998). The fluorescence intensity generally decreases with increasing temperature. Although this decrease of fluorescence is non-linear, it is usually satisfactory to assume a linear dependence (Eftink & Ionescu, 1997).

1.3.1.2. Differential scanning calorimetry

DSC has been widely employed during the last 20 years for the study of the thermodynamic parameters associated with processes that are initiated by either an increase or a decrease in temperature. It can be used to study the effect of environmental conditions (pH, ionic strength, nature of solvent) upon thermodynamic parameters. In DSC, the heat capacity of a protein in solution is directly measured as a function of temperature and the enthalpy change of the unfolding process can be obtained from the thermogram.

DSC is a valuable tool for determining the number of transition states obtained during the unfolding of a protein. It is widely used in studying the thermodynamics of protein unfolding because it does not need any models or assumptions. It enables precise determination of the key thermodynamic parameters such as melting temperature (T_m), change in heat capacity (ΔC_p) and enthalpy change (ΔH) (Pace &

Scholtz, 1998). However, some errors can arise in DSC and are normally due to aggregation and precipitation of the protein, which lead to irreversible denaturation.

1.3.1.3. Catalytic activity

In many cases, the protein under investigation will be an enzyme with a well-known biological activity. Changes in biological activity can therefore be used to monitor the unfolding of an enzyme. It is difficult to define the extent of conformational unfolding when the activity changes as activity loss can be the result of very small changes in the conformation at the active site.

1.4. Citrate synthase

1.4.1. Metabolic role

Citrate synthase is the enzyme that catalyses the initial reaction of the citric acid cycle – the synthesis of citrate from oxaloacetate and acetyl coenzyme A in an aldol condensation. Citrate synthase can directly form a carbon-carbon bond in the absence of metal ion co-factors. This reaction is the only step in the cycle that involves the formation of a carbon-carbon bond. Its role as a catalyst of the entry reaction of two carbon units into the citric acid cycle guarantees its importance for organisms with the complete cycle, but even where the complete cycle does not function, it is an essential step in the biosynthesis of amino acids related to glutamate (Nguyen *et al*, 2001).

The central role of citrate synthase in cell metabolism, in both aerobic energy production and carbon skeleton biosynthesis, is demonstrated by the presence of the enzyme throughout the three phylogenetic domains of life. Some organisms have a single citrate synthase, with a few such as *Saccharomyces cerevisiae* (Rosenkrantz *et al*, 1986) and *Bacillus subtilis* having as many as three (Jin & Sonenshein, 1994). Archaea and many Gram-positive bacteria possess a single citrate synthase, which is a homodimer. Some Gram-negative bacteria possess both a hexamer and a dimer. In eukaryotes, there are two isozymes of citrate synthase. Both eukaryotic enzymes seem to be dimers of identical chain length. Despite the oligomeric variation, the subunit molecular weight is very similar, between 42,000 and 50,000 in all cases (Muir *et al*, 1995).

Citrate synthases from several organisms have been well characterised and there is a large base of information on this enzyme. The structure of CS from several organisms spanning the biological range of growth temperatures (10-100°C) has

been determined (Russell *et al*, 1993, 1997; Muir *et al*, 1995; Gerike *et al*, 1997). In addition to this, the expressed recombinant protein is readily purified and its activity can be assayed simply and accurately.

Citrate synthase was chosen as our model protein with which to investigate the basis of conformational thermostability.

1.4.2. Structure

As mentioned earlier, a large number of citrate synthases have been sequenced and high-resolution structures of the dimeric enzyme from several sources have been determined. There are a number of similarities between these dimers including a number of regions of sequence similarity (shown in **Figure 1.3**) and structural similarity at three-dimensional level.

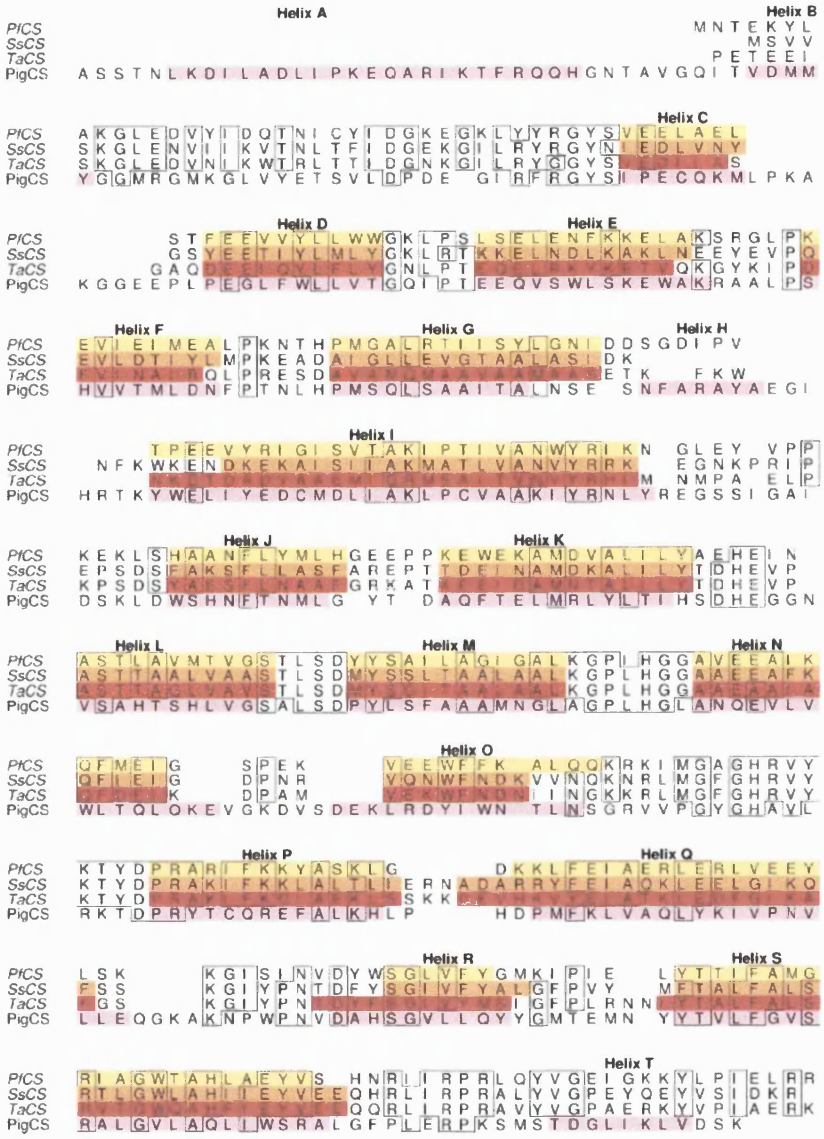

Figure 1.3. Structurally based alignment of the amino acid sequences of citrate synthases. Helices are shown in shown in pink (PigCS), red (TaCS), orange (SsCS) and yellow (PfCS).

Dimeric citrate synthase, known also as type 1 citrate synthase, is made up of two identical subunits. Each subunit has two domains – the small domain and the large domain. Most of the residues in the active site are from the small domain, and this is therefore referred to as the catalytic domain. The large domain is mainly responsible for the inter-subunit association – almost entirely but not exclusively. There is a high degree of structural homology between the crystal structures of the dimeric citrate synthases and the homology extends to the active site residues, which are conserved both in sequence and in three-dimensional space (Arnott *et al*, 2000). Crystal structure analysis has shown that citrate synthase is almost entirely α-helical with only a small region of β-sheet.

Much less is known of the hexameric (type II) citrate synthase. This enzyme is only found in Gram-negative bacteria (Weitzman, 1966). Whilst type I and II CSs show limited sequence identities (<30%), there is conservation of active site residues and the enzyme mechanism is likely to be very similar. (Nguyen *et al*, 2001).

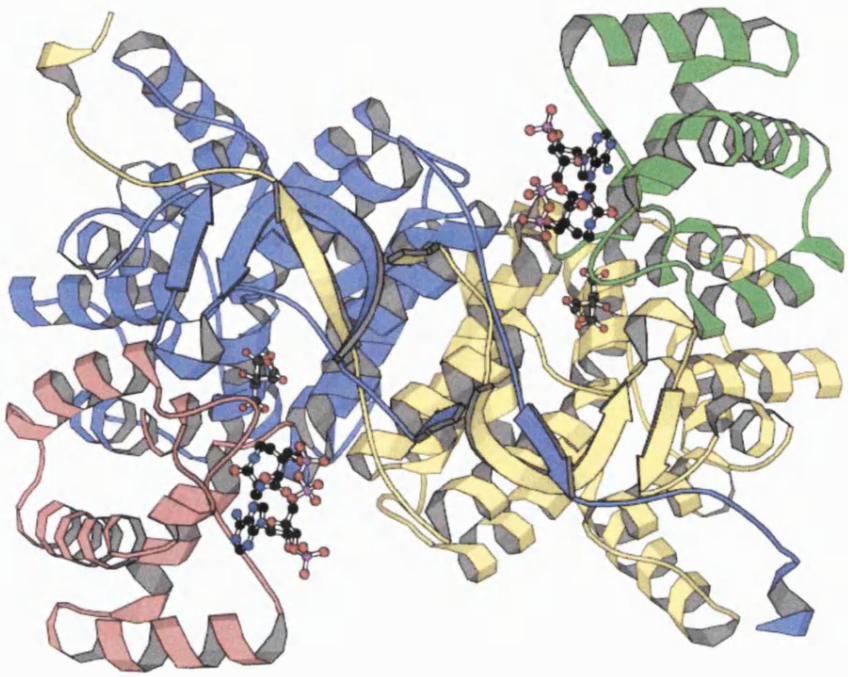

Figure 1.4: Crystal structure of *Pyrococcus furiosus* citrate synthase showing the two subunits. Each subunit consists of a small domain (shown in pink and green) and a large domain (shown in yellow and blue). The substrates, acetyl CoA and OAA, are shown in the active sites.

1.4.3. Reaction mechanism

Structures of the liganded form of pig citrate synthase show that the active site lies in the cleft between the large domain of one subunit and the small domain of the other subunit. There are therefore two active sites per molecule of the CS. Studies on the pig enzyme have shown that it is only active as a dimer due to the fact that active site residues reside on both monomers. The catalytic mechanism has been studied by kinetics, fluorescence, NMR, inhibitor studies and by site-directed mutagenesis (Handford *et al*, 1988; Kurz *et al* 1992a&b; 1995, 1997, 1998; Evans *et al*, 1996).

A flow diagram of the catalytic mechanism of pig CS is shown in **Figure 1.5**. The initial binding of oxaloacetate initiates the movement of the small domain relative to the large, giving the closed form of the enzyme. The reaction is thought to proceed via an acid/base mechanism (Remington, 1992). It proceeds via deprotonation of the methyl group of acetyl CoA by the aspartate 375, stabilisation of the resulting transition state by His 274, followed by a condensation reaction in which the carbanion attacks the carbonyl group of oxaloacetate, producing citryl CoA. The final reaction involves the hydrolysis of the thioester resulting in the formation of citrate and CoA. The rate-limiting step is the formation of the enolate intermediate of acetyl CoA. Of the total of 11 residues involved in substrate binding and catalytic action of the pig citrate synthase, 8 are conserved in the known archaeal enzymes.

Mesophilic and thermophilic citrate synthases have approximately the same specific activities at their physiological temperatures (pig 280 μmol/min/mg at 37°C, *Thermoplasma acidophilum* 170 μmol/min/mg at 60°C, *Sulfolobus solfataricus* 275 μmol/min/mg at 80°C and *Pyrococcus furiosus* 240 μmol/min/mg at 95°C. This shows that the increase in stability may probably be at the expense of catalytic activity. Standard chemical reaction theory predicts an exponential increase in rate with temperature. Therefore, if all CS enzymes were equally efficient catalysts, the rate of reaction with PfCS at 95°C should be 64 times the rate with pigCS at 37°C. It is therefore thought that the rigidity necessary for stability may be partially incompatible with the flexibility that is required for catalysis (Zavodsky *et al*, 1998), although temperature induced changes in the pKa values of ionisable amino acids may be another factor (Danson *et al*, 1996).

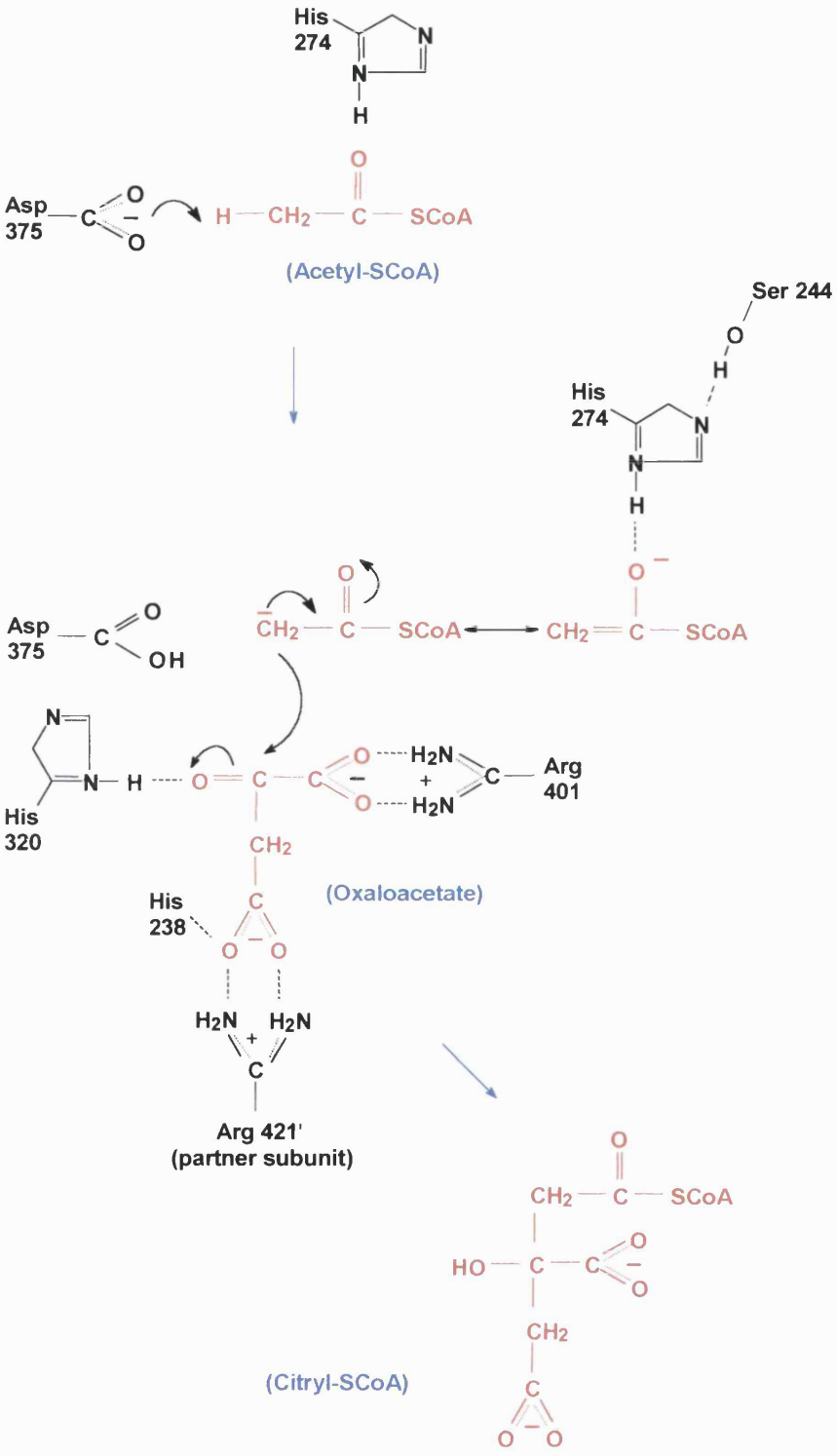

Figure 1.5: Catalytic mechanism of pig citrate synthase. The residues thought to be involved in the mechanism are shown in black. Substrates and products of the reaction are shown in red.

1.4.4. Structural basis of thermostability in citrate synthase

The work reported in this thesis concentrates on investigating the structural features responsible for thermostability in citrate synthase.

As discussed earlier, the dimeric citrate synthases that have been characterised are from the psychrophilic *Arthrobacter*, the eukaryote pig and the thermophilic Archaea *T. acidophilum*, *S. solfataricus* and *P. furiosus.* Their three-dimensional structures have been determined and compared, and there is a close structural similarity between all these enzymes. They show a common overall fold of the large and small domains of the monomer unit and also the nature of the subunit interface, which in each case comprises an eight α-helical sandwich of four antiparallel pairs of helices (Danson & Hough, 1998). Comparison of the active sites also indicates a similar mode of substrate binding and essential active site residues are conserved. Despite the close structural similarity, a detailed look at these structures has shown significant differences that may be linked to the differences in thermal stability.

Ionic interactions – Ion pairs are commonly associated with increasing stability. A comparison of the different citrate synthases reveals that PfCS, the most thermostable of these proteins, has the greatest number of ionic interactions (Russell *et al*, 1997). A number of these ion pairs are located in the loop regions, thought to reduce the flexibility of the loops. There are also two arginine residues at the C-terminal arm, which form ionic interactions with residues on the other monomer.

The number of ionic interactions found at the subunit interface of the different CSs increases with increasing thermostability as is seen in **Figure 1.6**. Compared to the less thermostable citrate synthases, PfCS has the greatest increase in the number of ionic interactions at the subunit interface. There are two five-membered ionic

networks located in helices G and M. These helices make up the central four helices of the right α-helical sandwich at the subunit interface.

Interestingly, the psychrophilic enzyme DSCS has two inter-subunit ionic interactions and two intra-subunit interactions at the surface. It is thought that the same interactions are required for stability at both extremes of temperature (high and low). The ionic interactions in PfCS will be discussed in more detail later on (Chapter 4).

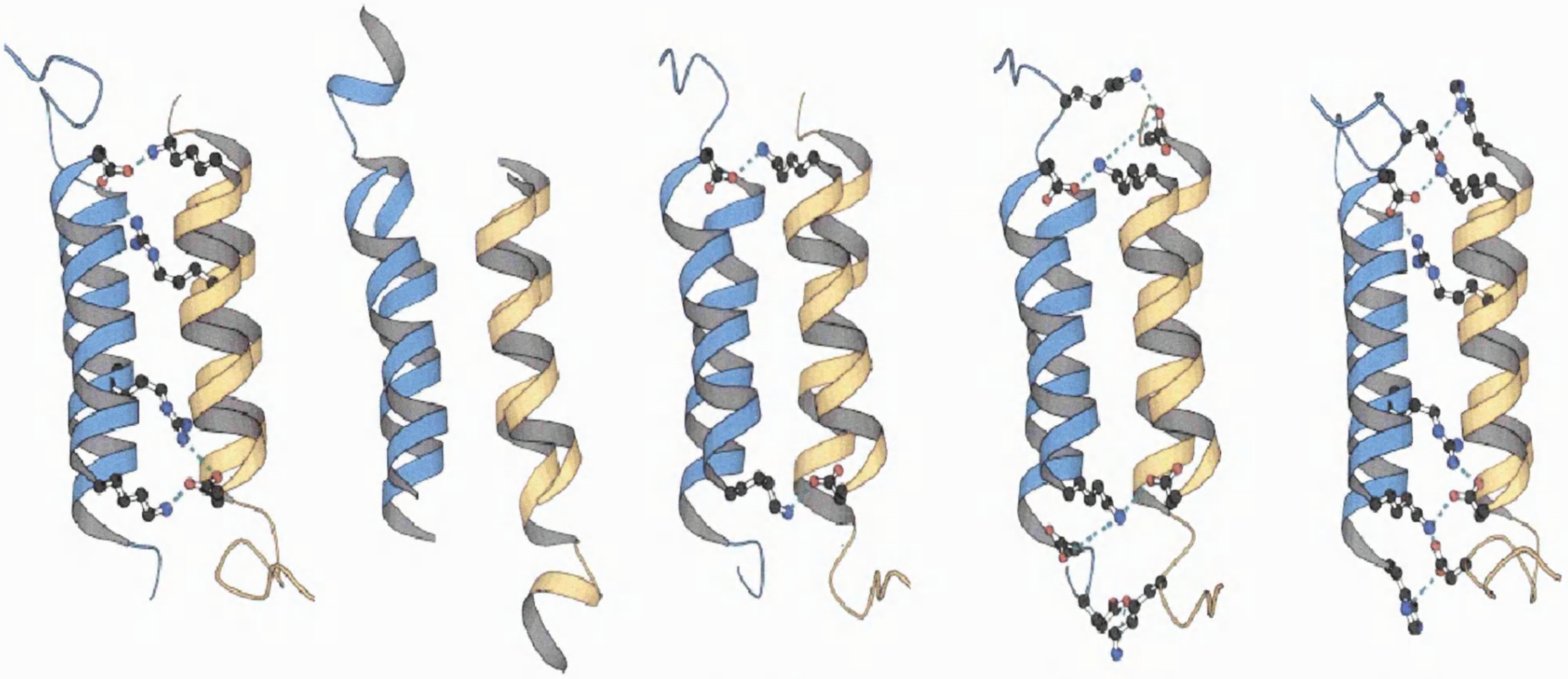

Figure 1.6: Comparison of the central four helices (G, G', M, M') of the dimeric citrate synthase enzyme showing the ionic interactions at the subunit interface. Helices from one subunit are shown in blue and the helices from the other subunit are shown in yellow. the temperatures are the optimal growth temperatures of the source organism.

Amino acid preferences The presence of thermolabile residues is thought to limit the thermostability of a protein because of their tendency to undergo oxidation (Cys, Met) or deamidation (Asn, Gln) at high temperature (Daniel *et al*, 1996). There is a reduction in Met content and an almost complete elimination of Cys residues in the thermophilic and hyperthermophilic citrate synthases. A comparison of PfCS with pigCS shows that PfCS has fewer methionine residues than PigCS, and the remaining methionine residues are buried in the solvent-free interior of the protein and hence are less susceptible to covalent modification. There is also a reduction in the number of asparagine and glutamine residues with increasing thermostability (Muir *et al*, 1995). Some asparagine and glutamine are replaced by charged residues, which are then involved in ionic interactions. There is, however, no trend in the glycine and proline contents in the citrate synthases studied, although the thermophilic citrate synthases have a lower number of intra-helical proline residues than pigCS.

Packing Density Better core packing may be linked to increased thermostability and an increase in the isoleucine content is thought to be closely involved in better packing (Britton *et al, 1995*). Clustering of isoleucine residues allows for a very well packed hydrophobic core. A comparison of the Ile content of DSCS, PigCS and PfCS shows an increase in Ile content and the formation of clusters in the hyperthermophilic enzyme (Muir *et al*, 1995).

PfCS also has one of the highest percentages of aromatic amino acid residues of the citrate synthases, which may lead to enhanced stabilizing packing interactions (Muir *et al*, 1995). This is shown in **Figure 1.7**. There is also a reduction in internal cavities and an increase in compactness of the CS structure with increasing thermal stability (Russell *et al*, 1997).

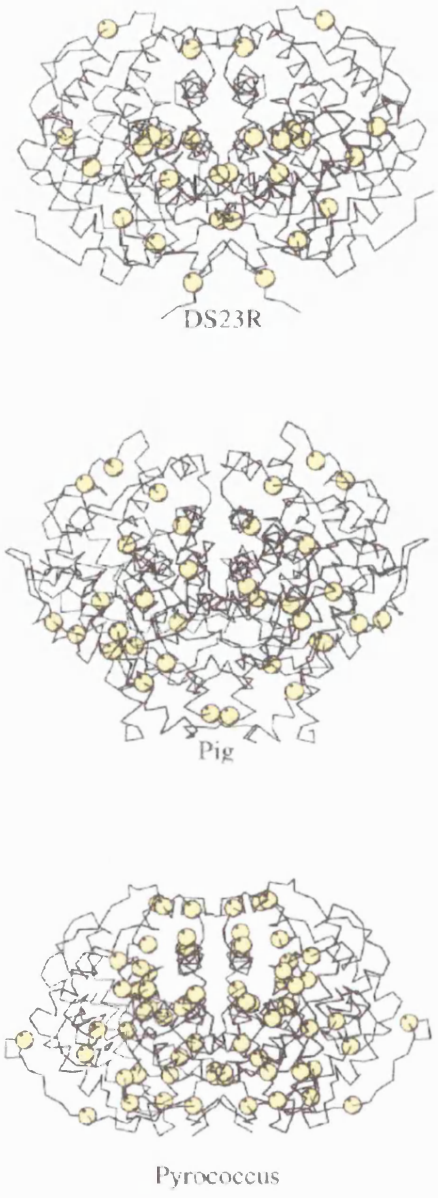

Figure 1.7: A comparison of the number of isoleucine residues present in citrate synthases from *Arthrobacter* (DS2-3R), pig and *Pyrococcus furiosus*. The schematic also shows the formation of clusters in PfCS.

Loops Loops tend to be highly mobile compared to the rest of the protein structure and are likely to unfold first. The shortening of loops between areas of secondary structure has been observed in thermophilic citrate synthases (Russell et al, 1994, 1997). In comparison to pigCS, there is a marked reduction in the length of loops of the thermophilic enzymes, which results in a more compact enzyme in the thermophilic Archaea (Muir *et al*, 1995). An example can be seen in **Figure 1.8**, which shows the loop region between helices C and D. In the *P. furiosus* enzyme, the loop is even shorter than in the TaCS and SsCS enzymes. This is thought to result in increased rigidity of the protein, thus increasing its thermostability. Another consequence of shorter loops is the elimination of some Asn and Gln residues in the thermozymes.

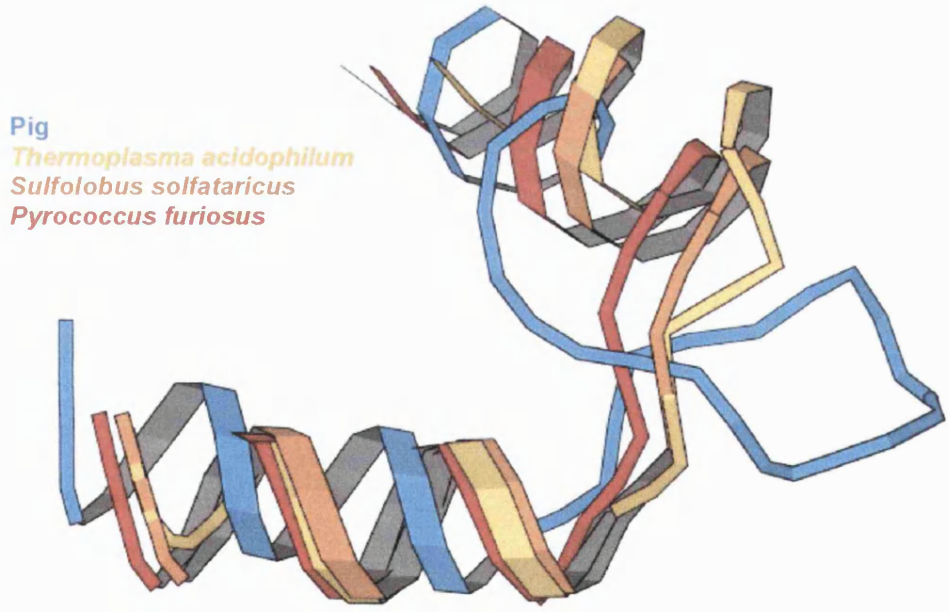

Figure 1.8: Comparison of loop regions between helices C and D for the different citrate synthase enzymes.

1.5. Experimental Aims

Part of the motivation for studying hyperthermophilic microorganisms is the extreme thermostability of their proteins and a logical question to ask is how stable are these proteins and how is their stability achieved?

The aim of this project is to use physical techniques to determine the denaturation mechanism and to understand the kinetic and thermodynamic basis for thermostability and thermoactivity of citrate synthase. A complete thermodynamic characterization will be performed for the *Pyrococcus furiosus* wild-type and mutant citrate synthases available in our laboratory.

The mechanism(s) via which thermal and chemical denaturation proceed in citrate synthases is to be characterised and the energy associated with the interactions stabilising the protein, calculated. One of the goals of this project is to provide a quantitative basis for the interpretation of experiments. These include thermodynamic studies of the entire unfolding process, including the study of the unfolding intermediates, and attempts to isolate the free energy contributions of individual groups using site-directed mutants of *P. furiosus* citrate synthase.

The main goal of this work is to arrive at a model capable of accounting for the small free energy changes that accompany protein unfolding while providing a more quantitative description of the effect of mutations on the thermostability of citrate synthase.

2. CHAPTER TWO

MATERIALS AND METHODS

Chemicals and reagents

All chemicals were of analytical grade or of the finest grade commercially available. Unless otherwise stated, culture media, chemicals and reagents were obtained from Sigma-Aldrich, Poole, UK, Fisher Chemcals, UK or Oxoid, UK. Guanidine hydrochloride and urea were of molecular biology grade and obtained from Sigma-Aldrich, Poole, UK.

Bacterial strains, culture conditions and plasmids

All the citrate synthase studied here had previously been cloned into the pREC7/*Nde*I expression vector using *Nde*I and *Kpn*I restriction sites. Plasmids had been transformed into the citrate synthase negative *E. coli* strains MOB154 and W620. The pREC7/*Nde*I vector was kindly supplied by Dr. Linda Kurz of Washington University School of Medicine (St. Louis, USA).

General Biochemical Methods

Storage of bacterial stocks

Cultures of *E.coli* MOB154 strain and W620 (CS^-) (acquired from glycerol stocks from U. Gerike, C. Thompson and R. Michael, University of Bath) carrying the citrate synthase gene on the expression vector pRec7/NdeI were grown overnight on LB-amp agar plates at 37°C (25°C for *Arthrobacter* DSCS). Bacteria were scraped into LB medium (see **Appendix I**) containing 15% sterile glycerol. The mixture was vortexed to ensure the glycerol was completely dispersed. The glycerinated culture

was dispensed into sterile tubes with screw caps. The cultures were frozen at –80°C for long term storage.

Growth and expression of citrate synthase

Bacterial cultures were grown in Terrific Broth (see **Appendix I**). Glycerol was used in the final fermentation to prevent foaming as foam can inhibit oxygenation. Cultures were incubated at 37°C (except DSCS which was incubated at 25°C) and shaken at 220 rpm. Overnight cultures were centrifuged at 5000g, 4°C, for 15 min to pellet the bacteria. Pellets were then stored at –20°C.

Purification of citrate synthase

Purification was carried out as described by James *et al* (1994). Frozen cell pellets were left to thaw at 4°C. The pellets were then resuspended in 12 ml extraction/ purification buffer (20mM Tris-HCl, pH 8, 2mM EDTA) and the cells were lysed using a high-pressure cell disrupter (One Shot Cell Disrupter, Constant Systems). Cell debris was removed by centrifuging the resulting suspension at 20,000g for 30 min. The supernatant was then heated at 85°C (PfCS enzymes) for 15 min (with the exception of the cell extract from the psychrophile which was applied to the column after centrifugation).

The heated cell extract was then centrifuged at 20,000g for 30 min to pellet denatured proteins. The resulting supernatant was applied to a Matrex Red Gel A or Pharmacia Red Sepharose affinity column. After washing with loading buffer, the enzyme was eluted with 5mM OAA and 1mM CoA.

Citrate synthase assay

The activity of citrate synthase can be assayed by measuring the CoA produced. Activity was measured spectrophotometrically by the method of Srere *et al* (1963). The thiol group of the coenzyme A produced reacts with 5,5'-dithio-bis(2-nitrobenzoic acid) (DTNB) to release thionitrobenzoate, which absorbs at 412 nm and has a molar extinction coefficient of $13,600M^{-1}cm^{-1}$. The assay was carried out at 55°C for thermophilic and hyperthermophilic CSs and at 25°C for the psychrophilic enzyme.

The assay is a sensitive procedure and simple to perform. The standard reaction mixture contained 0.2mM oxaloacetic acid, 0.15mM acetyl coenzyme A, 0.2mM DTNB and the enzyme sample made up to 1ml with Epps buffer (50mM Epps, 100mM KCl, 2mM EDTA), pH 8 (at 55°C). For assay at pH 7, the buffer was replaced with 50mM sodium phosphate, 2mM EDTA; at pH 5, the buffer was 50mM acetate, 2mM EDTA.

Enzyme assays were carried out in a Perkin Elmer Lambda 3B spectrophotometer and initial rates were calculated using the PECSS software supplied with the instrument. Specific activities of the samples were calculated as Units/mg of protein, where 1U is defined as 1μmol product formed per minute under standard assay conditions.

Estimation of protein concentration

Protein concentration was determined using the method of Bradford (1976) using the Bio-rad protein assay stock reagent as described by the manufacturer. A 0.9 ml volume of the reagent was mixed with 0.01 ml of protein sample and 0.09 ml of 0.9% sodium chloride solution and incubated at room temperature for 15 minutes.

The absorbance at 595 nm was measured and the protein concentration calculated from a calibration curve of bovine serum albumin (BSA) standard solutions ranging from 1-10μg.

Sodium dodecyl sulphate polyacylamide gel electrophoresis (SDS-PAGE)

Protein samples were analysed for purity by SDS-PAGE based on the method of Laemmli (1970). The resolving gel consisted of 10% (w/v) acylamide, 0.375 M Tris-HCl, pH 8.8, 0.1% (w/v) SDS, 0.025% (w/v) ammonium persulphate and 0.1% (v/v) N,N,N',N'-tetramethylethylenediamine (TEMED). The stacking gel consisted of 5%(w/v)acylamide, 0.13 M Tris-HCl, pH 6.5, 0.1% (w/v) SDS, 0.03% (w/v) ammonium persulphate and 0.001% (v/v) TEMED.

To prepare the protein samples for electrohoresis, an equal volume of loading buffer (0.18 M Tris-HCl, pH 6.5, 2% (w/v) SDS, 10% (w/v) glycerol, 2.6% (w/v) 2-mercaptoethanol, 0.005% (w/v) bromphenol blue) was added to a sample of protein and water. The samples were incubated at 100°C for 5 minutes. 5μg of protein sample was loaded into each well. Molecular weight markers were also loaded on to the gel. Electrophoresis was carried out with 1x tank buffer (0.025 M Tris-HCl, pH 8.8, 0.096 M glycine, 0.1 % (w/v) SDS) at a constant current of 10mAmps through the stacking gel and 20mAmps through the resolving gel until the bromophenol blue dye front was about 1cm from the edge of the gel.

The gels were stained for 30 minutes with Coomassie stain (0.5% (w/v) Coomassie Brilliant Blue R, 45% (v/v) methanol, 45% (v/v) acetic acid) and destained in a mixture of 10% (v/v) methanol, 10% (v/v) acetic acid and 80 % (v/v) water.

Denaturation Methods

Estimation of the conformational stability of a protein from denaturant- or thermally-induced unfolding curves is difficult for some proteins. A large amount of time was spent adapting and modifying experimental procedures used in the unfolding of monomeric proteins for this study.

The basis of the thermodynamic analysis of proteins is that the unfolding is an equilibrium process that is reversible. For the validity of calculations of thermodynamic parameters, it was necessary to establish that the unfolding of *P. furiosus* citrate synthase is an equilibrium process that is reversible.

Preparation of GdnHCl and Urea unfolding curves

Stock solutions of 8M GdnHCl and 10M urea were prepared as described by Pace & Scholtz, (1998); urea stock solutions were used within one week of preparation. The molarity of stock solutions was checked using refractive index measurements. Twenty to thirty different denaturant concentrations were typically used to define each denaturation curve and were prepared by adding a standard volume of a protein solution to a mixture of denaturant stock solution and a buffer solution to obtain different concentrations of denaturant. Actual experimental setups are described in the following chapters. The solutions were then incubated to allow an unfolding equilibrium to be reached before measurements were carried out.

Determination of fluorescence emission wavelength

To decide on a technique for following the unfolding of a protein, the spectra of the folded and unfolded conformations should be of interest. The fluorescence of the tryptophan residues can be investigated selectively by excitation at wavelengths greater than 295nm and tyrosine and tryptophan at wavelengths greater than

278nm. A comparison of the emission observed after excitation at 295nm and at 278nm shows that the shapes of the fluorescence spectra are virtually identical but excitation at 278nm results in a higher fluorescence intensity. **Figure 2.1** shows the fluorescence emission spectra of *P. furiosus* citrate synthase with fluorescence excited at 278nm and 295nm.

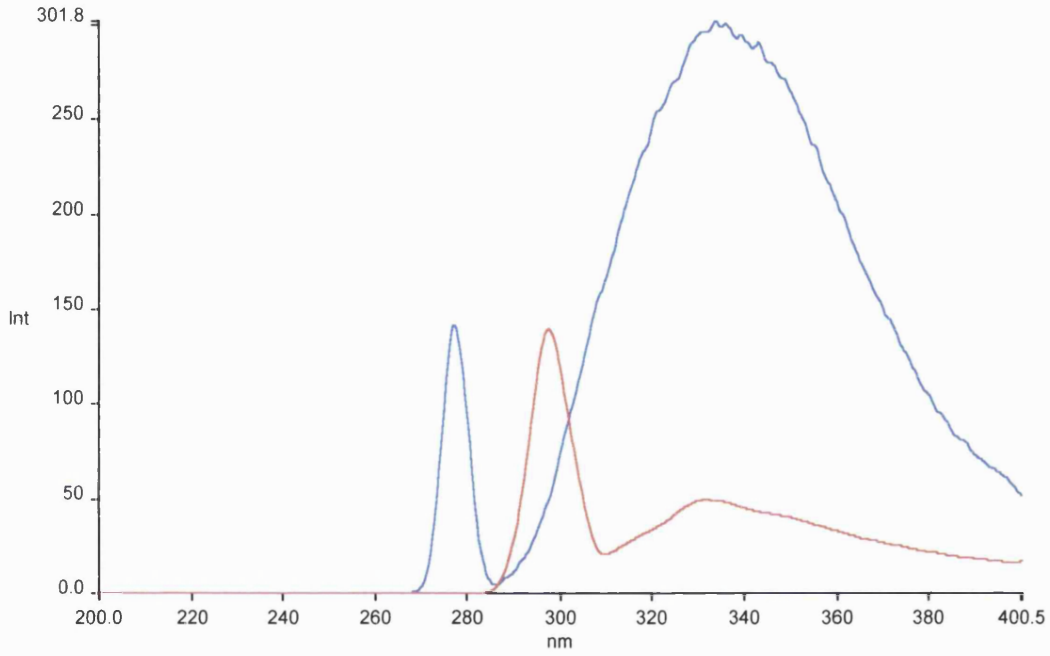

Figure 2.1: Fluorescence emission spectra of 10μg/ml folded *P. furiosus* citrate synthase. Fluorescence was excited at 278nm (-----) and 295 nm (-----). Spectra were recorded at 25°C.

Unfolding by GdnHCl results in a strong decrease of Trp fluorescence. For this reason, it was decided that an excitation wavelength of 278nm would be used.

Using fluorescence, it is necessary to pick a wavelength for which the spectra of the folded and unfolded conformations differ significantly. To determine the emission wavelength, the spectra of *P. furiosus* citrate synthase in phosphate buffer and 6M

GdnHCl were compared. **Figure 2.2** shows such a comparison of the fluorescence spectra of the PfCS, and from such data the emission wavelength was set at 340nm for subsequent unfolding studies. This corresponds to the wavelength at which there is a maximum difference between the native protein and the 6M GdnHCl unfolded protein.

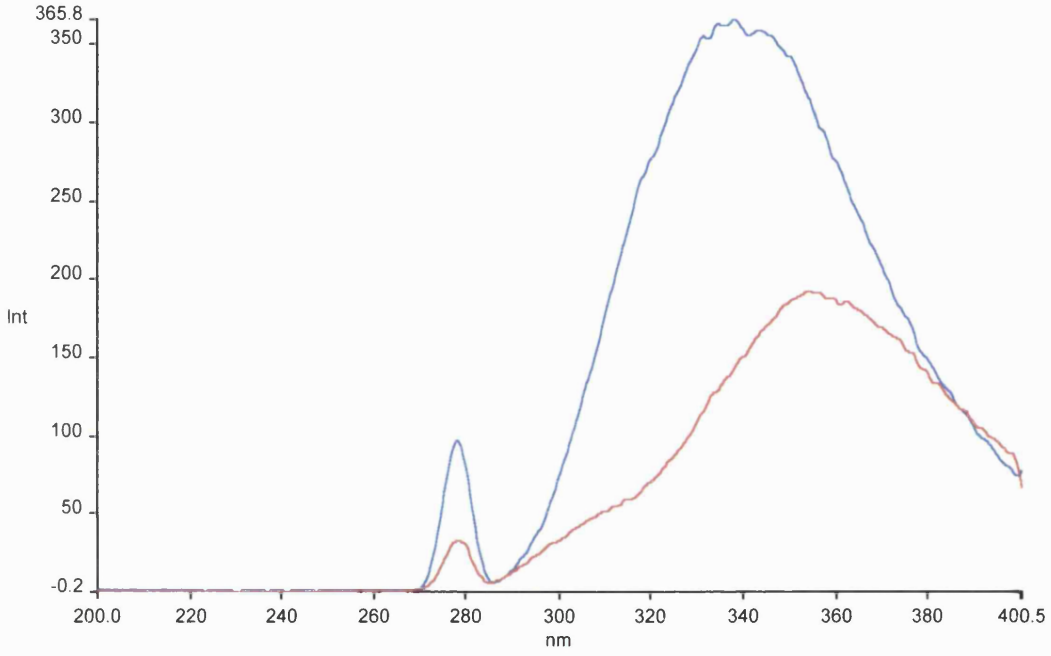

Figure 2.2: Fluorescence emission spectra of folded (-----) and unfolded (-----) *P. furiosus* citrate synthase. Folded PfCS was in 50mM sodium phosphate buffer pH 7; the sample of unfolded protein contained 6M GdnHCl. Spectra were recorded at 25°C.

Equilibrium studies

When dealing with thermodynamic measurements, it is essential that the unfolding reaction has reached equilibrium before spectroscopic or enzyme activity measurements are made. In general, the nearer the midpoint of the transition (i.e. the point at which fraction of unfolded = fraction folded), the longer it takes to reach

equilibrium (Pace & Scholtz, 1998). The time required by *P. furiosus* citrate synthase to reach equilibrium in GdnHCl was determined. This was done by measuring the fluorescence intensity as a function of time at the midpoint of transition and at both the pre- and the post-transition regions. The transition midpoint was determined as approximately 4M GdnHCl, whereas the pre- and post-transition periods determined as 0.8M and 6M respectively. The enzyme was incubated in GdnHCl at these concentrations at 25°C for three hours. Fluorescence measurements were taken at time intervals. Previous work done by Hanslip (2000) showed that when measuring the activity of the enzyme in the presence of GdnHCl, equilibrium was reached after fifteen minutes.

The data obtained when the fluorescence was measured are shown in **Figure 2.3**.

(a)

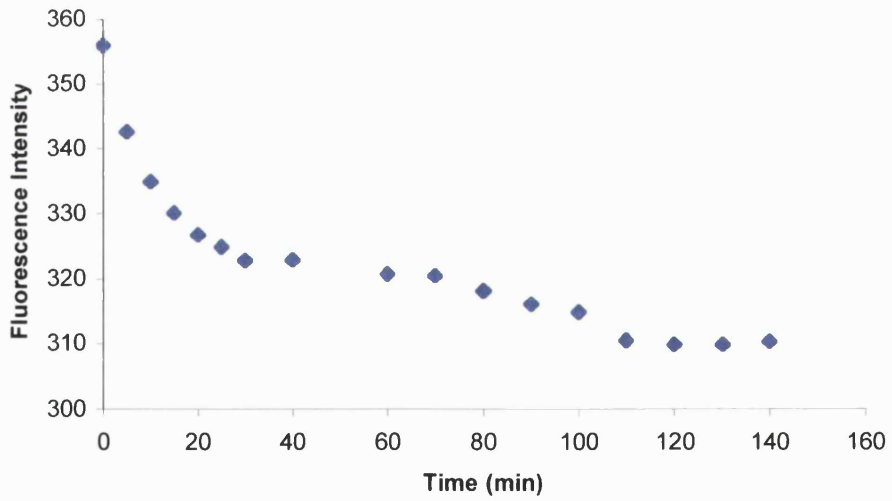

(b)

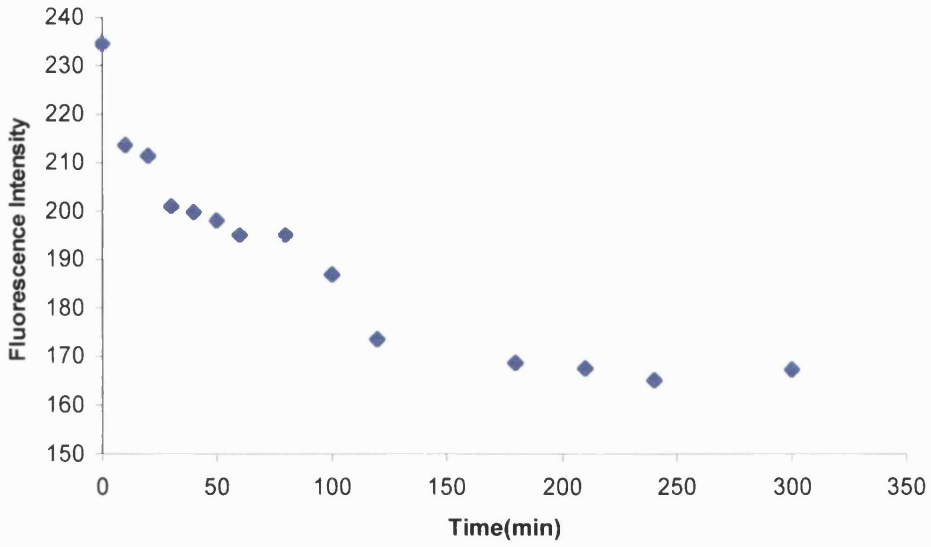

(c)

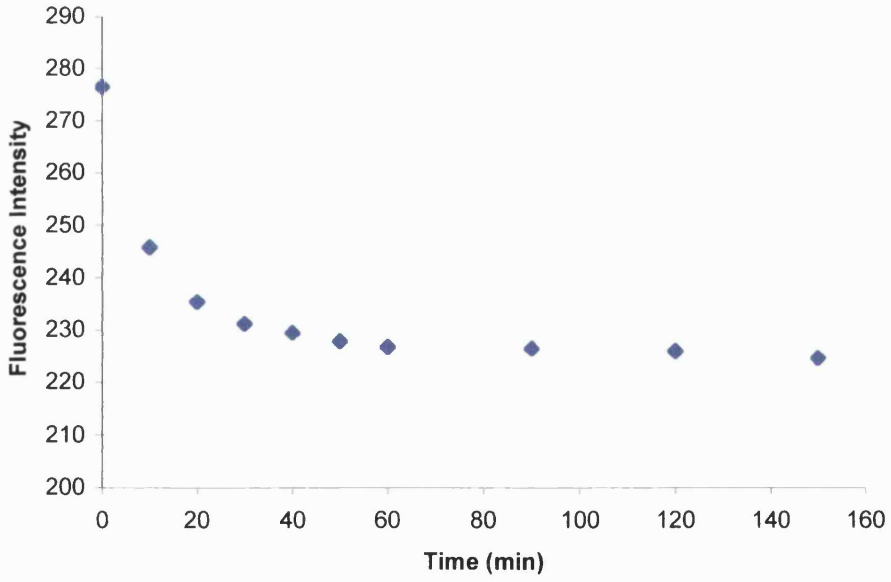

Figure 2.3: Fluorescence intensity measured as a function of time to establish the time required to attain equilibrium. Enzyme incubated in (a) 0.8M, (b) 4M and (c) 6M GdnHCl.

The data show that at the low and high GdnHCl concentration (0.8 and 6M), equilibrium was reached within the first thirty minutes whereas close to the transition region (4M GdnHCl) equilibrium was only reached after about 120 minutes. Protein solutions were therefore incubated overnight for fluorescence studies and for one hour for enzyme activity measurements.

Reversibility studies

It is essential for the accuracy of ΔG calculations that the unfolding of the enzyme is reversible. To test the reversibility of unfolding, protein incubated in 0.8, 2.4, 3.5 and 6M GdnHCl were allowed to reach equilibrium (overnight for fluorescence studies and one hour for enzyme activity measurements). The protein solution was then diluted in buffer giving a 1:20 ratio of protein solution to buffer, and left for an hour for refolding to occur. The fluorescence and enzyme activity were measured before and after dilution. In fluorescence measurements, the protein concentration before and after dilution was 50 and 2.5μg/ml, respectively. The protein concentration in the enzyme assay before and after dilution was 5 and 2.5μg/ml, respectively. The folding and refolding of the enzyme were carried out at 50°C.

Table 2.1: Determination of the reversibility of unfolding of *P. furiosus* citrate synthase. Enzyme activity and fluorescence measurements of protein solutions incubated in various GdnHCl concentrations (a) before and (b) after dilution.

(a)

[GdnHCl] (M)	Enzyme activity (μmol/min)	Fluorescence intensity
0	0.02	788.3
0.8	0.0254	750.9
2.4	0.0421	813.4
3.5	0.0249	549.4
6	0.0118	450.2

(b)

[GdnHCl] (M)	Enzyme activity (μmol/min)	% Recovery (from Enzyme activity)	Fluorescence intensity	% Recovery (from Fluorescence intensity)
0	0.0086	100	490.9	100
0.8	0.0087	100	453.5	92
2.4	0.0122	142	461.8	94
3.5	0.0131	152	315.4	64
6	0.0088	100	344.9	70

The emission scans were also recorded to determine whether the enzyme had unfolded/refolded. Emission scans obtained at the different GdnHCl concentrations show the conformational state of the enzyme.

(a)

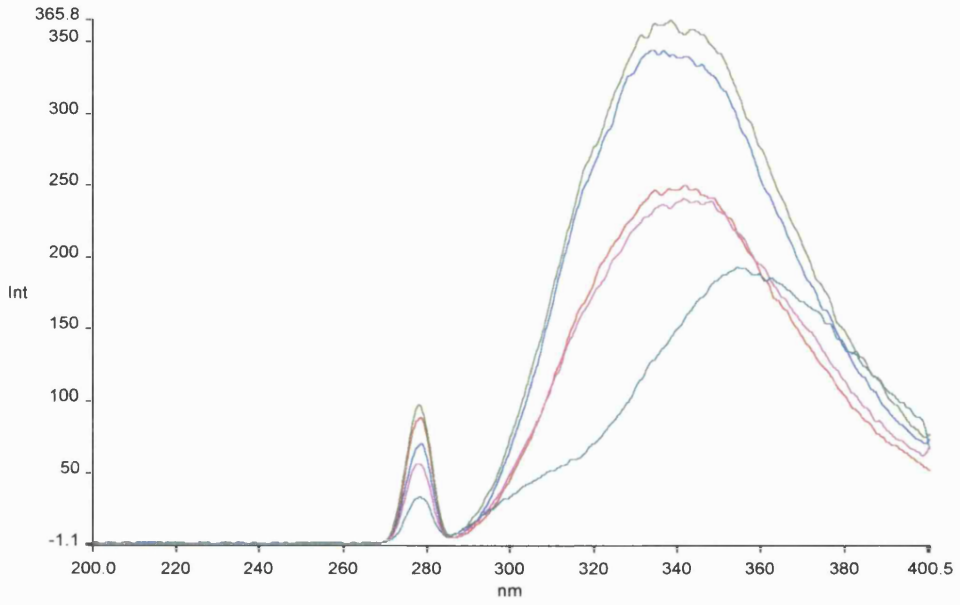

(b)

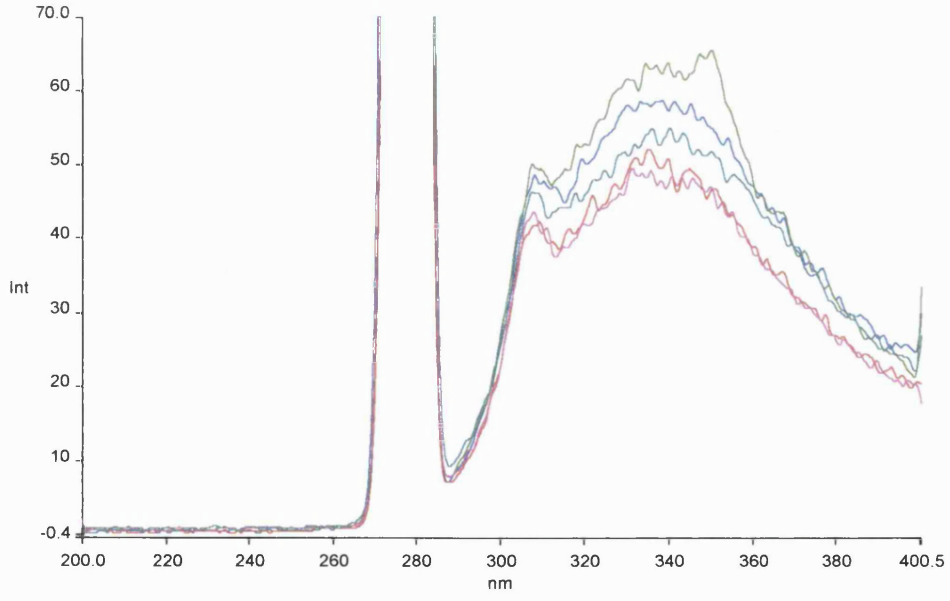

Figure 2.4: Intrinsic fluorescence emission spectra of folded and unfolded *P. furiosus* citrate synthase with excitation at 278nm. (a) PfCS was incubated in phosphate buffer (--), 0.8M (--), 2.4M (--), 3.5M (--) and 6M (--) GdnHCl. (b) The protein solutions were diluted in phosphate buffer and scans repeated. The initial peak represents the Rayleigh peak of water.

The emission spectra obtained for PfCS are all similar up until 6M GdnHCl, indicating that the enzyme is fully folded until this point. At 6M GdnHCl, there is a reduction in fluorescence intensity and a shift in fluorescence emission.

The fluorescence spectra obtained after the dilution of the enzyme in buffer show that all scans are similar although there is a slight difference in the fluorescence intensity. The majority of the refolding of the enzyme occurs within one hour of its dilution in buffer, but when incubated at 3.5M and 6M GdnHCl, the enzyme does not seem to recover its native structure fully.

The enzyme activity of the enzyme increased when incubated in GdnHCl up to two-fold. This activation of the enzyme is still present after the dilution of enzyme.

The overall process is, therefore, judged to be reversible by the complete recovery of enzymic activity and 70% recovery of tertiary structure within one hour of the dilution of the enzyme.

3. CHAPTER 3

EQUILIBRIUM UNFOLDING AND MEASUREMENT OF THE CONFORMATIONAL STABILITY OF CITRATE SYNTHASE FROM *PYROCOCCUS FURIOSUS*

3.1. Introduction

Citrate synthase from *Pyrococcus furiosus* has been particularly well studied with both amino acid sequence and X-ray structure determined (Russell *et al*, 1997). The thermal stability of *P. furiosus* citrate synthase has been characterised in detail using thermal denaturation studies (Arnott *et al*, 2000) and the observed properties have been compared with those of the analogous thermophilic, mesophilic and psychrophilic enzymes.

For this present study, the task was to characterise comprehensively the stability of *P. furiosus* citrate synthase, taking into account the knowledge gathered about this enzyme during the last few years. This represents a contribution to the investigation of the features responsible for enhancing the thermostability of (hyper)thermophilic proteins. Only a few studies have been reported in which thermostable proteins have been characterised thermodynamically (McCary *et al*, 1996, Pfeil *et al*, 1997, Backmann *et al*, 1998). In the present case, the citrate synthase from *P. furiosus* is of special interest as it is both thermostable and oligomeric.

In this chapter, the denaturant-induced unfolding of *P. furiosus* citrate synthase was monitored at equilibrium using enzyme activity and fluorescence spectrometry, and thermal unfolding of the enzyme was characterised using differential scanning microcalorimetry (DSC).

The term protein stability has been used to describe different phenomena that are generally characterised by the ability of a protein to maintain its native structure and normal function in a certain range of conditions and/or over a period of time (Backmann *et al*, 1998). The stability is determined by various interrelated physical and chemical properties of the protein including: (i) the free energy difference between the folded and the unfolded states (the thermodynamic stability), (ii) the unfolding kinetics (kinetic stability) and (iii) the tendency of the unfolded state(s) to aggregate. To study the thermodynamic stability of a protein, one has to reduce the number of processes affecting the sample. Experimental conditions have to be created under which it is possible to neglect all reactions except the equilibrium between the folded and the unfolded states. In the case of an irreversibly unfolded state, it is only possible to characterise the parameters and features of the irreversible loss of the protein structure and function.

In this study, it was intended to determine the mechanism via which denaturation occurs in *P. furiosus* citrate synthase and to obtain quantitative data on the stability of the enzyme using denaturant unfolding and calorimetry to provide reliable overall thermodynamic parameters. We know from previous thermal denaturation studies that the thermal unfolding of the enzyme is often irreversible. In addition to the irreversibility of thermally-induced denaturation of the enzyme, the analysis of unfolding data is complicated by the fact that the native protein is a dimer.

When studying the stability of a protein, an important issue is the determination of the model of unfolding. The evaluation of the thermodynamic parameters for unfolding of a protein is dependent on the model used and the model provides the context for drawing molecular interpretations (Eftink & Ionescu, 1997). The Occam's Razor approach is to assume a two-state transition between the native or folded state and the denatured or unfolded state with negligible population of any

equilibrium intermediate. This is because for small monomeric proteins, unfolding can often be reversible and can appear to be a two-state model.

P. furiosus citrate synthase is a homodimer. The assumption of a two-state unfolding model may not apply because intra- and inter-subunit interactions would make distinct contributions to the overall conformational stability. A conceptual problem is how to consider the intermediate and the unfolded states and how to relate the observed signal to these states.

Tests have been designed to determine the validity of the model chosen for the unfolding transition of a protein. One test is to determine whether the enthalpy change, ΔH, is constant throughout a transition (indicative of a two-state process) or goes through a maximum near the apparent midpoint of the transition, which indicates a multi-state process. The familiar method used to obtain the enthalpy change from a thermal unfolding curve is with the van't Hoff equation. The van't Hoff equation is an indirect determination of the enthalpy of unfolding (ΔH_{vH}). It is a linear equation relating the equilibrium constant, K, to temperature:

$$\mathbf{d(\ln K) / d(1/T) = -\Delta H_{vH} / R}$$

where **K** is the equilibrium constant, **T** is the temperature and **R** is the gas constant. Thus, ΔH_{vH} can be calculated.

ΔH can also be determined by differential scanning calorimetry (ΔH_{cal}). The analysis of thermal melting curves represents an important approach for evaluating protein stability (John & Weeks, 2000). The shape of a denaturation curve is determined by two physical properties, the melting temperature (T_m) and the transition enthalpy (ΔH_{vH}). T_m determines the transition midpoint and ΔH_{vH} is inversely proportional to

the width of the transition. The enthalpy (ΔH_{cal}) is a measure of the total heat involved in the unfolding process.

Another test of the two-state model is to compare the ΔH_{vH} with ΔH_{cal}, determined for the same process. This is the best evidence that thermal unfolding follows a two-state mechanism.

1. If $\Delta H_{vH} = \Delta H_{cal}$ then the unfolding transition can be considered to be well approximated by a two state process.
2. If $\Delta H_{vH} < \Delta H_{cal}$ (or vice versa) then most likely there is an intermediate (i.e. a multi-state process).

A third test, which is often used and was used in this study, is to monitor the unfolding of the protein by two or more independent observable quantities. If such different data sets do not provide identical unfolding patterns, this is an indication that the process is multi-state. Identical unfolding curves are normally an indication of a two-state transition, although this is not true in all cases. It may mean that the intermediate states cannot be observed by the methods used to study unfolding. For a three-state transition to be determinable, there must be some asymmetry in the thermodynamic parameters and/or signal changes for the steps. For the data to reveal the need for a three-state model (i.e., a two-state model is inadequate) the amplitude of the signal corresponding to the intermediate state must be higher or lower than that of both N and U states, and the maximum population of the intermediate state must be sufficiently high (Eftink & Ionescu, 1997).

The ability to distinguish between these models rests not only on the population of the intermediate but also on the signal being monitored. For example, for a three-state unfolding process, one might see a biphasic denaturation curve or non-

superimposable transitions when different methods are used to observe the unfolding.

The aim of this work was to determine the mechanism of unfolding of *P. furiosus* citrate synthase and to calculate thermodynamic parameters associated with this process. Although temperature is a convenient method with which to bring about the unfolding of a protein, many proteins do not show reversibility with respect to thermal unfolding, due largely to the aggregation of the unfolded state. Consequently, many studies of protein unfolding employ chemical denaturants to induce unfolding.

Denaturant-induced unfolding is a technique regularly used to characterise the energetics and mechanisms of conformational changes of proteins. It is the method of choice as in most cases it is reversible whereas thermal unfolding is not, and the equilibrium thermodynamic analysis of the denaturant-induced unfolding curve allows us to determine the number of intermediate states in the unfolding process. These agents provide ideal ways to gain insight into the stability of proteins. An obvious issue is whether there is agreement about the methods used to describe the unfolding reactions and whether all the unfolding processes (guanidine, urea, temperature) proceed via the same or similar mechanisms. For urea- or guanidine-induced unfolding, there has been a good deal of discussion regarding the appropriate relationships.

The thermodynamic understanding of stability requires measurement of the **Gibbs free energy of unfolding (ΔG)** of a protein.

$$\Delta G = -RT \ln K,$$

where **R** is the gas constant (8.314 joules mol^{-1} K^{-1}), **T** is the absolute temperature and **K** is the equilibrium constant of unfolding. ΔG measures the difference in energy between the folded state and the unfolded state and it represents how much more stable the native conformation of the protein is over the denatured form. Thermodynamic parameters are usually estimated from measurements of unfolding by fluorescence, CD or DSC.

For the purpose of introducing the methods used to determine the thermodynamic parameters of unfolding, a two-state folding mechanism will be assumed here i.e. the presence of only the native and denatured states at equilibrium. The denaturant or heat-induced unfolding transition of a protein as monitored by, for example, fluorescence will generate a curve as shown below.

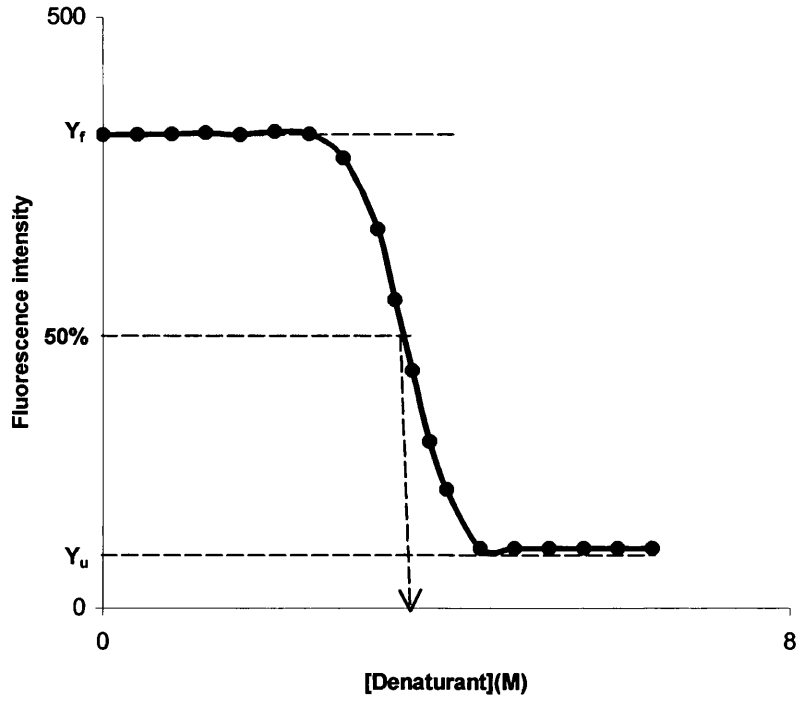

Figure 3.1: An example of denaturant-induced unfolding transitions of a protein monitored using a spectroscopic method (e.g. fluorescence spectroscopy).

For any point shown in **Figure 3.1**, only the folded and unfolded states are present at significant concentrations and $f_F + f_U = 1$, where f_F and f_U represent the fraction of protein present in the folded and unfolded states, respectively. The observed value of y at any point will be

$$y = y_F f_F + y_U f_U$$

where y_F and y_U represent the values of y (in this case fluorescence intensity) characteristic of the folded and unfolded states, respectively, under the conditions where y is being measured. Combining both equations gives:

$$f_U = (y_F - y)/(y_F - y_U)$$

The equilibrium constant, K and the free energy change, ΔG, can be calculated using

$$K = f_U/f_F = f_U/(1 - f_U)$$

and

$$K = (y_F - y)/(y - y_U)$$

Free energy change, ΔG is defined as :

$$\Delta G = -RT \ln K$$

Therefore

$$\Delta G = -RT \ln [(y_F - y)/(y - y_U)]$$

Values of y_F and y_U can be obtained by extrapolating from the pre- and post-transiton baselines of the unfolding curves using a least-squares analysis as shown in **Figure 3.9**. The process involves determining K and hence ΔG at a series of denaturant concentrations. ΔG_w is then calculated using one of the equations shown in **Table 3.1**. The values of K can be measured most accurately near the midpoint of the unfolding curve and ΔG values are, therefore, normally determined around the midpoint of the unfolding transition. The free energy of unfolding in the absence of denaturant and at ambient temperature (ΔG_w) can then be determined through the analysis of the calculated ΔG values using one of a number of relationships used to

describe the unfolding transitions in proteins, examples of which are shown in Table 3.1.

For thermal unfolding, a form of the Gibbs-Helmholtz equation is well established for the temperature dependence of the standard free energy change associated with a two-state transition.

Table 3.1: Relationships that have been used to describe the unfolding transitions in proteins assuming a two-state model. Adapted from Eftink & Ionescu, 1997.

Linear extrapolation model (LEM)	$\Delta G(D) = \Delta G_w - m[\text{Denaturant}]$ Where ΔGw is the free energy change in the absence of denaturant
Denaturant binding model	$\Delta G(D) = \Delta Gw + \Delta n.R.T.\ln (1+ K.\ a_d)$ where a_d is the activity at [Denaturant] Δn is the difference in the number of denaturant binding sites upon unfolding K is the average (or equivalent) association constant for D to both N and U states i.e. the affinity of the protein for the denaturant.

For denaturant-induced unfolding, either of the two models shown is normally used. In the denaturant binding model (Johnson & Fersht, 1995), it is assumed that unfolding results as a consequence of there being a greater number of identical, non-interacting binding sites for the denaturant molecules on the unfolded state than on the native state. Therefore, at a high enough concentration of denaturant, the

free energy difference between the native and the denatured states is shifted so that the unfolded state is more stable.

The linear extrapolation method (LEM) is the simplest method for estimating ΔG_w and is, therefore, the most frequently used model. In this model, the transition region is characterised by two parameters, *m*, which measures the steepness of the transition region and hence the cooperativity of the unfolding reaction, and ΔG_w which is the free energy change for the unfolding transition in the absence of denaturant. In the transition region of a denaturation curve, there is a linear dependence of ΔG on the concentration of denaturant and the LEM assumes that this dependence extends to zero denaturant concentration. Despite the evidence for denaturant binding and a non-linear dependence of ΔG_w on denaturant concentration, the LEM is still popular due no doubt to its simplicity and to the fact that the deviations from linearity are small.

In this work, equilibrium unfolding of *Pyrococcus furiosus* citrate synthase as a function of guanidine hydrochloride concentration was monitored by fluorescence spectroscopy and enzyme activity; the equilibrium intermediate was determined by analytical centrifugation. Loss of activity as a result of GdnHCl denaturation was therefore compared with the loss of the tertiary structure of the protein. The urea- and heat-induced unfolding of the enzyme was also monitored to determine whether the unfolding processes of these methods are comparable.

Analytical centrifugation is one of the most important tools in the characterisation of biological molecules. It provides two complementary views of solution behaviour. It can be divided into sedimentation velocity and sedimentation equilibrium. Sedimentation velocity provides information about the shape and conformation of a protein as well as the interaction between macromolecules whereas sedimentation

equilibrium provides information about the solution molar mass and stoichiometry of a molecule (Laue, 2001). Analytical centrifugation is an absolute method and is therefore the only method for accurately determining the native molecular weight of a protein. The obtained molecular weight is normally within 5% of the calculated value based on the protein sequence.

In this study, the oligomeric status and conformation of *P. furiosus* citrate synthase were determined in the presence and absence of GdnHCl. In each denaturant concentration, molecular weight (M_r) values and sedimentation coefficients (s) were determined by sedimentaion equilibrium and sedimentaion velocity centrifugation, respectively. Combining these values within the Svedberg equation:

$$M = RTs / D(1 - \bar{v}\rho_0)$$

and using the relationships

$$D = RT / Nf \quad \text{and} \quad f = 6\pi\eta r$$

where **M** is the relative molecular mass of the molecule, **R** is the gas constant, **T** is the temperature, **s** is the sedimentation coefficient, **D** is the diffusion coefficient, $\bar{v}$ is the partial specific volume of the protein, ρ_0 is the solvent density, **N** is Avogadro's number, **f** is the frictional coefficient, η is the viscosity of the solution and **r** is the hydrodynamic or Stokes radius of the macromolecule.

The Stokes radii of the protein in the respective conditions were calculated.

3.2. Methods and Results

3.2.1. Isothermal guanidine-induced unfolding of *P. furiosus* citrate synthase

Three stock solutions were prepared: a denaturant solution as described in **Appendix I**, a protein solution and a buffer solution. The solutions on which measurements were made were prepared volumetrically with an electronic Biocontrol Finnpipette. These solutions were allowed to equilibrate at the chosen temperature for 1 hour (enzyme activity) and overnight (fluorescence). The different incubation times were used depending on the attainment of equilibrium as determined by the various methods as described in the previous chapter.

Protein was incubated in different concentrations of GdnHCl (0-6M). A total of 36 solutions were prepared for fluorescence measurements and 23 solutions for enzyme activity measurements. A protein concentration of 10μg/ml was used for fluorescence and enzyme activity measurements. The fluorescence measurements were done on a Perkin Elmer FI 50B spectrofluorimeter in a 1cm water-jacketed cell. The excitation and emission wavelengths were fixed at 278 and 340nm, respectively, with slit widths of 5nm for both monochromators. Each measurement was a single reading with an integration time of 20s. The cuvette was left in the spectrofluorimeter and not rinsed between samples. This improves the quality of the measurements, and the error introduced by residual traces of the previous solution is negligible. The pH of the solutions in the transition region was measured after fluorescence with pH sticks. This is to ensure that no shift of pH had occurred at equilibrium. The unfolding Gibbs free energy change calculated by linear extrapolation from high GdnHCl data has been shown to depend very weakly on pH (Pace *et al*, 1990). Enzyme activity measurements were carried out in a Perkin Elmer Lambda 11 spectrophotometer. The DTNB/412nm CS assay was used to determine enzyme activity at varying denaturant concentrations.

Figure 3.2 shows an example of the unfolding curve as monitored by fluorescence.

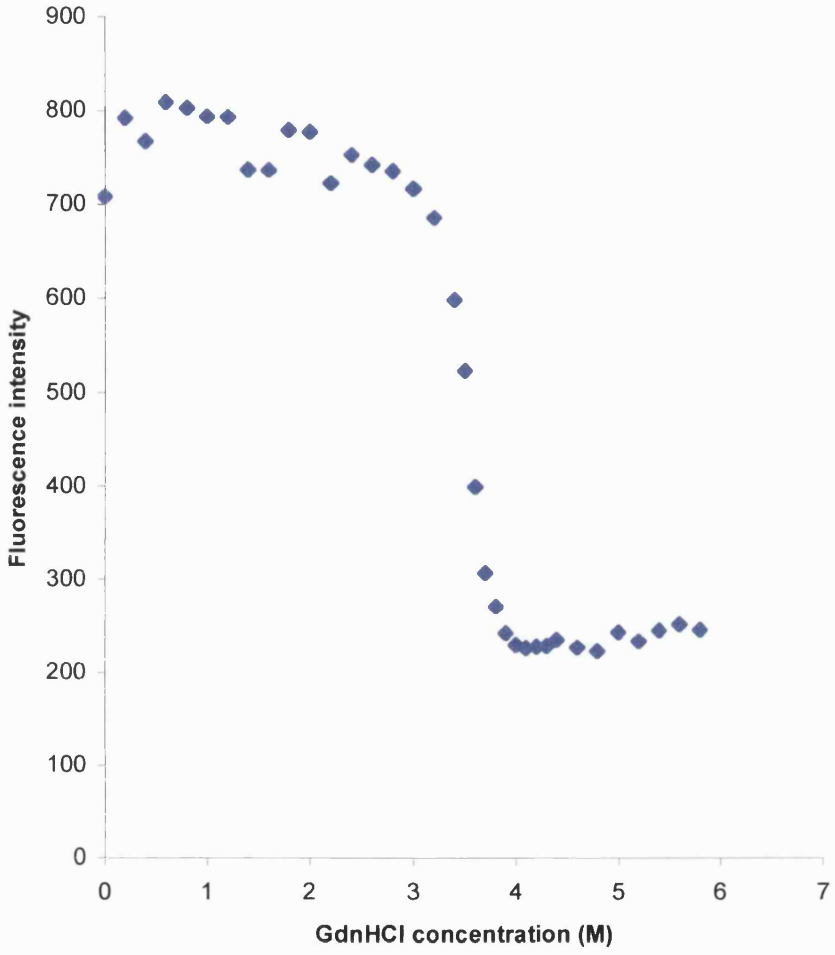

Figure 3.2: GdnHCl-induced unfolding transition of *P. furiosus* citrate synthase as monitored by fluorescence intensity at 340nm.

The single-transition unfolding curve as shown by the fluorescence data is consistent with the enzyme unfolding via a two-state mechanism. It is worth noting that a monophasic curve is also obtained when the GdnHCl-induced unfolding of the enzyme is monitored by circular dichroism (**Appendix V**). However, a single-transition unfolding curve does not prove that the unfolding is a two-state mechanism and further insight was gained by monitoring the loss of enzyme activity.

The enzyme activity that remains following incubation of the protein in denaturant is assumed to be directly proportional to the fraction of enzyme present in the native state at equilibrium i.e. a loss of activity represents a loss of the native conformation of the protein.

A typical curve obtained for the GdnHCl-induced unfolding of *P. furiosus* citrate synthase as monitored by enzyme activity is shown in **Figure 3.3**.

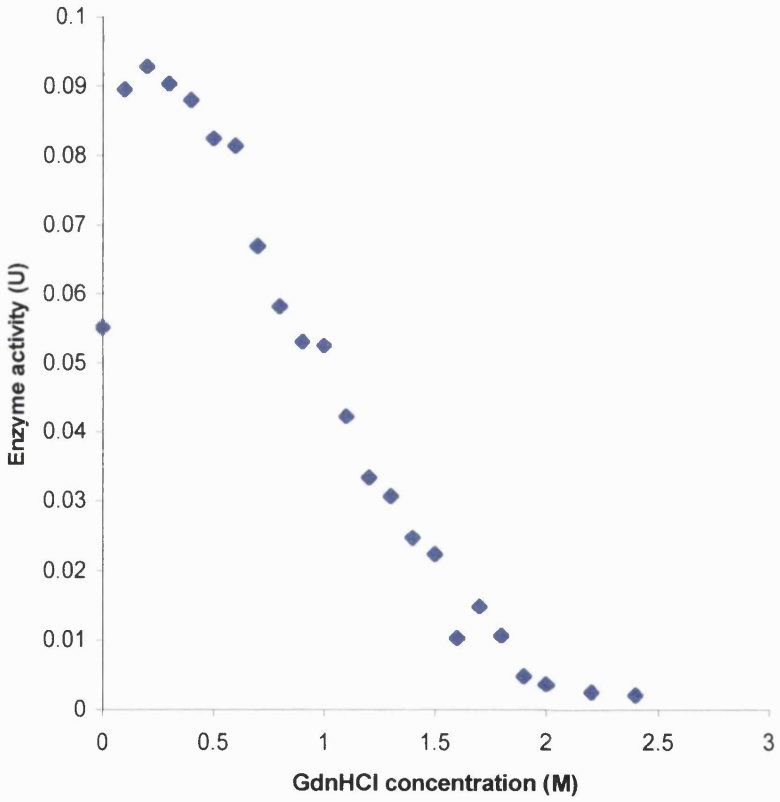

Figure 3.3: GdnHCl-induced unfolding of *P.furiosus* citrate synthase as monitored by loss of activity.

Figure 3.3 shows that the enzyme activity is completely lost at around 2.4M GdnHCl. At this concentration, however, there is no change in the fluorescence measured. A change in fluorescence intensity is not observed until around 3.1M GdnHCl. There is

also an observed increase in the enzyme activity at low concentrations of GdnHCl (up to 0.5M). This increase in activity does not coincide with a change in fluorescence.

Figures 3.2 and **3.3** have been combined in Figure 3.4 to show the comparison.

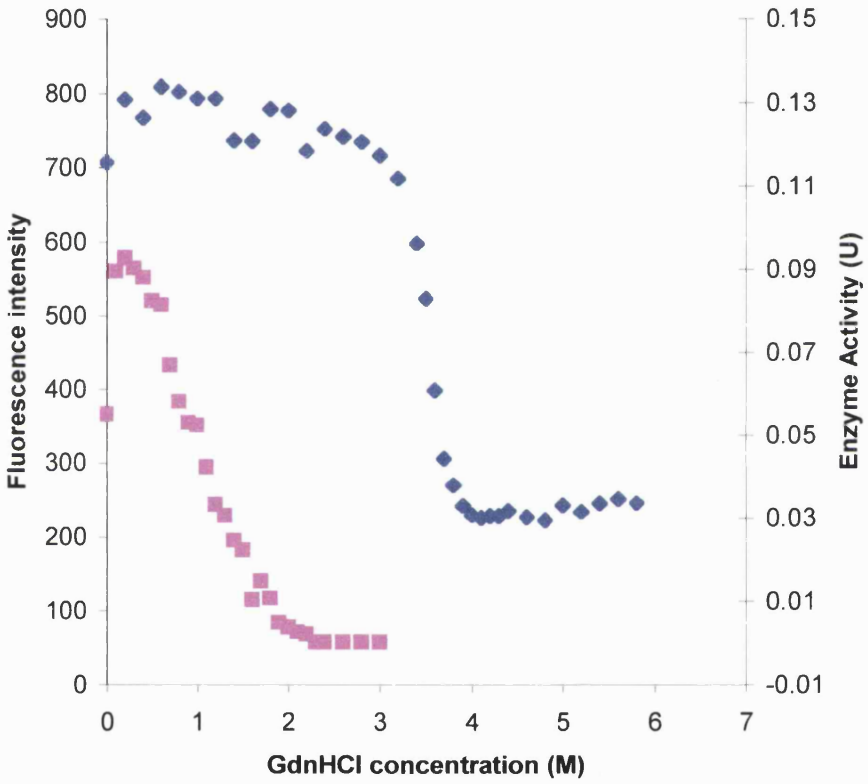

Figure 3.4: GdnHCl-induced unfolding of *P. furiosus* citrate synthase at 50°C as monitored by fluorescence and enzyme activity.

PfCS is a dimer with two identical catalytic centres that are shared between the two subunits. It is therefore only active in the dimeric state. The loss of activity at low GdnHCl concentration without a change in the fluorescence signal suggested a loss

of the dimer integrity or a small conformational change at the active site without any significant change in the global conformation of the monomers. The unfolding intermediate (2.4-3.1M GdnHCl) is enzymically inactive but retains the spectral properties of a fully folded protein and therefore it was of interest to determine its oligomeric nature.

Analytical centrifugation was chosen to determine the M_r and conformation of PfCS in zero and 2.4 M GdnHCl.

3.2.2. Analytical centrifugation of *P. furiosus* citrate synthase

Centrifugation was performed on a Beckman Optima XL-A analytical centrifuge by Dr. Olwyn Byron and Gordon Campbell at the University of Glasgow.

3.2.2.1. Sedimentation equilibrium

PfCS stock solution was diluted in buffer to give nine samples for an equilibrium run. Four samples were diluted in 50mM Sodium phosphate, 2mM EDTA, pH 7 buffer and the remaining five samples were diluted 50mM Sodium phosphate, 2mM EDTA, pH 7 buffer containing 2.4M GdnHCl. The samples were run at speeds of 18,000 rpm and 24,000 rpm at 4°C, and the protein concentration in the centrifuge cell was monitored by absorbance at 280nm. An example of the data obtained is shown in **Figure 3.5**.

(a) (b)

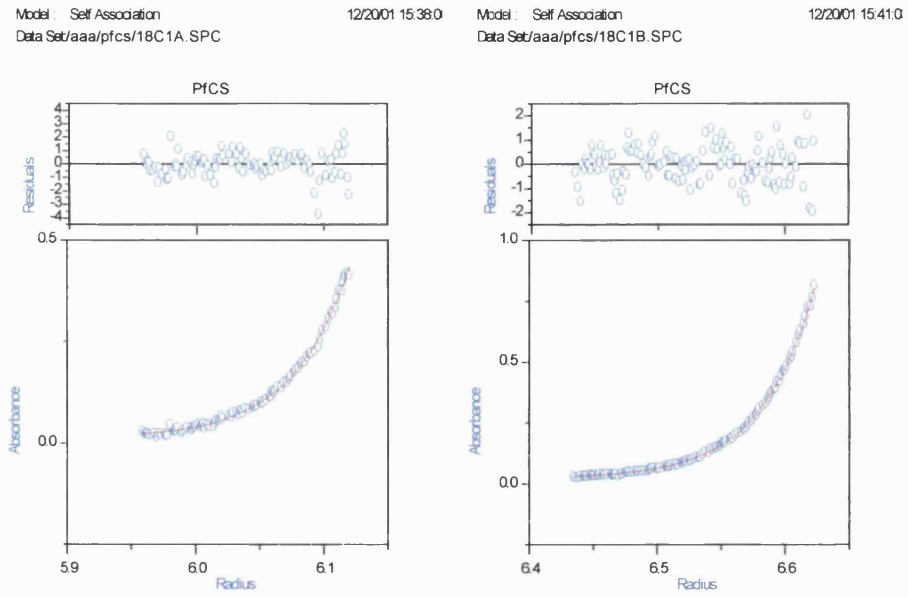

Figure 3.5: The distribution data obtained for (a) 0.16 au of protein and (b) 0.46 au of protein from the equilibrium runs spun at 18 000 and 24 000 rpm, respectively. The data were fitted using a single ideal species model. Residual plots (i.e. the scatter about the line of fit) obtained are shown above and the curve fits are shown at the bottom of each plot. The line of best fit is given in red.

Table 3.2: The molecular weight determination of *P. furiosus* citrate synthase in the presence and absence of GdnHCl.

	Absorbance (A280nm)	Rotor speed (rpm)			
		18 000		24 000	
		$M_{r,app}$ (kDa)	(+/-)	$M_{r,app}$ (kDa)	(+/-)
Phosphate	0.16	90.5	1.9	89.3	2.2
	0.26	87.3	1.0	83.5	1.2
	0.34	84.3	1.6	83.1	2.9
	0.46	86.2	1.2	82.5	1.5
2.4M GdnHCl	0.06	43.2	1.9	42.5	1.4
	0.16	45.0	1.3	45.5	1.1
	0.28	46.4	0.5	45.5	0.4
	0.40	46.2	0.5	44.9	0.5
	0.51	46.2	0.5	46.0	0.7

The data have been plotted into two graphs (**Figure 3.6a & b**), showing the concentration dependence of the molecular weight determined.

(a)

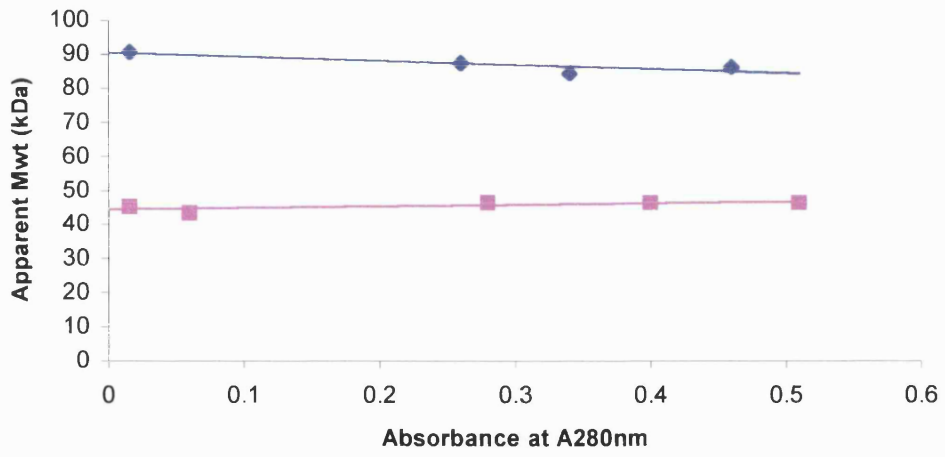

(b)

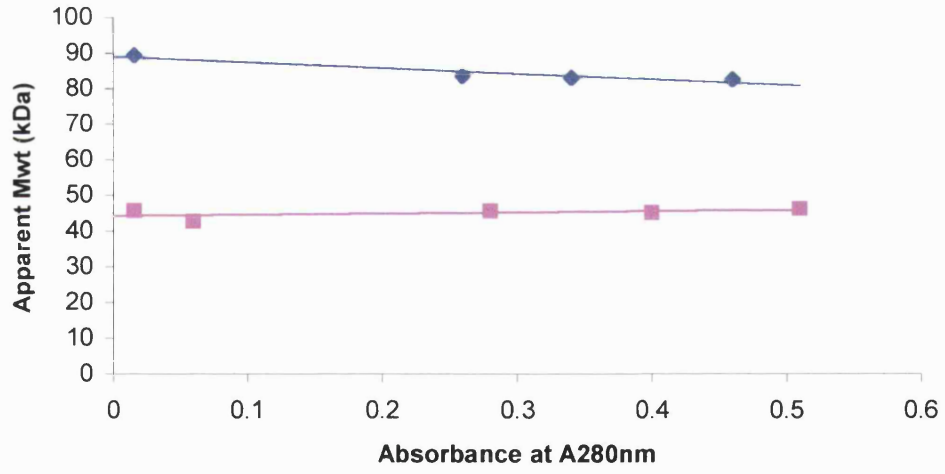

Figure 3.6: Concentration dependence of molecular weight of *P. furiosus* citrate synthase in phosphate buffer (◆) and 2.4M GdnHCl (■). Centrifugation was carried out at a number of protein concentrations and at two different speeds (a) 18 000 rpm and (b) 24 000 rpm.

The molecular weight of each monomer calculated from the available sequence is 43290. From the sedimentation equilibrium experiments, the molecular weight of *P. furiosus* citrate synthase in phosphate buffer is shown to be around 91400 ± 2400 (linear regression) and 85800 ± 1100 (mean). In the presence of 2.4M GdnHCl, the molecular weight of the PfCS is around 43500 ± 600 (linear regression) and 45100 ± 440 (mean). This means that the native structure of the enzyme is a homodimer and in the presence of the 2.4M GdnHCl, the dimer dissociates into two monomers. Sedimentation velocity was then used to determine the conformation of the monomer at 2.4M GdnHCl.

3.2.2.2. Sedimentation velocity

Sedimentation velocity runs were performed to ascertain whether at 2.4M GdnHCl PfCS is a folded monomer.

A sample of PfCS was split into two and dialysed overnight against phosphate buffer and 2.4M GdnHCl. Three concentrations were prepared of each dialysed sample for a sedimentation velocity run (neat, neat/2 and neat/4). The concentration of the original sample was unknown due to initial precipitation. Samples were loaded into the centrifuge cells and left at 4°C until thermal equilibrium had been reached. The rotor was then spun at 50000 rpm and scans were taken every 2.5 minutes for 8.3 hours.

Detailed analyses of scans to determine the sedimentation coefficients are shown in **Appendix II**. The raw data scans from the different runs were imported into the Sedfit program to obtain distribution plots of the sedimenting species. The analysis of the data provides the sedimentation and diffusion coefficients, and the percentage of each species present. The data are presented in **Table 3.3**.

Table 3.3: Sedimentation coeffiecients (s) and relative amounts of sedimenting species

Buffer	A280nm	Species 1		Species 2		Species 3	
		(S)	(%)	(S)	(%)	(S)	(%)
Phosphate	1.6	1.7	1	3.2	82	4.4	17
	0.8			3.2	91	4.8	9
	0.5	1.6	10	3.3	90		
2.4M GdnHCl	2.5	1.6	84	2.6	16		
	1.5	1.5	100				
	1.3	1.5	70	3.2	30		
	1.1	1.5	70	3.2	30		

Sedimentation coefficients are expressed in Svedberg units (1S = 10^{-13} seconds)

Sedimentation coefficients are normally expressed at a standard temperature of 20°C, with water as solvent. The sedimentation coefficients obtained were therefore converted to $s_{20,w}$ using the the equation of $s_{20,w} = s_{obs} \times F$, where F is a factor common for each buffer condition. The value of F for phosphate is 1.6274 and for GdnHCl is 2.1903. **Table 3.4** gives the corrected values.

Table 3.4: Sedimentation coefficients (s) converted to $s_{20,w}$ vlaues and relative amounts of sedimenting species.

Buffer	A280nm	Species 1		Species 2		Species 3	
		(S)	(%)	(S)	(%)	(S)	(%)
Phosphate	1.6	2.8	1	5.2	82	7.2	17
	0.8			5.2	91	7.8	9
	0.5	2.6	10	5.4	90		
2.4M GdnHCl	2.5	3.5	84	5.7	16		
	1.5	3.3	100				
	1.3	3.3	70	7.0	30		
	1.1	3.3	70	7.0	30		

The Stokes' radii were calculated from the experimental data obtained. The $s_{20,w}$ of the predominant species for each buffer condition was used in these calculations. The Stokes' radii were also predicted using the crystallographic co-ordinates for PfCS. The radii calculated are shown in **Table 3.5**.

Table 3.5: Calculated Stokes radii of *P. furiosus* citrate synthase. The radii were calculated using two different molecular weights - one obtained by linear regression ($Radius_{LR}$) and the other by taking the mean of the molecular weights obtained ($Radius_{Mean}$). Stokes radii also predicted from crystallographic data.

	$Radius_{LR}$ (Å)	$Radius_{Mean}$ (Å)	Predicted radii (Å)
Phosphate buffer (dimer)	39	37	36
2.4M GdnHCl (monomer)	29.5	30.6	28 (- termini) 31(+ termini)

A comparison of the experimental and predicted Stokes radii suggests that in phosphate buffer, *P. furiosus* citrate synthase is a fully folded dimer while in 2.4M GdnHCl, the enzyme exists as a folded monomer with perhaps the C-terminal arm not completely wrapped around the monomer.

The data obtained from the analytical centrifugation, combined with the fluorescence and enzyme activity results suggest that *P. furiosus* citrate synthase unfolds via a three-state mechanism:

$$N_2 \rightleftharpoons 2N \rightleftharpoons 2U.$$

For a three state model, one expects biphasic unfolding transitions and/or noncoincident unfolding transitions if the method used to study unfolding can distinguish between the different conformational states. The fluorescence and enzyme activity data show non-coincident unfolding curves. Protein concentration dependent behaviour can be used to test the three-state model. In such a model, the first transition is bimolecular, with subunit dissociation giving the monomeric intermediate; therefore, the transition observed for this process should be protein concentration dependent. The second transition, however, is unimolecular and is not expected to be protein concentration dependent.

3.2.3. The effect of protein concentration on the equilibrium unfolding of *P. furiosus* citrate synthase

The effect of protein concentration on the unfolding transitions and the thermodynamic measurements of *P. furiosus* citrate synthase was determined at 5, 8 and 10μg/ml in order to differentiate between unimolecular (concentration-independent) and bimolecular (concentration dependent) steps of the unfolding process. Unfolding was carried out in GdnHCl as described previously, at 40°C. Enzyme activity and fluorescence intensity measurements were made and unfolding curves analysed. **Figure 3.8** shows the plots of the data obtained in this study.

(a)

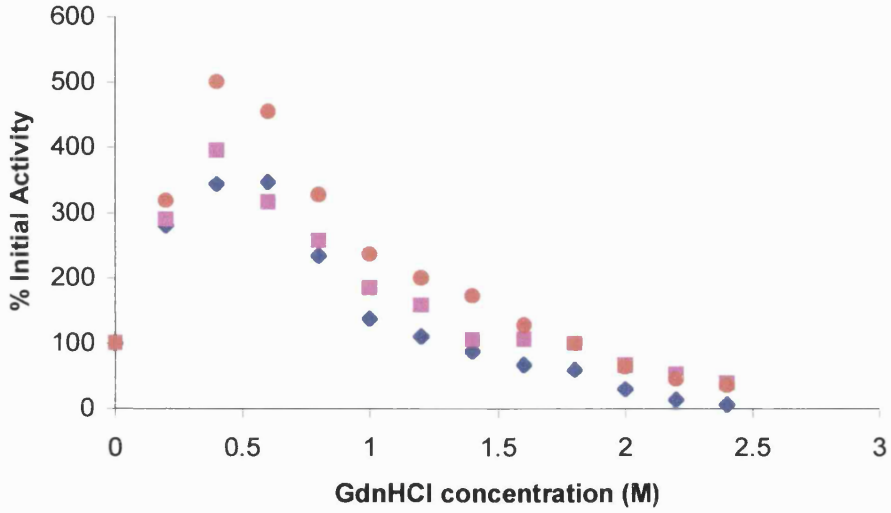

(b)

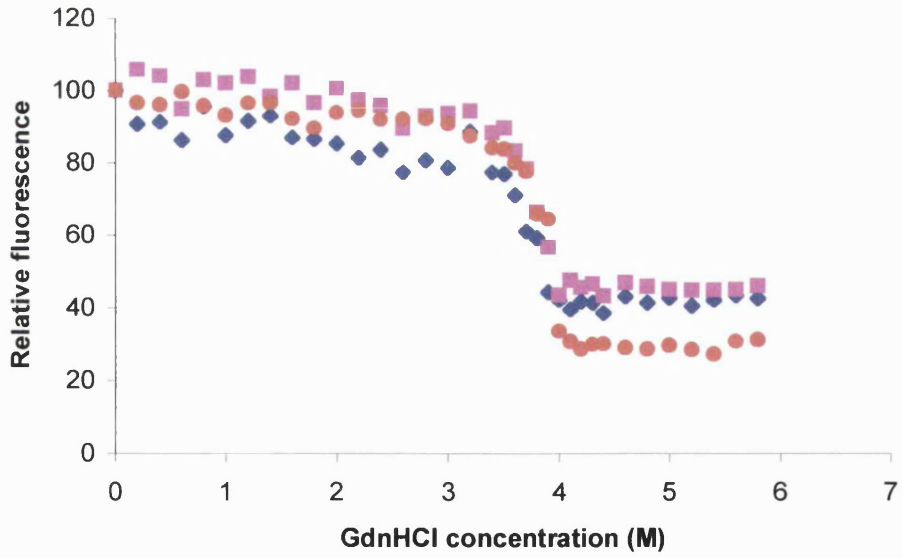

Figure 3.9: GdnHCl-induced unfolding curves of *P. furiosus* citrate synthase at different protein concentrations. The protein concentration dependence of (a) the enzyme activity and (b) the fluorescence intensity unfolding transitions were determined at 5μg/ml (◆), 8μg/ml (■) and 10μg/ml (•).

The enzyme *P. furiosus* citrate synthase is a dimer. For a two-state model of the unfolding of this enzyme, the transition observed should be protein concentration dependent. The unfolding monitored by fluorescence does not seem to be affected by a change in protein concentration. The enzyme activity, however, seems to be affected by the change in protein concentration. At 5μg/ml protein concentration, the enzyme activity is lost (6.6%) at around 2.4M GdnHCl. At this denaturant concentration, the residual activity is around 50% for the 8μg/ml and 10μg/ml protein concentration.

The data from this study suggest an unfolding model involving an initial protein concentration dependent (bimolecular) step followed by a protein concentration independent (unimolecular) step.

The protein concentration dependent data are consistent with the suggestion that dimer dissociation occurs prior to the disruption of the tertiary structure of the protein and that the equilibrium unfolding of *P. furiosus* citrate synthase most likely proceeds via a three-state process of

$$N_2 \rightleftharpoons 2N \rightleftharpoons 2U.$$

3.2.4. Isothermal urea-induced unfolding of *P. furiosus* citrate synthase

It has been seen that the GdnHCl-induced unfolding of *P. furiosus* citrate synthase proceeds via a three–state mechanism. It was therefore of interest to determine whether both GdnHCl- and urea-induced unfolding of *P. furiosus* citrate synthase proceed via the same three-state mechanism.

Three stock solutions were prepared: a urea solution (as described in **Appendix I**), a protein solution and a buffer solution. The solutions on which measurements were made were prepared volumetrically with an electronic Biocontrol Finnpipette. These solutions were allowed to equilibrate at the chosen temperature for 1 hour (enzyme activity) and overnight (fluorescence).

Protein was incubated in different concentrations of urea (0-9.8M). A total of 36 solutions were prepared for fluorescence measurements and 23 solutions for enzyme activity measurements. A protein concentration of 10μg/ml was used for fluorescence and 5 μg/ml for enzyme activity measurements.

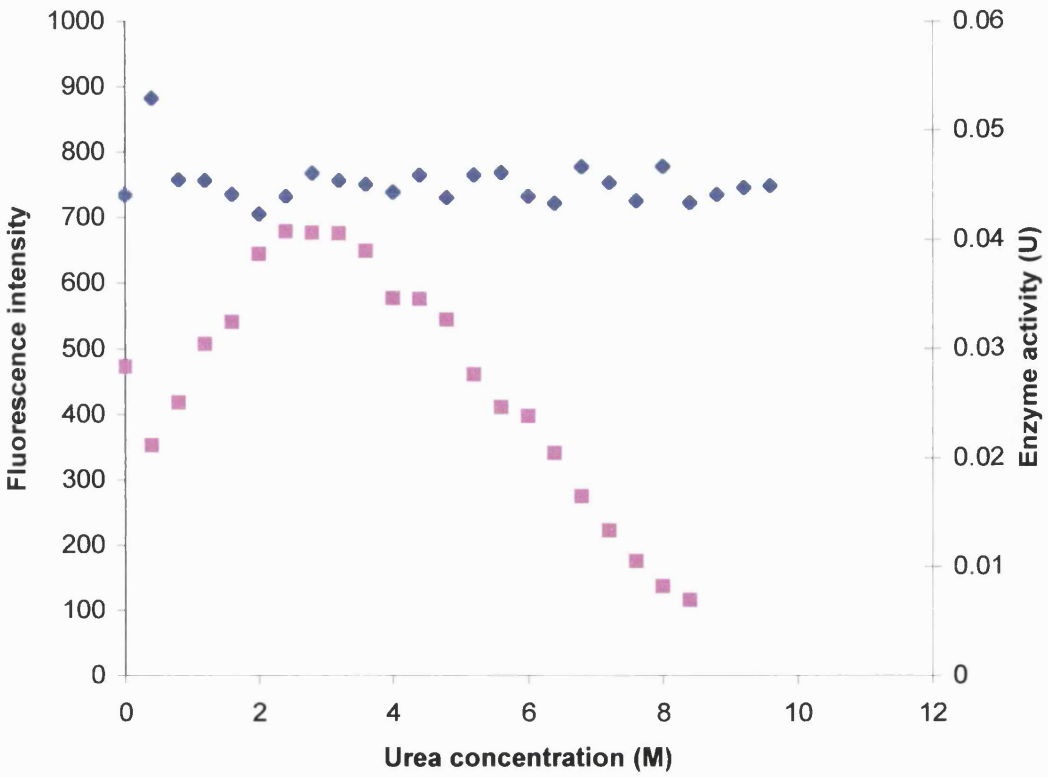

Figure 3.7: Urea-induced unfolding of PfCS at 40°C as followed by fluorescence (◆) and enzyme activity (■).

The data presented here show that the PfCS enzyme remains folded at up to 9.8M urea, as there is no change in fluorescence measured. The activity of the enzyme is almost completely lost at around 8.4M even though there is no change in the fluorescence intensity. The loss of enzyme activity suggests a loss in the dimer integrity. This would suggest a similar mechanism of unfolding to that seen for the GdnHCl-induced unfolding of PfCS, that is, that the dimer first dissociates without unfolding and then unfolds at a higher denaturant concentration. In this case, the highest saturating concentration does not effect the unfolding of the enzyme. Clearly this would need to be confirmed by similar centrifugal analysis, but time did not permit these experiments to be carried out. There is also an activation of the enzyme in low concentrations of urea (up to 3M) as previously seen with GdnHCl. This increase in activity does not coincide with a change in fluorescence.

3.2.5. Thermal unfolding of *P. furiosus* citrate synthase

Differential scanning calorimetry was carried out both at pH 5 and pH 7. At pH 5, 50mM sodium acetate, 2mM EDTA buffer was used. At pH 7, the buffer used was 50mM sodium phosphate, 2mM EDTA. Calorimetric measurements were carried out at a protein concentration of 1.5mg/ml. Protein concentration was determined after dialysis.

The protein sample was dialysed overnight in the appropriate buffer at 4°C with continuous stirring. The ratio of sample to dialysate was 1:1000. Dialysis was carried out using Pierce Slide-A-Lyser dialysis cassettes with 3500 MWCO. The dialysate was then used as a reference solution for the calorimetry experiments. Measurements were carried out with a Microcal MCS apparatus from 15-110°C. A scan rate of 60°C per hour was chosen for the study. An example of the DSC scan obtained for the thermal unfolding of the enzyme at pH 5 is shown in **Figure 3.8**.

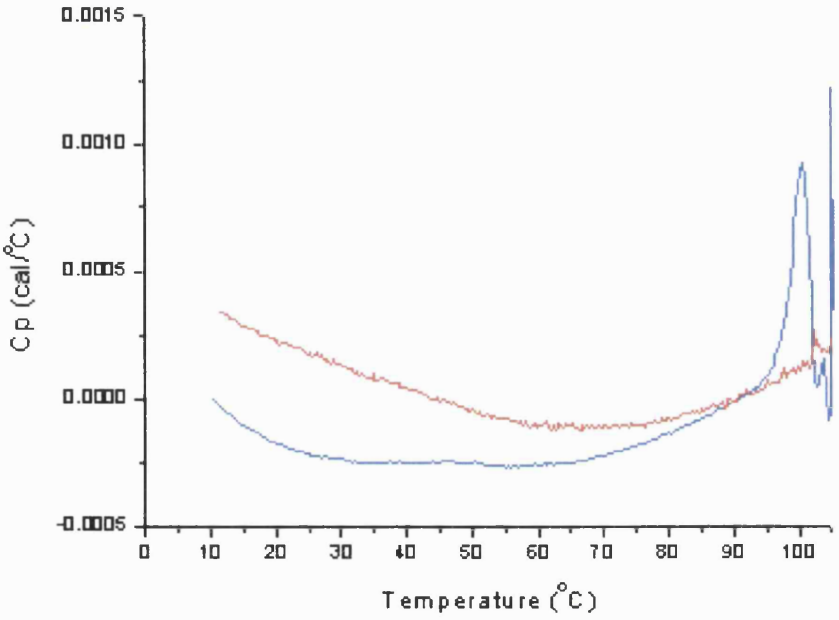

Figure 3.8: Thermal unfolding of *P. furiosus* citrate synthase at pH 5 as monitored by DSC. Protein from the first scan at 110°C was cooled and then rerun. The irreversibility of the unfolding was demonstrated with a second scan shown in red. Scans have not been baseline-corrected as a consistent baseline could not be obtained, due to a instrumental problems.

The DSC scan shows a single peak of excess heat capacity. The temperature at this peak is defined as the melting temperature (T_m) of the protein. No fits of the data were carried out due to the irreversibility of the unfolding of the enzyme and the unavailability of a post-transition baseline. The lack of a post-transitional arm of the unfolding scan was due to noise experienced at high temperatures and aggregation of the protein. For reversible thermal unfolding, the T_m can be obtained from a fit of the DSC data to the model of unfolding and by analysis using the Gibbs-Helmholtz equation. The T_m was, however, determined by inspection of the raw data and was estimated at 100.4°C and 103.2°C at pH 5 and pH 7, respectively.

3.3. Formulation of the Model

The importance of subunit interactions are being investigated with respect to stability and therefore it is important to know the mechanism via which unfolding (thermal or solvent) proceeds. Earlier thermal inactivation studies suggested a loss of conformation at the active site of the enzyme. However, it was not clear whether this was an effect of the dissociation of the dimer or whether this was due to a micro-unfolding at the active site. Therefore, a more extensive study of the denaturation of the protein by guanidine hydrochloride was carried out. This allowed us to understand the process via which denaturation occurs and also to calculate the conformational stability of the enzyme in terms of its Gibbs free energy.

The fluorescence data showed that a two-state model could describe the system. The two-state model is a concerted and bimolecular dissociation/unfolding for which one expects monophasic unfolding curves, superimposable for all spectroscopic methods used to monitor unfolding at fixed denaturant concentration. The transitions observed with this model should also be protein concentration dependent. The other experimental tests, however, led to doubt regarding the two-state model. The unfolding curves obtained with fluorescence spectroscopy and enzyme activity measurements were not super-imposable. There was a loss of activity at 2.4M GdnHCl but this was not accompanied by a change in fluorescence. The next logical model was a three-state model.

For three-state models, biphasic unfolding curves and/or non-coincident unfolding transitions are expected if the methods used can distinguish between the different conformational states. PfCS is a dimer and this led to a necessity to determine the nature of the equilibrium intermediate. The observation was that the intermediate is catalytically inactive and displays a native-like secondary and tertiary structure. The dimer could either dissociate and then unfold as shown in Case 2 or there could be

a slight conformational change in the dimer which then dissociates into two unfolded monomers as in Case 3.

Case 1: $N_2 \rightleftharpoons 2U$

Case 2: $N_2 \rightleftharpoons 2N \rightleftharpoons 2U$

Case 3: $N_2 \rightleftharpoons U_2 \rightleftharpoons 2U$

Two methods were used to determine the nature of the intermediate species of the equilibrium unfolding of PfCS. Analytical centrifugation was carried out to determine the molecular weight and shape of the molecule, and the results suggest that the enzyme is a folded monomer at 2.4M GdnHCl. Protein concentration dependent behaviour can also be used to differentiate between the three-state models i.e. between Cases 2 and 3, in that only the bimolecular step should be protein concentration dependent. If the first transition is bimolecular, subunit dissociation may be occurring and the intermediate is a monomer. If, however, it is the second transition that is protein concentration dependent, then subunit dissociation occurs after the formation of a dimeric intermediate. Protein concentration studies revealed an initial step that was protein concentration dependent and a second step that was protein concentration independent.

Therefore, for the GdnHCl-induced unfolding of *P. furiosus* citrate synthase, dimer dissociation occurs prior to the disruption of the secondary and tertiary structure and the equilibrium unfolding proceeds via a three-state process:

$$\mathbf{N_2 \rightleftharpoons 2N \rightleftharpoons 2U}$$

The aim of this work was to fully characterise the conformational stability of citrate synthase from *P. furiosus* using denaturant-induced unfolding and thermally-induced

unfolding. The enzyme could only be fully unfolded in GdnHCl and with heat; it could not be fully unfolded in urea. Denaturant-induced unfolding is reversible but thermally-induced unfolding of *P. furiosus* is irreversible. Calorimetry has been successfully applied to many small globular monomeric proteins. Although theoretical models have been developed for some irreversible denaturation (Sanchez-Ruiz *et al*, 1988), the calorimetric determination of thermodynamic parameters is full of complications. It is worth discussing under which conditions thermodynamic parameters can be estimated from a DSC scan of an irreversible process.

Strictly the thermodynamic analysis of an unfolding process is only permissible in the case of an equilibrium process. The calorimetric equilibrium criterion is the reproducibility of a DSC scan on the second heating of the same sample. The thermal denaturation of *P. furiosus* citrate synthase was shown to be irreversible. The results of the calorimetric measurements were, therefore, not applied for the determination of thermodynamic parameters. For the reasons mentioned, thermodynamic parameters have only been determined for the GdnHCl-induced unfolding of the enzyme over the temperature range of 20-60°C.

The measured enzyme activity and fluorescence unfolding transitions were fitted to two two-state analytical equations. The enzyme activity data were fitted to an equation of the model:

$$N_2 \rightleftharpoons 2N$$

where **K** the equilibrium constant is described as:

$$K = [U]^2/[N_2] = 2P_t [f_U^2/(1 - f_U)]$$

with P_t being the total protein concentration and f_U the fraction of unfolded protein. ΔG is calculated from $\Delta G = - RT \ln K$.

The fluorescence data were fitted to an equation for the model:

$$\mathbf{N} \quad \rightleftharpoons \quad \mathbf{U}$$

Where K is described as:

$$K = f_U/(1-f_U)$$

The ΔG values were then least-squares fitted to the equation:

$$\Delta G = \Delta G_w + m[D]$$

These equations allow the fitting of the parameters ΔG_w, m, y_F^0, y_U^0, m_F and m_U where, ΔG_w is the extrapolated free energy in the absence of denaturant, **[D]** is the denaturant concentration, m is the slope of the unfolding transition, also known as the extrapolation coefficient of the LEM, m_F is the slope of the pre-transitional baseline of the unfolding curve, m_U is the slope of the post-transitional baseline of the unfolding curve, y_F is the intersection of the extrapolated linear pre-transitional baseline of the unfolding curve with the Y-axis, and y_U is the intersection of the extrapolated linear post-transitional baseline of the unfolding curve with the Y-axis. The fitting functions were obtained using the LEM, a fact that should be considered when one applies these functions and interprets the results.

Two non-linear curve fitting functions incorporating the equations previously described and the pre- and post-transition baseline fits were used in the analyses of the data. The actual fitting functions used in Microcal Origin 6.0 are shown in **Appendix III**. **Figure 3.9** shows the analysis of a typical unfolding curve.

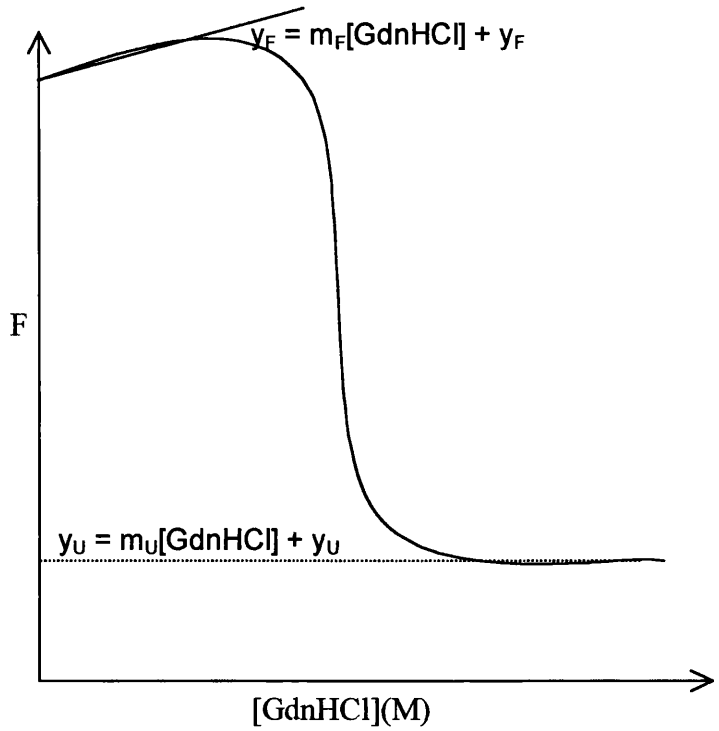

Figure 3.9: Typical GdnHCl-induced unfolding curvefit that can be obtained with either of the proposed models. The linear extrapolations of the pre and post-transitional parts of the curve (broken lines) and the corresponding expressions are shown.

An example of the fitting of fluorescence and enzyme activity data carried out using Microcal Origin 6.0 are shown in Figure 3.10. The figure shows the non-linear fitting of data obtained at 50°C (**Figures 3.2 & 3.3**).

(a)

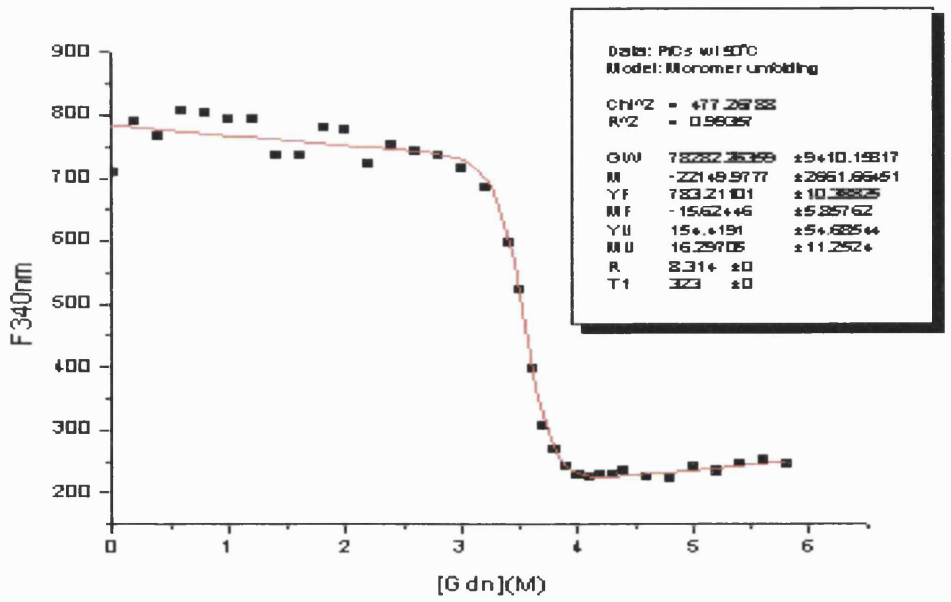

(b)

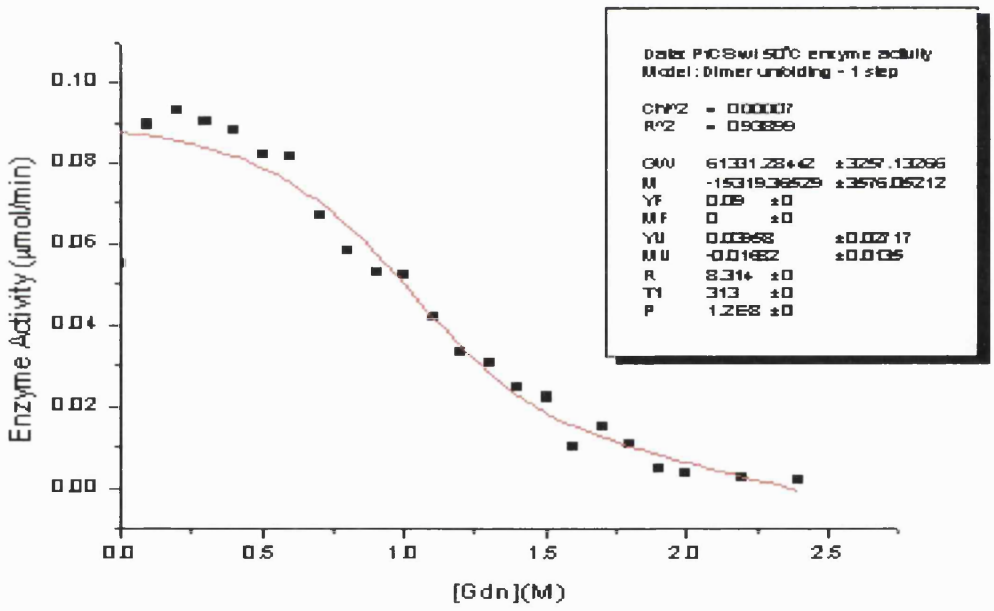

Figure 3.10: Non-linear least-squares analysis of the GdnHCl-induced unfolding of *P. furiosus* citrate synthase at 50°C as monitored by (a) fluorescence and (b) enzyme activity. (a) was fitted to N ⇌ U and (b) was fitted to N_2 ⇌ 2N.

3.4. Calculation of thermodynamic parameters

The effect of temperature on the ΔG values obtained for the GdnHCl-unfolding of *P. furiosus* citrate synthase was determined. This strategy is sometimes used to determine the melting temperature (T_m) of a protein, the temperature at which the equilibrium constant, K = 1 and $\Delta G = 0$.

Thermodynamic parameters obtained for the GdnHCl-induced unfolding of PfCS at 20-60°C are shown in **Table 3.6**. There are no enzyme activity data available at 20°C, as the catalytic activity is too low to record at this temperature.

The midpoint of unfolding, C_m, was determined for the transitions of the unfolding curves. C_m is the denaturant concentration where $f_U = f_F$. Two equations were used to determine these values.

The relationship for monomeric proteins as given by Schellman (1978) is:

$$C_m = -\Delta G_w / m \qquad \text{(i)}$$

And for the dissociation of dimer proteins as described by Neet and Timm (1994):

$$C_m = -\{RT[\ln[\text{protein}] + \Delta G_w\}/m \qquad \text{(ii)}$$

Therefore, C_m for the first transition as monitored by enzyme activity is described by equation (ii) whereas for the second transition monitored by fluorescence the C_m is described by equation (i).

The data (shown in the table) have also been plotted (without the errors) in **Figure 3.11**. The effect of protein concentration on the thermodynamic parameters at 40°C is also shown in **Table 3.7**.

Table 3.6: Thermodynamic parameters obtained for the GdnHCl-induced unfolding of 10μg/ml of *P. furiosus* citrate synthase between 20°C – 60°C. Values obtained from enzyme activity unfolding curves are termed ΔG_1, m_1 and C_{m1} and values from fluorescence unfolding curve analysis are termed ΔG_2, m_2 and C_{m2}.

Temp (°C)	ΔG_{w1} (kJ/mol)	m_1 (kJ/mol/M)	C_{m1} (M)	ΔG_{w2} (kJ/mol)	m_2 (kJ/mol/M)	C_{m2} (M)
20	-	-	-	101 ± 18	26 ± 4	3.97 ± 0.9
30	42 ± 2	7.8 ± 0.6	0.43 ± 0.04	174 ± 35	44 ± 9	4.00 ± 1.1
40	47 ± 7	8.5 ± 1.8	0.92 ± 0.5	118 ± 19	30 ± 5	3.89 ± 0.9
50	61± 4	15.3 ± 3.8	1.33 ± 0.4	78 ± 9	22 ± 3	3.54 ± 0.6
60	55 ± 5	8.2 ±1.7	1.50 ± 0.4	31 ± 4	10 ± 1	3.24 ± 0.6

(a)

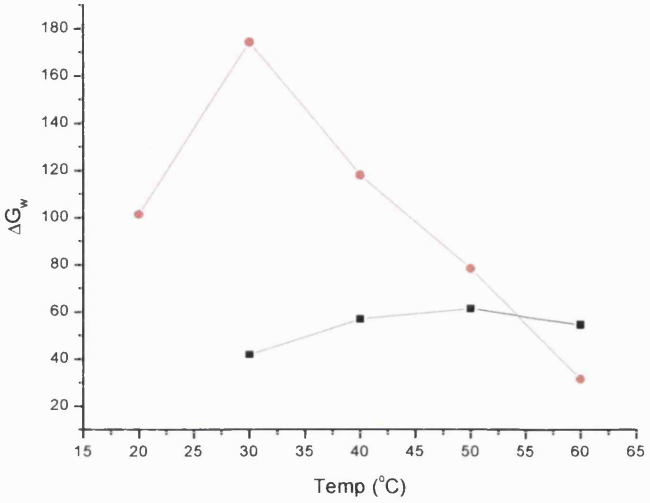

(b)

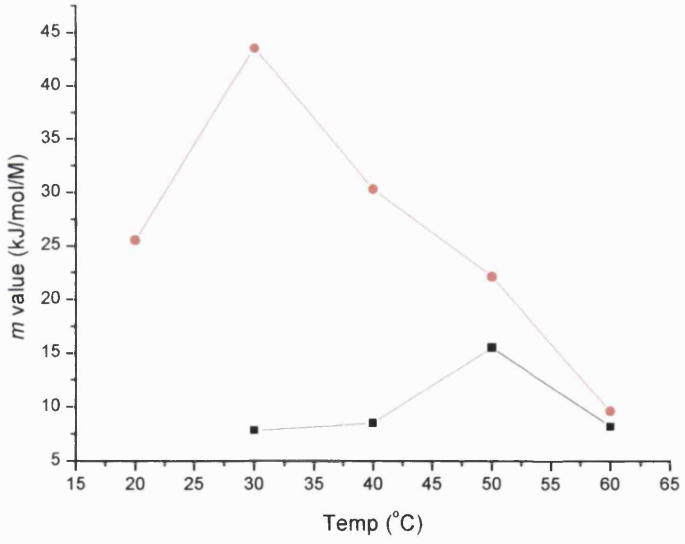

Figure 3.11: ΔG_w (a) and *m* (b) values obtained from the analysis of GdnHCl-induced unfolding curves of *P. furiosus* citrate synthase as monitored by enzyme activity and fluorescence spectroscopy. Values obtained from enzyme activity unfolding curves (■) and from fluorescence unfolding curve analysis (●) are plotted.

The values of the thermodynamic parameters ΔG_w and m vary as a function of temperature for both the unfolding of the monomer and the dissociation of the dimer. The parameter m is the absolute value of the slope of the unfolding transition and it relates the observed ΔG for the unfolding process to the GdnHCl concentration (Pace, 1990). This parameter is usually interpreted as a measure of the difference between the numbers of GdnHCl interaction sites in the native and denatured states of the protein.

If this model provides a reasonable thermodynamic description of the denaturation of *P. furiosus* citrate synthase, then one should calculate the same ΔG for the dissociation of the dimer from experiments performed at different protein concentrations. The values obtained for the thermodynamic parameters calculated at different protein concentrations are shown in **Table 3.7**.

Table 3.7: A comparison of thermodynamic parameters obtained for the GdnHCl-induced unfolding of *P. furiosus* citrate synthase at different protein concentrations. Values obtained from enzyme activity unfolding curves are termed ΔG_1, m_1 and C_{m1} and values from fluorescence unfolding curve analysis are termed ΔG_2, m_2 and C_{m2}.

[Protein] (μg/ml)	ΔG_{w1} (kJ/mol)	m_1 (kJ/mol/M)	C_{m1} (M)	ΔG_{w2} (kJ/mol)	m_2 (kJ/mol/M)	C_{m2} (M)
5	37.7 ± 2.7	7.5 ± 0.8	0.53 ± 0.1	99.2 ± 23.8	26.4 ± 6.3	3.76 ± 1.3
8	36.7 ± 3.2	8.1 ± 1.4	0.63 ± 0.1	109.3 ± 18.9	28.9 ± 5.0	3.78 ± 0.9
10	37.6 ± 3.4	8.0 ± 1.7	0.71 ± 0.2	111.3 ± 17.5	28.6 ± 4.5	3.89 ± 1.9

Thermodynamic parameters have been determined over a small temperature and protein concentration range. It is unclear in the literature how the total ΔG_w should be calculated for the complete unfolding of the protein – whether the ΔG_{w2} is a combination of the dissociation and unfolding of the protein (ie the total ΔG_w of the protein) (Hornby *et al*, 2000) or whether it is a separate component (Grimsley *et al*, 1990). It is possible that ΔG_{w2} is the total ΔG_w of the system as the fluorescence data incorporate the dissociation and the unfolding of the enzyme. The ΔG values obtained at 60°C , ΔG_{w1} = 55kJ/mol and ΔG_{w2} = 31kJ/mol would, however, not support this theory. If ΔG_{w2} is indeed the ΔG_w of the overall process, then between 20 and 40% of the enzyme stability is found at the dimer interface. This means that the subunit association is an important feature in the stability of the protein. There is an entropic cost to forming a dimer, but it is clear that this is more than offset by the gain in the stability of forming the dimer.

If the view that ΔG_{w2} is a combination of the dissociation and unfolding of the protein, the data show that *P. furiosus* citrate synthase is a very stable protein with a ΔG_w of the unfolding of the monomers of around 100 kJ/mol. The ΔG_w values reported for mesophilic, monomeric proteins are between 20-60kJmol^{-1} (Pace, 1990).

The *m* values, the dependence of the free energy of unfolding on denaturant concentration, obtained can be related to the global changes occurring during the unfolding of the protein. Myers *et al* (1995) collected denaturant *m* values for a large number of proteins and found them to correlate strongly with the amount of protein surface exposed to solvent upon unfolding. The *m* values reported in this thesis show that 70-75% of the total change occurs in the second transition. This is consistent with the observation that unfolding of the monomers occurs in the second transition.

It must be stressed that the quality of the thermodynamic data obtained here is certainly dependent on the original unfolding data and the method of fitting the data.

3.5. Discussion

The overall unfolding pathway for homodimeric proteins must begin with folded dimer (N_2) and end with two unfolded monomers (2U). The way in which this is achieved depends on the nature of the intermediates along the way.

The data from the GdnHCl-induced unfolding of *P. furiosus* citrate synthase suggest an unfolding model of the dimer dissociating into two folded monomers prior to the unfolding of the monomers. Enzyme activity appeared to be the more sensitive method toward the dissociation of the dimer, whereas fluorescence spectroscopy was only sensitive toward the unfolding of the monomers.

So why is there no change in fluorescence observed for the dissociation of the dimer? Fluorescence is usually dominated by the contribution of the tryptophan residues because the absorbance at the wavelength of excitation is greater than the respective values for tyrosine and phenylalanine (Schmid, 1998). This can be seen in the sensitivity parameter as shown in the table below.

Table 3.8: Fluorescence properties of aromatic amino acids. Sensitivity = molar extinction coefficient x quantum yield. Table adapted from Schmid (1998).

Amino acid	Fluorescence (λmax) nm	Quantum yield	Sensitivity $M^{-1}cm^{-1}$
Tryptophan	355	0.13	730
Tyrosine	304	0.14	200
Phenylalanine	282	0.12	4

In proteins that contain both Tyr and Trp residues, fluorescence for Tyr is barely detectable because Trp emission is strong. The emission wavelength of 340nm

corresponds to the fluorescence maximum of the Trp residues. Therefore, although both Tyr and Trp residues are excited in these experiments only the emission of the Trp is detected. The change in fluorescence would therefore be dependent on the environment of the Trp residues. Calculation of the solvent accessibility of residues within PfCS shows that no Trp residues change accessibility with monomerisation. This means that there are no Trp residues at the subunit interface, hence no change in Trp environments on dissociation.

A change in fluorescence would, therefore, indicate a change in the environment of the Trp residues. The Trp residues in PfCS are mainly found within the folded monomer structure. Hence to observe a change in the fluorescence, the structure needs to be unfolded. The change of fluorescence seen at around 3.4M GdnHCl shows the onset of the unfolding of the tertiary structure of the protein. The Trp residues in PfCS are shown in **Figure 3.11**.

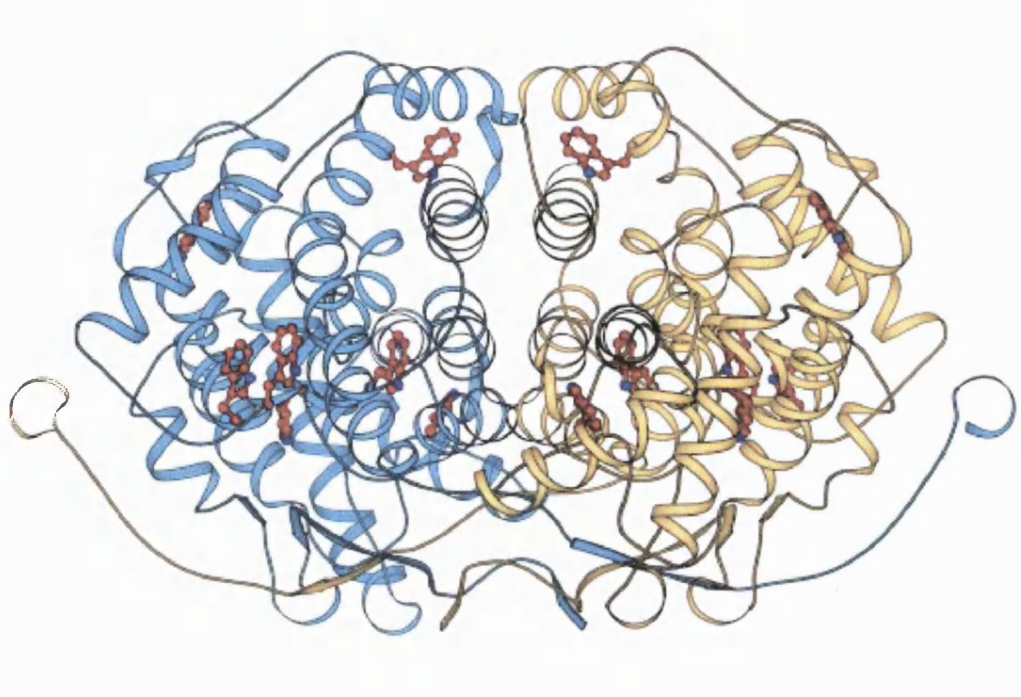

Figure 3.11: Ribbon diagram of *P. furiosus* citrate synthase showing the position of tryptophan residues. The Trp residues are shown in red as ball and stick models.

The mechanism and kinetics of denaturant- and thermally-induced unfolding are obviously of great practical interest. It is an important problem for protein engineering and the understanding of the mechanisms of protein stabilisation. Nevertheless, only a few quantitative studies have been presented for oligomeric and thermostable proteins (Backmann *et al*, 1998). Many reports suggest that thermostability and stability towards denaturants are correlated. A question that remains unanswered by this study, and that could only be answered only after the accumulation of a representative set of data, is whether the thermal unfolding of this enzyme proceeds via the same mechanism. At such high temperatures, the probability of destructive processes is generally greater.

The observation that a multi-state system can be well described by a two-state model illustrates the major difficulty in analysing equilibrium unfolding data. Still, the experimental results have clearly shown that the GdnHCl-induced unfolding of PfCS proceeds via a three-state mechanism:

$$\mathbf{N_2} \quad \rightleftharpoons \quad \mathbf{2N} \quad \rightleftharpoons \quad \mathbf{2U}.$$

This three-state unfolding model of citrate synthase is the first time a model has been proposed for the guanidine-induced unfolding of this dimeric protein.

There is no doubt that our understanding of the unfolding of *P. furiosus* citrate synthase has grown, but some uncertainties still persist.

4. CHAPTER FOUR

INVESTIGATING THE ROLE OF THE INTER-SUBUNIT IONIC NETWORK AND THE C-TERMINAL REGION ON THE CONFORMATIONAL STABILITY OF *PYROCOCCUS FURIOSUS* CITRATE SYNTHASE

4.1. Introduction

Two main strategies have been used to investigate protein thermostability. One is a comparative approach whereby either the amino acid sequences or the atomic structures of homologous enzymes from mesophilic and (hyper)thermophilic organisms are compared. Another approach is the use of mutagenesis either by site-directed mutagenesis or directed evolution to create mutants to determine the effects of amino acid changes on the protein's stability. Site-directed mutagenesis is normally carried out to test the predictions made by structural or amino acid comparisons. Work in our lab has used this combination strategy to study the structural basis of thermostability in citrate synthase.

The genes of citrate synthases from *Arthrobacter*, Pig, *Thermoplasma acidophilum*, *Sulfolobus solfataricus*, and *Pyrococcus furiosus* have been cloned, sequenced and expressed in *E. coli*. The recombinant enzymes have been characterised and shown to possess thermostability properties that correspond with the environmental temperature of the organisms from which their native counterparts were isolated. The five proteins show a high degree of structural homology and almost identical active site structures and conformations. The atomic structures of these enzymes have been compared to study the structural basis of thermostability.

A comparison of the atomic structures of the thermophilic and hyperthermophilic citrate synthases with the citrate synthase from pig, a mesophile, reveals a number of features, both intra- and inter-subunit, that may be responsible for enhancing thermostability. Intra-subunit features include: (i) a reduction in thermolabile residues and an increase in isoleucine and glutamic acid residues, (ii) an increase in compactness, achieved by shortening of loops between helices and a reduction in both the size and number of internal cavities. All these measures serve to increase the conformational stability of the folded monomers and, hence, increasing the thermostability (Fontana *et al*, 1998; Arnott *et al*, 2000). Differences in the inter-subunit features include: (i) an increase in complex ion-pair networks, and (ii) variations in the nature of dimer formation including additional interactions involving the C terminus.

Four anti-parallel pairs of helices (F, G, M & L) constitute the subunit interface in the dimeric citrate synthases. In the *Thermoplasma acidophilum* CS (TaCS) and *Sulfolobus solfataricus* CS (SsCS) enzymes, there is a marked increase in the alanine content of helices G and M compared with the pig enzyme (PigCS) (Russell *et al*, 1994; Bell, 1999). This may contribute to the thermostability of these enzymes by increasing the hydrophobicity of the subunit contacts and also through stabilising the individual helices. Alanine is the most stabilising residue (Serrano *et al*, 1992 a&b) and a high alanine content is thought to increase the rigidity of the helix.

In the *Pyrococcus* enzyme, this hydrophobicity is largely replaced by ionic interactions. There is a single ionic interaction in TaCS, SsCS has two interactions that are not networked, PfCS possesses a five-membered ionic network at either end of the central helices (G &M), while the psychrophilic *Arthrobacter* CS (DSCS) has two intersubunit ionic interactions and two intrasubunit interactions at the surface. This is consistent with the theory that such networks play an important role

in the adaptation of enzymes at extreme temperatures. The structures of several other thermostable proteins have appeared recently, some of which point to the importance of ion-pairs in conferring hyperthermostability and some of which point to compactness. Ionic networks have been observed in glutamate dehydrogenase from *P. furiosus* (Yip et al, 1995) and β-glycosidase from *S. solfataricus* (Aguilar *et al*, 1997).

Another difference in structure between PfCS and less thermostable CSs is in the C-terminal arm of the enzymes. The closed form of PfCS has revealed an intimate association of the monomers (Russell *et al*, 1994), where the C-terminal arms are in an extended conformation and wrap over the surface of the partner subunit in the form of an embrace. Of the two terminal arginines, the penultimate residue (Arg 375) forms an ionic bond with Glu 48 in the partner monomer. It was predicted that this interaction might contribute to maintaining the integrity of the dimer at extreme temperatures (Russell *et al*, 1997). This subunit interaction has not been observed in low-resolution studies of the open form of TaCS. By comparing amino acid sequence alignments, it is clear that this region varies between different organisms (see **Figure 4.2**). It can be seen that the CS from the *Arthrobacter* and from pig have shorter C-terminal arms than the PfCS. It was supposed that the shortening of this region might be one reason for this difference in themostability.

Some of these features mentioned are being analysed by site-directed mutagenesis, to gain an insight into their relative contributions to overall thermostability. Site-directed mutants were created of PfCS to test the importance of the additional C-terminal subunit interaction and of the 5-membered subunit interface ionic network (Arnott *et al*, 2000).

The first set of mutants, the ionic interaction mutants, consisted of the replacement of the central Asp 113 on Helix G which forms ionic bonds with Lys 219, His 93 and Arg 99 (**Figure 4.1**). Hence the substitution of this residue could disrupt the ionic network considerably by up to 60%. The acidic aspartate was replaced in the first mutation by serine, a polar residue and in the second case by an alanine, which is a hydrophobic residue. Serine was chosen as a relacement for Asp 113 because its side chains cannot form ionic interactions but it contains a hydroxyl group, which is capable of forming hydrogen bonds. Therefore, serine may be able to retain a degree of interaction with the other residues in the ionic network. In the second case, alanine was chosen because its side chain cannot form any interactions with the other residues in the ionic network, thus destroying the majority of the ionic interactions in the network.

The second set of mutants was the C-terminal deletion mutants. The first C-terminal mutant created involved the removal of the two terminal arginine residues. The penultimate residue is present in all the thermophilic citrate synthases. The removal of this residue was to determine the importance of the ionic bond between the penultimate arginine residue (Arg 375) and the glutamate residue (Glu 48) on the partner subunit in PfCS. This ionic bond is thought to anchor the whole C-terminal arm. The second C-terminal deletion mutant created involved removing the whole arm (of 13 residues) from where it emerges from the core domain of the PfCS molecule.

(a)

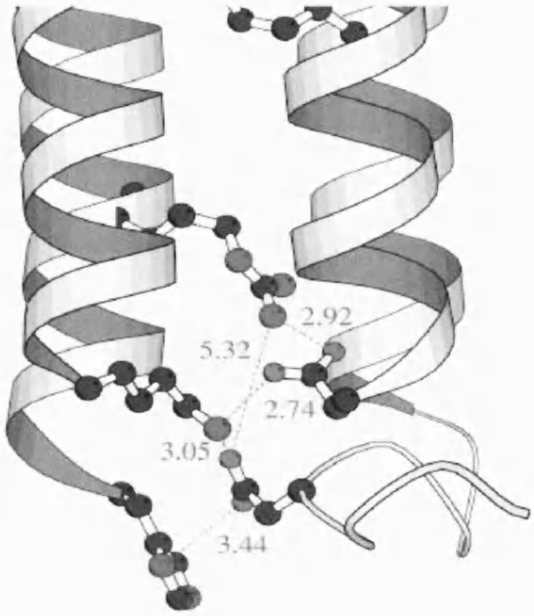

(b)

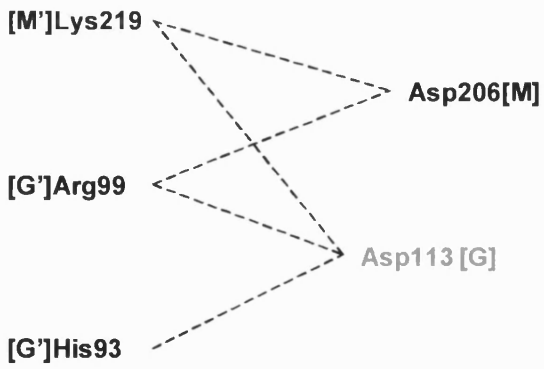

Figure 4.1: Ionic interactions at the subunit interface of *P. furiosus* citrate synthase: (a) the positioning of the ionic network with bond lengths between helices M, M', G and G', and (b) a schematic of the ionic network. The residue Asp 113 subjected to site-directed mutagenesis is shown in red.

(a)

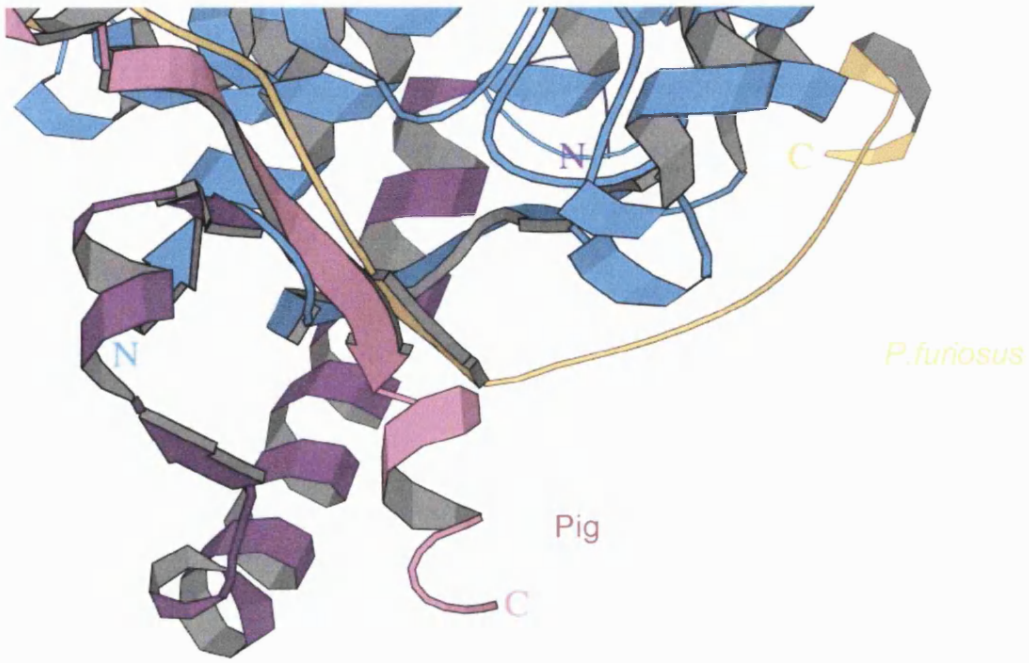

(b)

Arthrobacter	L	S	E	Y	N	G	P	E	Q	R	Q	V	P					
Pig	K	S	M	S	T	D	G	L	I	K	L	V	D	S	K			
T. acidophilum	R	A	V	Y	V	G	P	A	E	R	K	Y	V	P	I	A	E	R	K
S. solfataricus	R	A	L	Y	V	G	P	E	Y	Q	E	Y	V	S	I	D	K	R	
P. furiosus	R	L	Q	Y	V	G	E	I	G	K	K	Y	L	P	I	E	L	**R**	**R**

-13 -2

Figure 4.2: Comparison of the C-terminal region of citrate synthases. (a) Ribbon diagram of the C-terminal regions of *P. furiosus* shown in yellow and Pig CS shown in pink. The partner subunits are shown in blue and magenta, respectively. (b) Sequence alignment of the C-terminal arms of various citrate synthases. The mutations created in the enzyme are shown as –2 (the two terminal arginine residues removed) and –13 (the whole arm of 13 residues removed).

4.2. Methods

All citrate synthase genes were cloned into the pREC7/*Nde*I expression vector and transformed into a citrate synthase negative *E. coli* strain, MOB 154, for expression (Arnott *et al*, 2000). All the enzymes were expressed as soluble, active proteins and they were purified as described in **Chapter 2**. The purified enzymes were homogenous as determined by SDS-PAGE analysis and had polypeptide Mr values of ~43 kDa. The effect of the mutations on the thermostability of PfCS is investigated in this chapter, by comparing the thermodynamic parameters of the enzymes.

4.2.1. Guanidine-induced unfolding of PfCS enzymes

Guanidine-induced unfolding was carried out as described in the previous chapter for the *P. furiosus* citrate synthase wild-type enzyme. Enzyme activity and fluorescence measurements were obtained for each enzyme at a range of temperatures (20-60°C). 36 solutions were prepared for the fluorescence measurements as previously described (0-6M Gdn-HCl); 23 solutions were prepared for enzyme activity measurements (0-2.4M Gdn-HCl). An example of data obtained for all the mutants at 50°C is shown below.

(a)

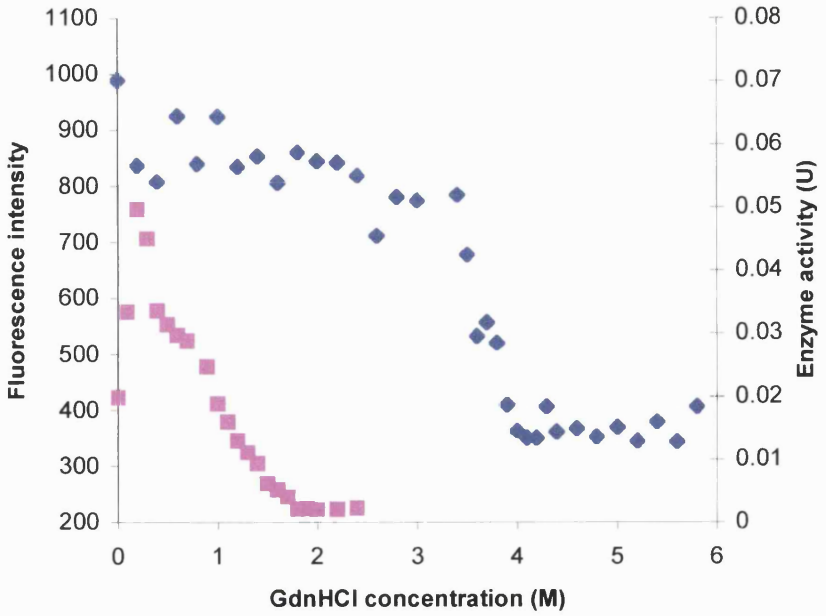
Fluorescence intensity
Enzyme activity (U)
GdnHCl concentration (M)
1100
1000
900
800
700
600
500
400
300
200
0.08
0.07
0.06
0.05
0.04
0.03
0.02
0.01
0
0
1
2
3
4
5
6

(b)

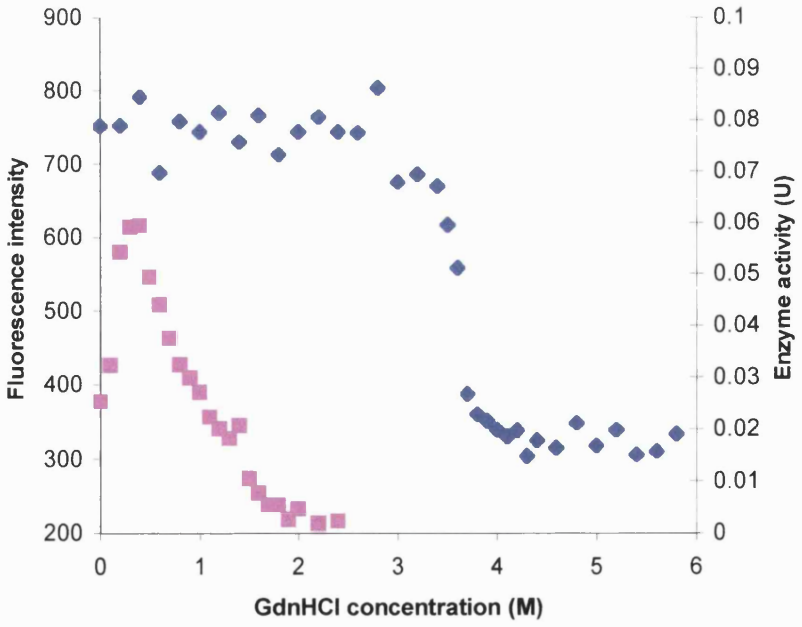
Fluorescence intensity
Enzyme activity (U)
GdnHCl concentration (M)
900
800
700
600
500
400
300
200
0.1
0.09
0.08
0.07
0.06
0.05
0.04
0.03
0.02
0.01
0
0
1
2
3
4
5
6

(c)

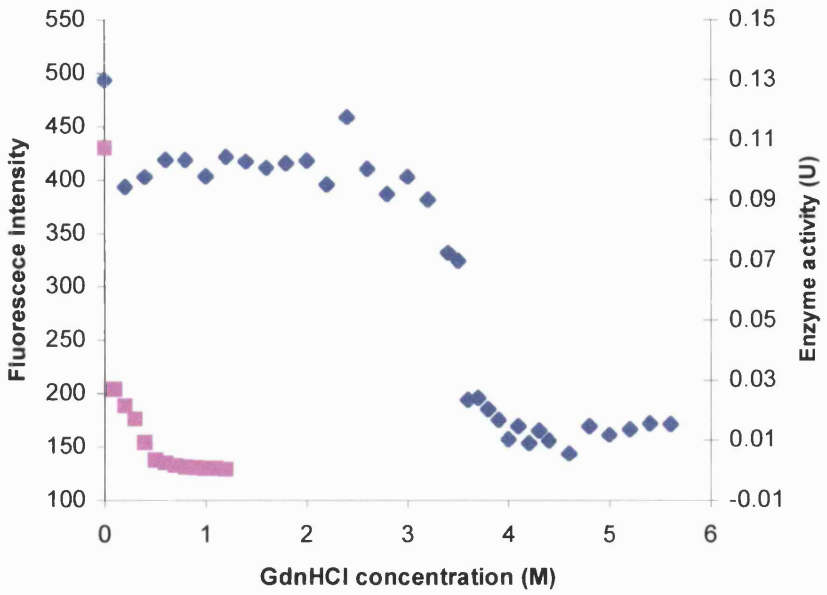

(d)

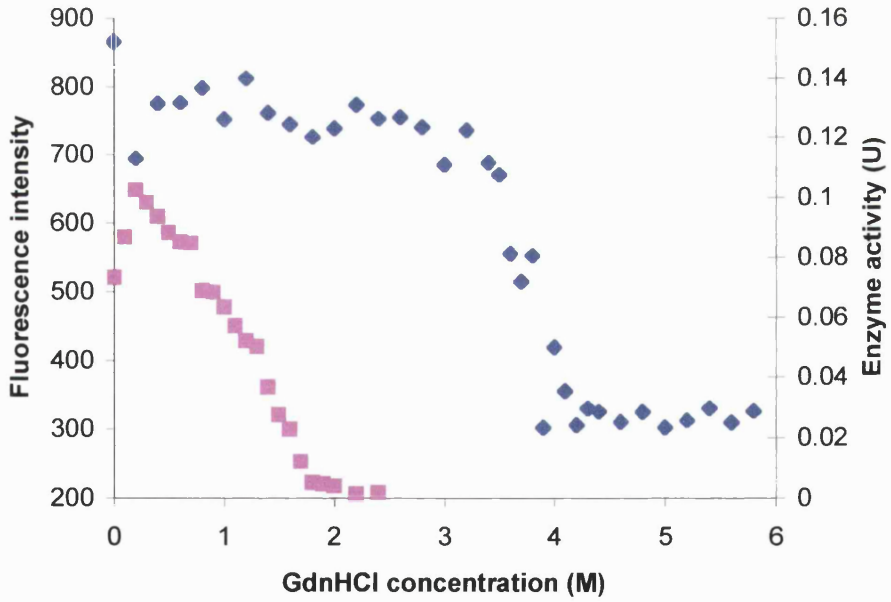

Figure 4.3: Guanidine-induced unfolding of alanine (a), serine (b) –13 (c) and –2 (d) mutants of *P. furiosus* citrate synthase. The proteins were incubated in varying concentrations of GdnHCl at 50°C and monitored for loss of activity (■) and change in fluorescence(◆).

As with the wild-type enzyme, the data presented in **Figure 4.3** show that there is a loss of activity around 2M GdnHCl for all the mutants (0.5M for the PfCS –13 enzyme). However, this is not accompanied by a change in fluorescence, which only occurs around 3M GdnHCl. This suggests that for all the mutant enzymes, as with the wild-type *P. furiosus* citrate synthase (data shown in **Chapter 3**), the dimer dissociates followed by the unfolding of the monomers. That is, these results support the prediction that the mutant enzymes unfold via the same mechanism as the wild-type enzyme:

$$\mathbf{N_2 \rightleftharpoons 2N \rightleftharpoons 2U}$$

The unfolding data were therefore fitted to equations as described in **Chapter 3**.

4.2.1.1. Determination of free-energy values for unfolding

Data shown in **Figure 4.3** have been analysed as described in **Chapter 3** and typical fits are shown in **Figure 4.4**. The fitted data for PfCS ala at 50°C are shown as examples in **Figure 4.4**. The thermodynamic parameters ΔG, m and C_m values for all proteins were determined as follows. The enzyme activity measurements were fitted to a two-state unfolding method of $N_2 \leftrightharpoons 2N$. The fluorescence data were also fitted to a two-state unfolding transition of $N \leftrightharpoons U$ as described previously. All data were fitted using Microcal Origin 6.0.

(a)

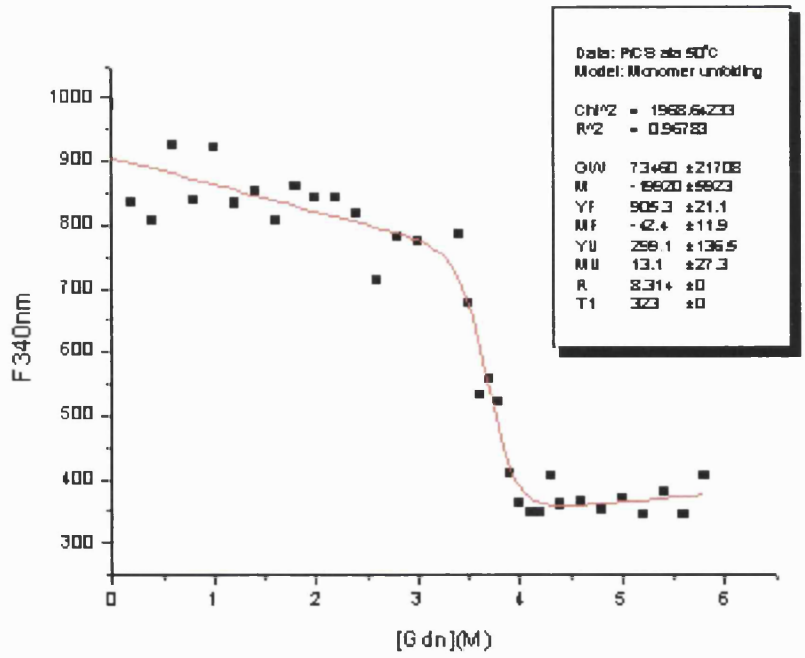

(b)

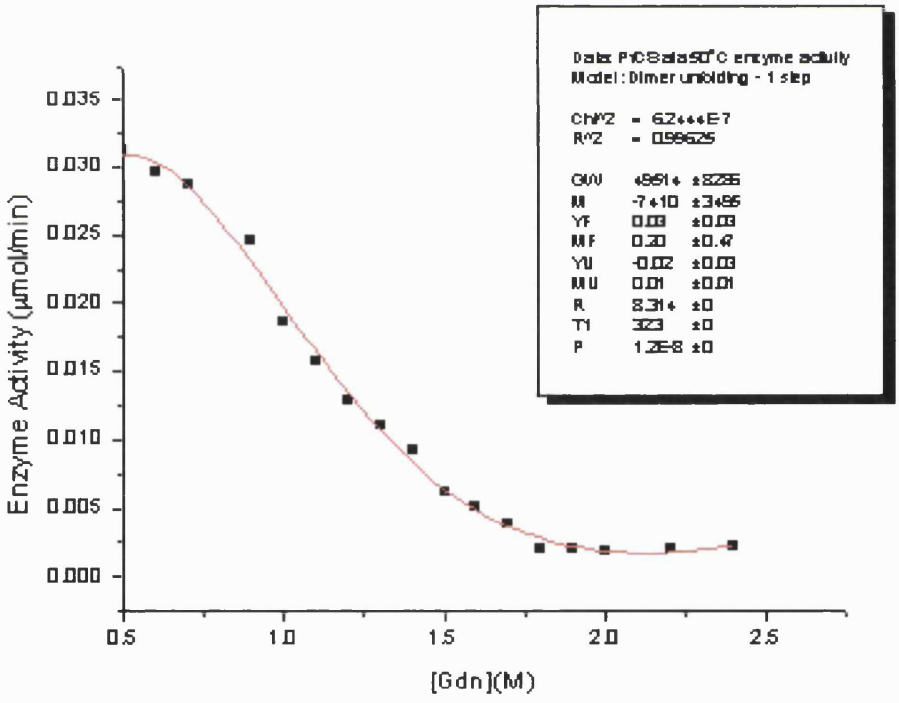

Figure 4.4: Non-linear least squares analysis of the GdnHCl-induced unfolding of PfCS –2 at 50°C as monitored by fluorescence and enzyme activity. Each data set was fitted to a two-state transition. (a) was fitted to $N \leftrightharpoons U$ (b) was fitted to $N_2 \leftrightharpoons 2N$.

The thermodynamic data obtained for the different enzymes at a temperature range of 20-60°C are displayed in **Tables 4.1a&b**. There are no enzyme activity data available for the PfCS (–13) enzyme. Unfortunately, the PfCS (–13) enzyme data could not be analysed due to the fact that the activity is lost presumably due to the dissociation of the dimer at around 0.5mM GdnHCl, thus a suitable pre-transition baseline could not be obtained. There are also no activity data for any of the enzymes at 20°C because the catalytic activities of the enzymes are too low to record.

Table 4.1: Comparison of ΔG values obtained for the dissociation of the *P. furiosus* wild-type and mutant enzymes at different temperatures. ΔG values calculated from (a) the enzyme activity data and (b) the fluorescence data. There are no enzyme activity values available for the PfCS(–13) enzyme.

(a)

Temp (°C)	ΔG_W(kJ/mol)			
	PfCS wt	**PfCS(D113A)**	**PfCS(D113S)**	**PfCS (-2)**
30	42 ± 2	51 ± 2	53 ± 2	44 ± 2
40	57 ± 7	52 ± 4	44 ± 6	56 ± 5
50	61 ± 4	50 ± 8	54 ± 5	64 ± 1
60	55 ± 5	65 ± 2	63 ± 1	66 ± 1

(b)

Temp (°C)	ΔG_w(kJ/mol)				
	PfCS wt	PfCS(D113A)	PfCS(D113S)	PfCS (-2)	PfCS (-13)
20	101 ± 18	115 ± 34	98 ± 32	124 ± 45	119 ± 11
30	174 ± 35	105 ± 47	169 ± 89	150 ± 28	170 ± 34
40	118 ± 19	88 ± 28	104 ± 31	85 ± 15	203 ± 38
50	78 ± 9	74 ± 22	106 ± 22	66 ± 17	98 ± 25
60	31 ± 4	25 ± 10	65 ± 14	79 ± 19	27 ± 5

A comparison of the ΔG of unfolding and *m* values obtained for the different enzymes for both transitions suggests that there are no differences between the wild-type and mutant PfCS enzymes. At 60°C, however, the PfCS (D113S) and PfCS (-2) appear more stable than others. The *m* value, the gradient of the transition region of the unfolding curve, is a measure of the cooperativity of unfolding.

Table 4.2: Comparison of m values for *m* values calculated from (a) the enzyme activity data and (b) the fluorescence data at 30-60°C.

(a)

Temp (°C)	*m* value (kJ/mol/M)			
	PfCS wt	PfCS (D113A)	PfCS (D113S)	PfCS (-2)
30	8 ± 0.6	15 ± 2	16 ± 3	8 ± 1
40	9 ± 2	16 ± 4	8 ± 3	24 ± 8
50	15 ± 4	7 ± 3	20 ± 6	10 ± 0.4
60	8 ± 2	15 ± 2	12 ± 1	16 ± 1

(b)

Temp (°C)	*m* value (kJ/mol/M)				
	PfCS wt	PfCS (D113A)	PfCS (D113S)	PfCS (-2)	PfCS (-13)
20	26 ± 4	29 ± 9	25 ± 8	31 ± 11	31 ± 3
30	44 ± 9	27 ± 12	43 ± 23	38 ± 7	44 ± 9
40	30 ± 5	23 ± 7	27 ± 8	22 ± 3.1	53 ± 10
50	22 ± 3	20 ± 6	30 ± 6	18 ± 5	28 ± 7
60	10 ± 1	7 ± 3	18 ± 4	21 ± 5	8 ± 1

The C_m value, the concentration at which the protein is 50% unfolded can be used to compare the stability of the different proteins. It is difficult to discern particular trends from the values obtained.

Table 4.3: Comparison of the C_m values (denaturation concentration at which the enzyme is 50% unfolded) obtained for (a) the enzyme activity data and (b) the fluorescence data at 30-60°C.

Temp (°C)	C_m (M)			
	PfCS wt	PfCS (D113A)	PfCS (D113S)	PfCS (-2)
30	0.43 ± 0.04	0.86 ± 0.1	0.89 ± 0.1	0.61 ± 0.1
40	2.02 ± 0.5	0.74 ± 0.4	0.48 ± 0.2	0.65 ± 0.2
50	1.33 ± 0.4	1.16 ± 0.7	0.66 ± 0.2	2.15 ± 0.1
60	1.50 ± 0.4	1.51 ± 0.2	1.74 ± 0.04	1.53 ± 0.1

(b)

Temp (°C)	C_m (M)				
	PfCS wt	PfCS (D113A)	PfCS (D113S)	PfCS (-2)	PfCS (-13)
20	3.97 ± 0.9	3.99 ± 1.7	3.95 ± 1.8	4.03 ± 2.0	3.88 ± 0.5
30	4.00 ± 1.1	3.95 ± 1.4	3.94 ± 1.7	3.97 ± 1.2	3.87 ± 1.1
40	3.89 ± 0.9	3.86 ± 1.7	3.86 ± 1.6	3.86 ± 0.9	3.82 ± 1.0
50	3.54 ± 0.6	3.69 ± 1.8	3.60 ± 1.1	3.73 ± 1.4	3.52 ± 1.3
60	3.24 ± 0.6	3.43 ± 2.0	3.72 ± 1.1	3.76 ± 1.3	3.35 ± 0.9

4.2.2. Differential scanning calorimetry of PfCS enzymes

Differential scanning calorimetry was carried out as described previously. Melting temperatures (T_m) were determined for *P. furiosus* wild-type and mutant enzymes at pH 5 and 7. Representative DSC scans at pH 5 are shown in **Figure 4.5**.

(a)

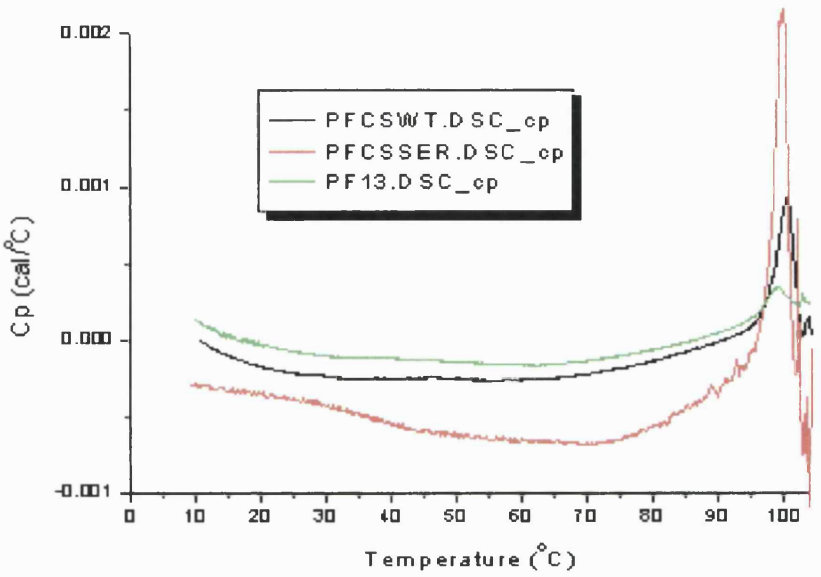

(b)

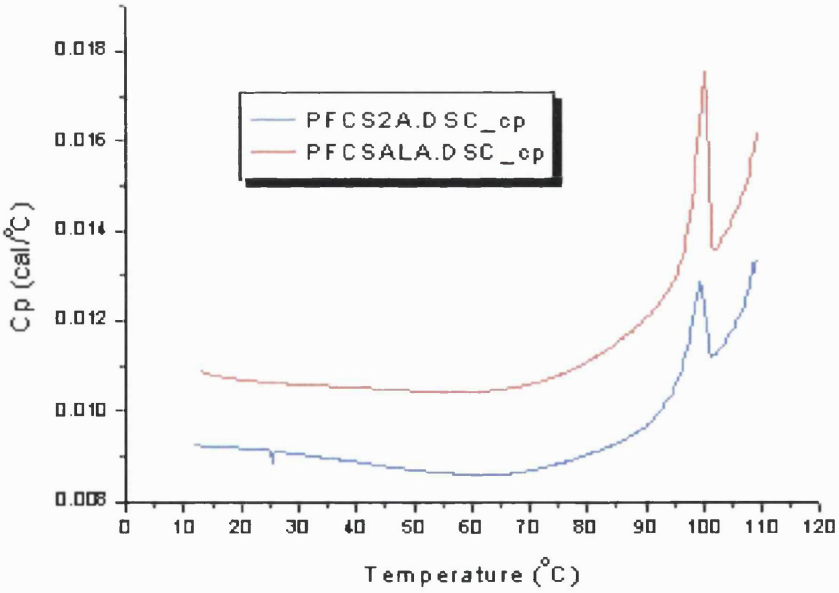

Figure 4.5: Thermal unfolding of PfCS wt and mutants as monitored by DSC at pH 5. (a) shows the scans of PfCS wt, PfCS (D113S) & PfCS (-13). (b) shows the scans of PfCS (-2) & PfCS (D113A). Scan rate of 60°C/h. Scans have not been baseline-corrected as a consistent baseline could not be obtained, due to instrumental problems.

DSC scans of all the enzymes revealed one unfolding peak. This is consistent with a two-state model of unfolding. On the basis of these observations, it appears that a two-state model might define the thermal unfolding of the mutants as with the wild-type enzyme. There is, however, a shoulder to each of these scans. It is not sure whether this is an instrumental baseline distortion or whether these are unfolding effects.

An equilibrium thermodynamic analysis of DSC scans allows us to check whether the process is two-state or in the case of a multi-state denaturation, to determine the number and character of the significantly populated intermediate states (Sanchez-Ruiz *et al*, 1988). However, the thermal unfolding data obtained were not fitted to determine the mechanism of unfolding or to obtain thermodynamic parameters because of the irreversibility of the process.

Estimates of the melting temperature (T_m) values were obtained from the observed peaks of the scans (**Table 4.4**) and it can be seen that there is no difference in the T_m values between the wildtype and the mutants. This agrees with the previous findings from the calculated ΔG values.

Table 4.4: Melting temperatures of *P. furiosus* wild-type and mutant enzymes. DSC was carried out at pH 5 and 7.

	Melting Temperature (°C)				
	PfCS wt	**PfCS (D113A)**	**PfCS (D113S)**	**PfCS (-2)**	**PfCS (-13)**
pH 5	100.4	100.0	99.8	99.4	99.1
pH 7	103.2	102.7	102.6	102.4	102.1

4.2.3. Thermal inactivation studies of PfCS enzymes

For all the enzymes, thermal inactivation studies were carried out by incubating 100ml aliquots of citrate synthase (50ug/ml) in (a) 50mM Epps, pH 8.0, 2mM EDTA, (b) 50mM sodium phosphate buffer, pH 7.0, 2mM EDTA and (c) 50mM sodium acetate, pH 5.0, 2mM EDTA. The stock solution was aliquoted into 0.5 ml PCR tubes and the tubes were incubated at the defined temperature in an Eppendorf Mastercycler and removed at known intervals and rapidly cooled in an ice/water bath. Enzymic activity was then measured using the DTNB/412nm assay at pH 8.0

Figure 4.6 shows the thermal inactivations of PfCS wt and mutant enzymes carried out at 99°C. A comparison of the wildtype and mutant enzymes at pH 5 and pH 7 is shown in **Figure 4.7**.

(a)

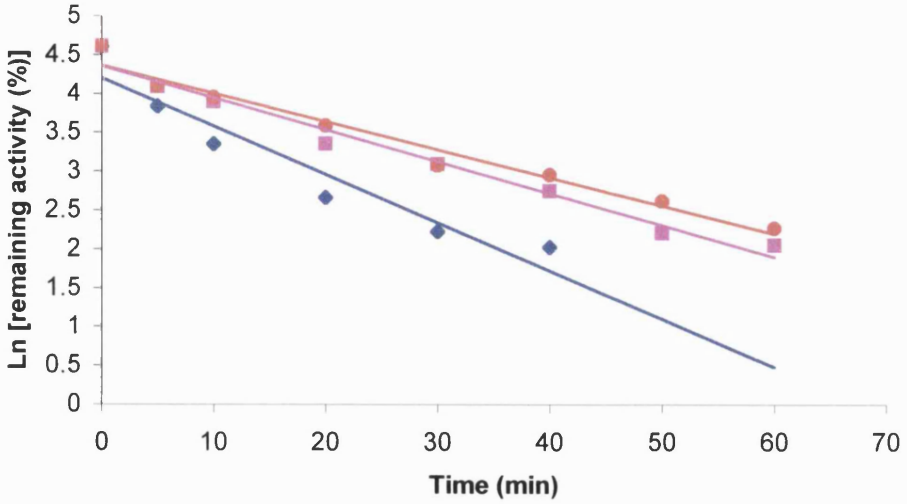
Ln [remaining activity (%)]
5
4.5
4
3.5
3
2.5
2
1.5
1
0.5
0
0
10
20
30
40
50
60
70
Time (min)

(b)

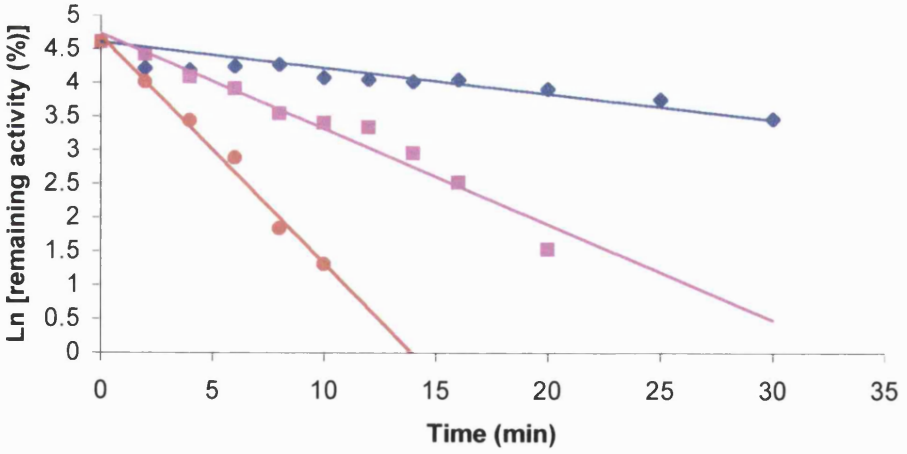
Ln [remaining activity (%)]
5
4.5
4
3.5
3
2.5
2
1.5
1
0.5
0
0
5
10
15
20
25
30
35
Time (min)

(c)

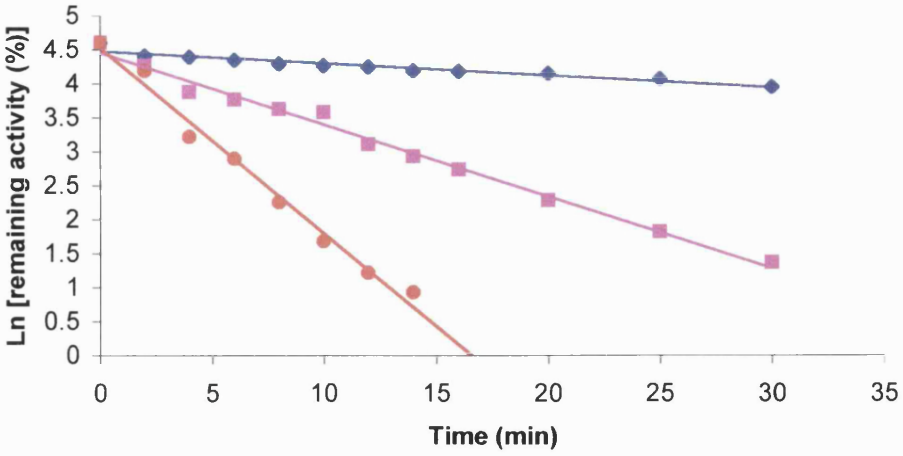

(d)

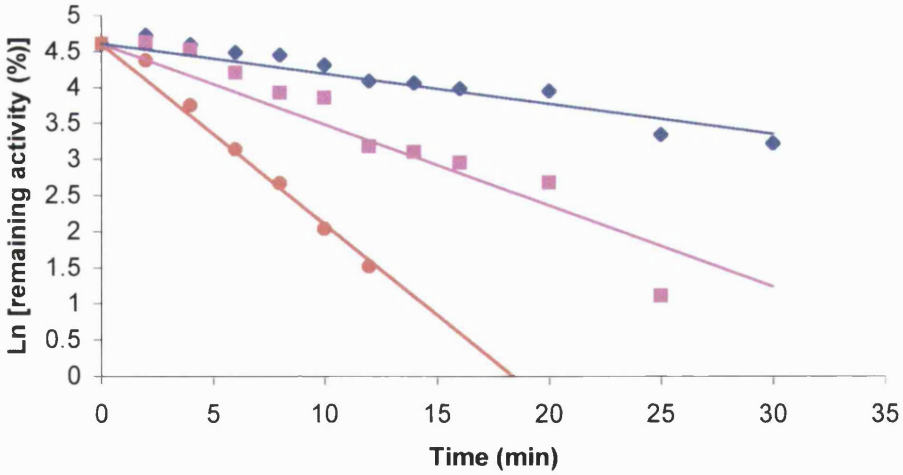

Figure 4.6: Thermal inactivations of (a) PfCS wt, (b) PfCS (D113A), (c) PfCS (D113S), (d) PfCS –2, carried out at 99°C. The enzymes were incubated in buffers at pH 5 (◆), pH 7 (■) and pH 8 (●).

(a)

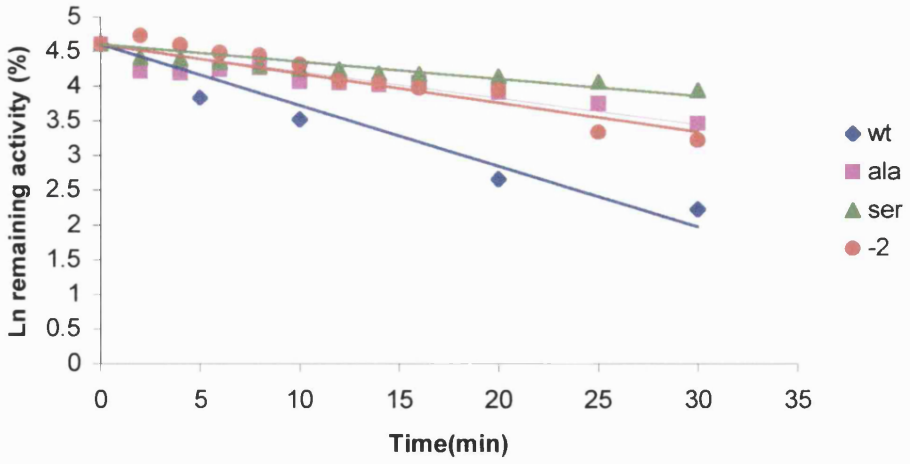

(b)

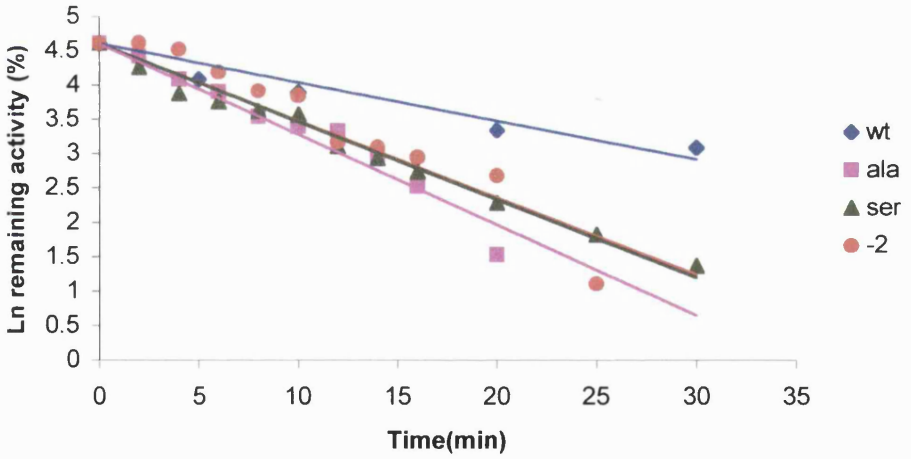

Figure 4.7: Thermal inactivations of PfCS wt and mutant enzymes. Enzyme samples were incubated at 99°C at (a) pH 5 and (b) pH 7. The remaining activity measured at known time intervals at 55°C and pH 8.

The results of this investigation show that the mutants become more stable as the pH is lowered (k_{inact} data shown in **Table 4.6**). They also suggest that the ionic network mutants and the PfCS (–2) C-terminal mutant of *P. furiosus* citrate synthase are markedly more stable to thermal inactivation at pH 5 than the wild-type enzyme (the reverse is true at pH 7). Unfortunately, after prolonged storage at 4°C, the PfCS (–13) enzyme had lost all its activity prior to this experiment; therefore no temperature inactivation data are available for this mutant.

Table 4.5: Thermal inactivation rate constants (k_{inact}) of PfCS wt and mutants. k_{inact} data were calculated from the slopes of the thermal inactivations at 99°C at different pH shown in **Figure 4.6**.

	k_{inact} (min^{-1})		
Enzyme	**pH 5**	**pH 7**	**pH 8**
PfCS wt	0.062 ± 0.002	0.0411± 0.003	0.0361± 0.001
PfCS (D113A)	0.0287 ± 0.004	0.1414 ± 0.003	0.3371 ± 0.006
PfCS (D113S)	0.0181 ± 0.001	0.1057 ± 0.004	0.2731 ± 0.002
PfCS -2	0.042 ± 0.002	0.1123 ± 0.001	0.2504 ± 0.004

4.3. Discussion

Comparing the structure and stability of mutants of a protein from a particular organism is an established approach for relating structure to thermostability. These stability studies normally involve a comparison of the catalytic properties of the enzymes. The mutants studied here were created to determine the role of the inter-subunit interactions in the increased thermostability of *P. furiosus* citrate synthase. As this study is concerned with determining the molecular basis of thermostability, it is important that only defined regions of the protein concerned are altered.

The mutations created in the enzyme are thought not to have caused any large disruptions in its structure. Any disruptions in the subunits for example could affect the enzyme activity as the active site is situated between the two subunits. The kinetic data obtained at 55°C, with the exception of the PfCS (–13) mutant, are consistent with those obtained for the wild-type enzyme (**Table 4.6**). The PfCS (–13) mutant shows a reduction in the affinity for both substrates. The k_{cat} at 55°C is unaltered, suggesting that it is the binding affinity that is affected by the complete removal of the C-terminal region. This region has been shown in crystallographic studies to be involved in the association of the subunits (Russell *et al*, 1994).

Table 4.6: Kinetic parameters determined for PfCS wt and mutants. K_M and V_{max} values were calculated using the Direct Linear plot. The table is reproduced with permission from Arnott *et al* (2000).

Enzyme	K_M AcCoA (μM)	K_M OAA (μM)	V_{max} (μmol/min/mg)
PfCS wt	4 ± 0.3	15 ± 1	23 ± 1
PfCS (–2)	5 ± 0.3	20 ± 1	17 ± 1
PfCS (–13)	51 ± 5	212 ± 18	14 ± 1
PfCS (D113A)	7 ± 0.3	17 ± 1	24 ± 1
PfCS (D113S)	7 ± 0.6	12 ± 1	19 ± 1

A comparison of the temperature dependence of enzyme activity of PfCS wt and mutants enzymes shows that the mutants have similar specific activities to the wild type enzyme up until 65°C. This suggests that the mutants have no significant change in the catalytic activity compared to PfCS wt. The mutants are, however, sensitive to thermal inactivation above 80°C. **Figure 4.8** shows the temperature dependence data for the wild-type and mutant PfCS enzymes.

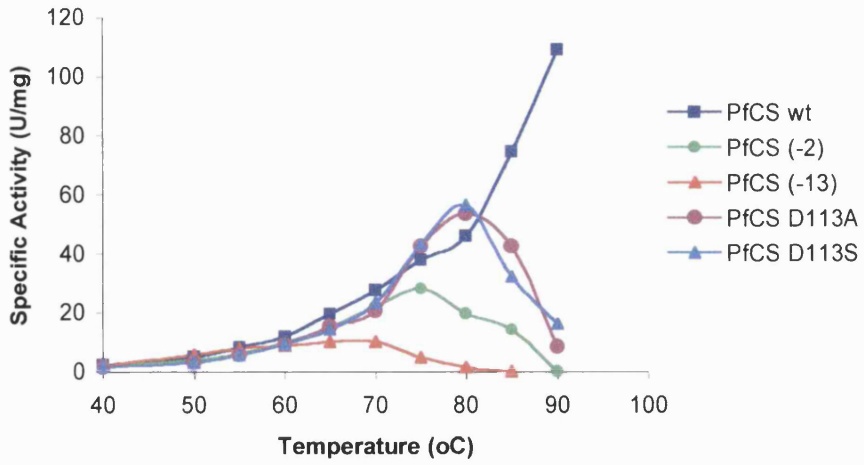

Figure 4.8: Temperature dependence of the catalytic activities of PfCS wt and mutants at pH 7. Data used with permission from Arnott *et al* (2000).

However, the studies reported in this thesis on GdnHCl-induced unfolding suggest that the ΔG of *P. furiosus* citrate synthase is relatively insensitive at the free energy level to the mutations introduced at the subunit interface and C-terminal region. This is also seen with the melting temperature, which seems not to be affected by the mutations in the enzyme. This means that the loss of activity seen above 80°C could be due to the dissociation of the dimer or just unfolding at the active site region of the protein. As the active site of the enzyme is situated between the two subunits requiring residues from both for activity, the dissociation of the dimer would result in a loss of activity.

The analysis of the GdnHCl-induced unfolding of these enzymes resulted in estimates of ΔG values with large errors. As a consequence of these errors, the estimates of ΔG values may not be ideal for making comparisons between the wildtype and mutant enzymes. However, as the thermal unfolding data support the

ΔG values obtained, it can be assumed that the ionic network and C-terminal region mutants are indeed just as stable as the wildtype to thermally- and GdnHCl-induced unfolding.

The observation that the mutants are just as thermodynamically stable as the wild type is unexpected when the proposal that the inter-subunit interactions have been disrupted in these mutants is taken into account. From the proposal, it would be expected that these mutants would be more susceptible to guanidine- and temperature-induced denaturation due to the necessity for the maintenance of the dimer integrity for enzyme activity. The disruptions made to the enzyme as a result of the mutations would be expected to increase the possibility of losing this integrity. The GdnHCl-induced data are consistent with the following suggestions:

1. Mutations give rise to large changes ΔH and ΔS of unfolding, which compensate to give a smaller effect on the ΔG of interaction; this is known as the entropy-enthalpy compensation (Cooper *et al*, 2001).
2. The ionic property of GdnHCl is presumably masking positive and negative side chains, thereby reducing or even totally eliminating any stabilizing or destabilizing electrostatic interactions (Monera *et al*, 1994).
3. The unfolding curve obtained by fluorescence is tracking the progress of the unfolding of the monomer; therefore, one would not expect the ΔG value to change for mutations that do not affect the stability of the monomer. The results would therefore be consistent with the $N_2 \rightleftharpoons 2N \rightleftharpoons 2U$ for Gdn unfolding.

ΔG is defined as: $\Delta G = \Delta H - T\Delta S$. The phenomenon of entropy-enthalpy compensation is widely invoked as an explanation in thermodynamic analyses of proteins (Sharp, 2001). This means that in many chemical processes any change in

enthalpy is partially or completely compensated for by a corresponding change in entropy, resulting in a small net free energy change. Entropy-enthalpy compensation has been suggested to be an intrinsic property of complex, fluctuating or aqueous systems but the physical origin of the behaviour is unclear (Liu *et al*, 2000).

Although mutations such as those introduced in the *P. furisous* citrate synthase may give rise to large changes in ΔH and ΔS, such changes compensate to give a much less effect on the ΔG of interaction (Cooper *et al*, 2001). This suggests that many of the interactions at the subunit interface may be thermodynamically neutral. Cooper and coworkers suggest crucial locations or 'hot spots' i.e. a situation in which just a few interactions at the subunit interface might be responsible for the majority of the free energy of stabilisation but the remainder control structural specificity. The latter may make zero contribution to ΔG in the correct conformation. For this reason, these interactions would be thermodynamically neutral in the sense that they do not contribute to the overall free energy of the interaction but are nonetheless vital for the correct conformation for enzyme activity.

Another conclusion that can be reached is that the ionic property of guanidine is presumably masking positive and negative side chains, thereby rendering or even totally eliminating any stabilizing or destabilizing electrostatic interactions. Monera and coworkers have shown that guanidine cannot discern the contributions of electrostatic interactions (Monera *et al*, 1993, 1994).

A possible explanantion is that the unfolding curve obtained by measuring fluorescence intensity of guanidine-induced unfolding of the enzymes only tracks the progress of the unfolding of the monomer; therefore one would not expect the ΔG value to change for mutations that do not affect the stability of the monomer. The

results are therefore consistent with the three state denaturant-induced unfolding of PfCS wt. It is also reasonable to suggest that the events seen in the denaturant-induced unfolding of the enzyme are distinct from those involved in the thermal inactivation and temperature dependence of catalytic activity studies. Thermal inactivation studies and the temperature dependence of the enzyme activity studies may reflect the stability of the enzyme active site and not the stability of the enzyme as a whole.

The conclusion reached from the data presented here is in contrast to thermal inactivation data collected for each of these proteins at pH 7 (**Figure 4.6**). Thermal inactivation data show that both the C-terminal deletion mutants and the ionic network mutants are considerably less thermostable that the wild-type enzyme when incubated in the absence of substrates at pH 7. This reduction in thermostability is reversed at lower pH values, in that at pH 5 the mutant enzymes seem to be more stable than the wild-type enzyme. The data suggest that, to counteract the loss of ionic interactions, lowering the pH of the environment of the enzyme increases the stability. This is not an expected result of these mutations. In the ionic network mutants, for example, a negatively charged amino acid is replaced with a neutral and a polar amino acid. This is, therefore, not expected to increase the stability of the ionic interactions at the subunit interface.

With the wildtype enzyme, k_{inact} increases with decreasing pH. This suggests a protonation of the aspartate residue (pKa ~ 4.5) as the pH is decreased; which in turn reduces the strength of the ionic interactions at the subunit interface. The enzyme is therefore less stable. The substitution of aspartate causes a change in the position of the remaining three positive charges. Those positive charges might no longer be able to stabilise (i.e. electrostatically interact with) the remaining aspartate residue. Thus as pH decreases, the aspartate becomes partially

protonated and so the enzyme is stabilised. It is unclear as to why the mutants seem to be more stable than the wildtype enzyme at pH 5.

In conclusion, creation of these mutants seems to have altered the rate of thermoinactivation of the enzyme but not the overall stability of the protein.

5. CHAPTER FIVE

ACTIVATION OF CITRATE SYNTHASE AT LOW DENATURANT CONCENTRATIONS

5.1. Introduction

Proteins are dynamic molecules whose motions are important for folding, function and stability. The induced fit theory of enzyme reaction proposes that the structure of an enzyme active site does not fit the substrate exactly but that the presence of substrate induces changes in the active site structure to fit substrate binding (Koshland, 1958). It is also implies that the changed active site (with substrate) is sufficiently structured to perform catalysis efficiently. The occurrence of substrate-induced conformational changes in enzymes has been well documented by a number of x-ray studies. Examples include the closure of the two domains of phosphoglycerate kinase upon the binding of substrates (Berstein *et al*, 1997) and the domain closure of the pig heart citrate synthase enzyme in the presence of the substrates (Remington, 1992). These conformational changes are required to bring the substrates into the correct proximity and orientation for reaction (Price, 2000).

It is possible that each intermediate step of the whole cycle of enzyme catalysis requires the enzyme molecule, especially the active site region, to be in specific conformational states different from one another (Tsou, 1998; Price, 2000). This means that the structural changes accompanying substrate binding and those allowing the products to dissociate will be different. Enzymes must have flexible active sites that undergo rapid conformational transitions to catalyse sequential chemical transformations and to accommodate different chemical intermediates (Fan *et al*, 1996). These conformational changes will generally occur on a very fast

time scale, which means that direct experimental evidence for this theory is difficult to obtain.

Denaturants such as guanidine hydrochloride and urea are commonly used to unfold native proteins and to determine the ΔG of stabilization, but the effects of these chaotropic agents on the enzyme active site flexibility and enzyme catalysis have been rarely studied. GdnHCl dissociates into $GdnH^+$ and Cl^- and because of its ionic character, GdnHCl might not always act as a denaturant only (Mayr & Schmid, 1993). Many enzymes seem to be either activated or inactivated by concentrations of guanidine hydrochloride, urea or organic solvents that are lower than those needed to cause demonstrable structural changes (Tsou, 1998).

It has long been thought that some enzymes are activated by chaotropic agents or limited proteolysis and the activation has been suggested to be the result of the perfection of the active site structure required for maximal catalytic efficiency (Tsou, 1998). Dihydrofolate reductase and alkaline phosphatase have been observed to be markedly activated by salts and chaotropic agents such as urea and guanidine (Duffy *et al*, 1987; Rao & Nagaraj, 1991).

There are two theories as to why there is an increase in enzymic activity in low concentrations of denaturants. The first is that they induce small conformational changes leading to the perfection of the active site and thus increasing catalytic efficiency; the other is they cause the micro-unfolding at the active site region which may make easier the conformation necessary for catalysis. Both theories involve an increase in the flexibility at the active site region.

The specificity of substrate binding depends on the precisely defined arrangements of atoms in an active site, and a substrate will bind better to some conformations

and not to others (Koshland, 1958). The enzyme and the substrate interact via means of short-range forces and, therefore, an increase in the flexibility of the active site could ensure that the enzyme and substrate are in close contact. Micro-unfolding is a phenomenon that has been observed in enzymes (Fontana *et al*, 1998). This is said to be due to the local disruption of a few weak interactions so that initially buried sites become exposed to solvent. This phenomenon has been observed as a function of temperature and certain other denaturants.

Several approaches have been used to investigate protein dynamics and the role of active site flexibility in enzyme catalysis. These include x-ray crystallography, hydrogen exchange experiments, NMR and fluorescence quenching. Fluorescence quenching was used to study the conformation and folding of PfCS in the presence of guanidine hydrochloride.

Fluorescence quenching is a process that decreases the intensity of the fluorescence emission. Fluorescence quenching reactions are an important tool for studying the location of fluorescent groups in proteins. Quenching may occur by several mechanisms: collisional or dynamic quenching, static quenching, quenching by energy transfer and by charge transfer reactions (Lakowicz, 1999). Only collisional quenching will be discussed in this chapter. Collisional quenching is one of the most important mechanisms where close contact of the quencher and the fluorophore in an excited state is required. The fluorescence intensity and lifetime of the excited state of the fluorophore are governed by the kinetics of the reaction. In an analysis employing fluorescence quenching, first the fluorophore whose fluorescence is quenched by target species is identified and, then, using known concentrations of the quencher, a number of measurements are performed. It is customary to treat the quenching data using the Stern-Volmer equation to determine the extent of quenching and hence the accessibility of a fluorophore.

A number of compounds have been identified as quenchers of molecular fluorescence. In fact, it is always possible to find a quencher that will quench a fluorophore, but the problem is to find a fluorophore that is selectively quenched by the target quencher (Lakowicz, 1999). Due to the non-specific nature of fluorescence quenching, practically any event can affect one or more of the aspects related to the fluorophore. However, there are several molecules that are commonly used as quenchers. Their advantages are that they are small, aqueous, soluble and do not denature proteins by themselves. These include:

- Iodide - because of its charged nature it efficiently quenches surface residues.
- Oxygen - small and can penetrate the protein to some degree.
- Acrylamide, succinimide, nitroxides - neutral.

Quenchers with different size and charges differentiate the charge versus steric effect. Acrylamide and succinimide are effective quenchers because they are large molecules. With these molecules there is a good relationship between the extent of quenching and the accessibility of the fluorophore, as judged by the emission maximum (fluorescence intensity) (Eftink & Ghiron, 1976). The limited quenching of buried residues is mainly due to limited penetration of the quencher into the protein structure, with the quenching being determined by the opening of pores large enough to accomodate a quencher molecule. The larger the quencher the more deformations of the protein structure must occur in order to allow access of the quencher to the buried fluorophore. The accessible fluorophores experience a decrease in fluorescence upon collision with collisional quenchers. Thus, quenching measurements can give general information about protein flexibility.

Interpretation of data

The apparent quenching rate constant is determined by either a fluorescence intensity or lifetime Stern-Volmer plot. When quenching occurs by a collisional mechanism, the quenching is an additional process that deactivates the excited state; therefore, the decrease in fluorescence intensity equates to the decrease in fluorescence lifetime. In a quenching reaction between an excited state of a chromophore, M*, and a quencher Q

$$M^* + Q \rightleftharpoons (M^*....Q) \rightarrow (M....Q)$$

The encounter complex (M*....Q) that is formed reacts to dissipate the electronic energy by some internal mechanism. Stern and Volmer derived the following relationship to describe collisional quenching under steady state conditions (Stern & Volmer, 1919).

$$\mathbf{F_0/F = 1 + k_Q\tau_O[Q] = 1+ K_D\,[Q]}$$

In this equation, F_0 and F are the fluorescence intensities in the absence and presence of quencher respectively. k_q is the apparent bimolecular rate constant for the collisional quenching process, τ_0 is the lifetime of the fluorophore in the absence of quencher and [Q] is the concentration of the quencher. The Stern-Volmer quenching constant is given by $k_q\tau_o$ represented by K_{SV}. Quenching data are usually presented as plots of F_0/F versus [Q]. This is because F_0/F is expected to be linearly dependent on the concentration of quencher. A plot of F_0/F, known as a Stern-Volmer plot, has an intercept of unity at the y-axis and a slope equal to K_{SV}. K_{SV}, the Stern-Volmer constant determines the accessibility of the fluorescent residues and hence can be used to determine the dynamics of a protein. It is useful to note that $1/K_{SV}$ is the concentration at which $F_0/F = 2$ or 50% of the fluorescence intensity is quenched.

A linear Stern-Volmer plot is generally indicative of all fluorophores being equally accessible to the quencher. It does not prove, however, that collisional quenching has occurred. If two groups of fluorophores are present i.e. one group is not accessible to the quencher, then the Stern-Volmer plot can deviate from linearity. This is the result frequently found for the quenching of tryptophan fluorescence in proteins as quenching molecules do not readily penetrate the hydrophobic interior of the proteins and only tryptophan residues on the surface are quenched (Lakowicz, 1999). The Stern-Volmer equation can be used to determine the portion of these fluorophores that are exposed to the aqueous solvent. This has resulted in the use of tryptophan fluorescence quenching to determine the fluctuation of a protein structure (Eftink & Ghiron, 1987).

Citrate synthase contains tryptophan residues some of which are buried within the protein structure, *b* and others that are exposed on the surface, *a*. In this case, the Stern-Volmer plot may display a downward curvature (Lakowicz, 1999). The total fluorescence in the absence of quencher is given by:

$$F_0 = F_{0a} + F_{0b}$$

where F_0 is the total fluorescence, F_{0a} is the fluorescence of the surface residues and F_{0b} is the fluorescence of the buried residues.

In the presence of quencher, the intensity of the accessible fluorophores decreases according to the Stern-Volmer equation whereas the buried fraction is not quenched. Therefore the observed intensity is given by:

$$F = F_{0a} / (1+K_{SV}[Q]) + F_{0b}$$

Then

$$dF = F_o - F = F_{oa}\{K_{SV}[Q] / (1+K_{SV}[Q])\}$$

$$F_o/dF = 1 / (f_a K_{SV}[Q]) + 1/f_a$$

K_{SV} is known as the Stern-Volmer constant and **[Q]** is the concentration of quencher.

This is the Stern-Volmer equation first described by Lehrer (1971) where f_a is the fraction of accessible fluorophores and f_b is the fraction of buried fluorophores.

$$f_a = f_{0a} / (f_{0a} + f_{0b})$$

This modified Stern-Volmer equation allows f_a and K_{SV} to be determined from a plot of F_o/dF versus $1/[Q]$. The intercept is $1/f_a$ and $1/f_aK_{SV}$ is the slope.

When performing quenching experiments, it is important to ensure that the quencher does not have an adverse effect on the protein. Some quenchers such as 2,2,2 trichloroethanol are known to bind to proteins and induce conformational changes (Eftink & Ghiron, 1976). For the purposes of this study it is imperative that the quencher, succinimide, does not bind to the protein. Several studies have shown that quenchers such as succinimide and acrylamide do not bind to proteins (Eftink & Ghiron, 1987), although some studies have suggested otherwise (Bastyns & Engelborghs, 1992).

Although the interaction of succinimide and the aromatic residues in citrate synthase is not known, it is assumed that no protein-succinimide interaction occurs, quenching is collisional and the efficiency is equal to unity.

5.2. Methods and Results

5.2.1. Activation of citrate synthase in the presence of GdnHCl

For the purposes of these activation studies, it was essential that the enzyme possessed a suitable level of activity in the absence of GdnHCl in order to follow the activation process. 10μg/ml enzyme solutions were incubated in varying concentrations of GdnHCl (0-6M). The GdnHCl-induced unfolding of the enzyme was then monitored via the DTNB citrate synthase activity assay. Assays were carried out after an incubation of one hour and were carried out at the incubation temperature. Enzyme activity was also measured both in the absence and in the highest concentration of denaturant in which the enzyme was incubated. This illustrated that the change in absorbance at 412 nm was not affected by the presence of GdnHCl. The enzyme activity at each GdnHCl concentration was expressed as a percentage of the activity in the absence of GdnHCl. The data are shown in **Figure 5.1**. **Figure 5.1** is the same as **Figure 3.4** but has been reproduced here for clarity.

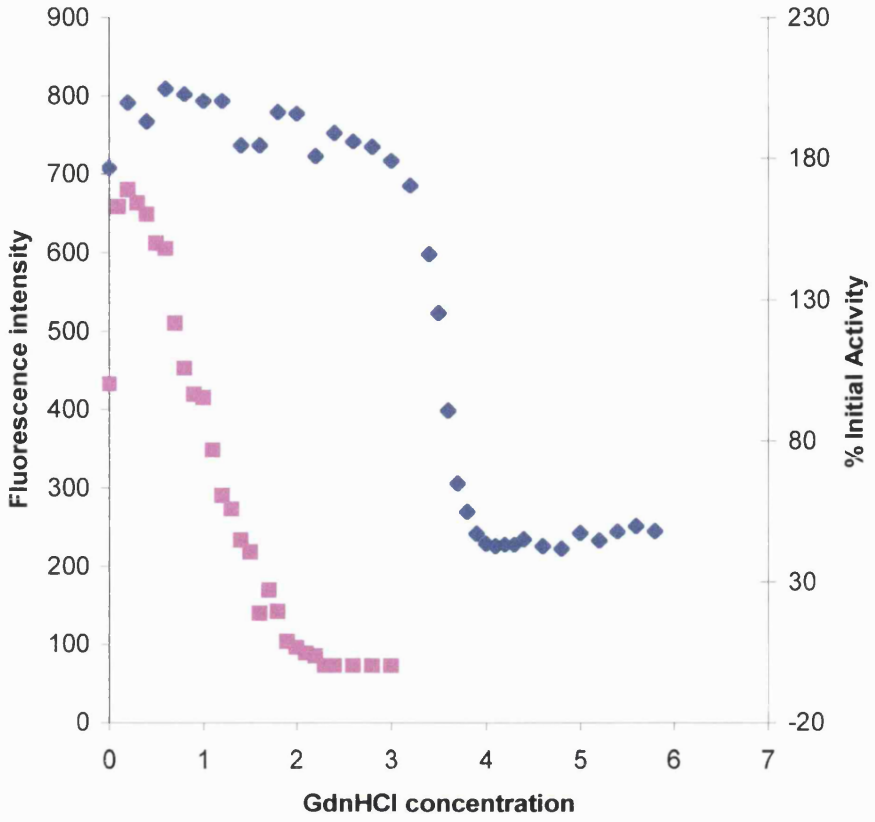

Figure 5.1: GdnHCl-induced unfolding of *P. furiosus* citrate synthase at 50°C as monitored by fluorescence spectroscopy and enzyme activity. The protein was incubated in varying concentrations for one hour (before enzyme activity assays) and overnight (for fluorescence measurements). Activities are expressed as a percentage of initial activity of the enzyme in the absence of GdnHCl.

At low concentrations of GdnHCl, an increase in activity was observed for the enzyme. This increase in activity does not seem to affect the structure to an extent that a change in the fluorescence signal is registered. The activity increases markedly with increasing concentrations of GdnHCl up to 0.5M. With further increases in GdnHCl concentration, the activity drops, and the enzyme becomes completely inactivated at GdnHCl concentrations higher than 2.4M. Changes in fluorescence emission are also shown in **Figure 5.1**. At GdnHCl concentrations

lower than 2.4M, the range over which the enzyme is activated and then completely inactivated, there is no observable change in fluorescence emission

An analysis of the denaturant-induced activation/inactivation of the enzyme at different temperatures was carried out to determine the effect of temperature on this increased activity.

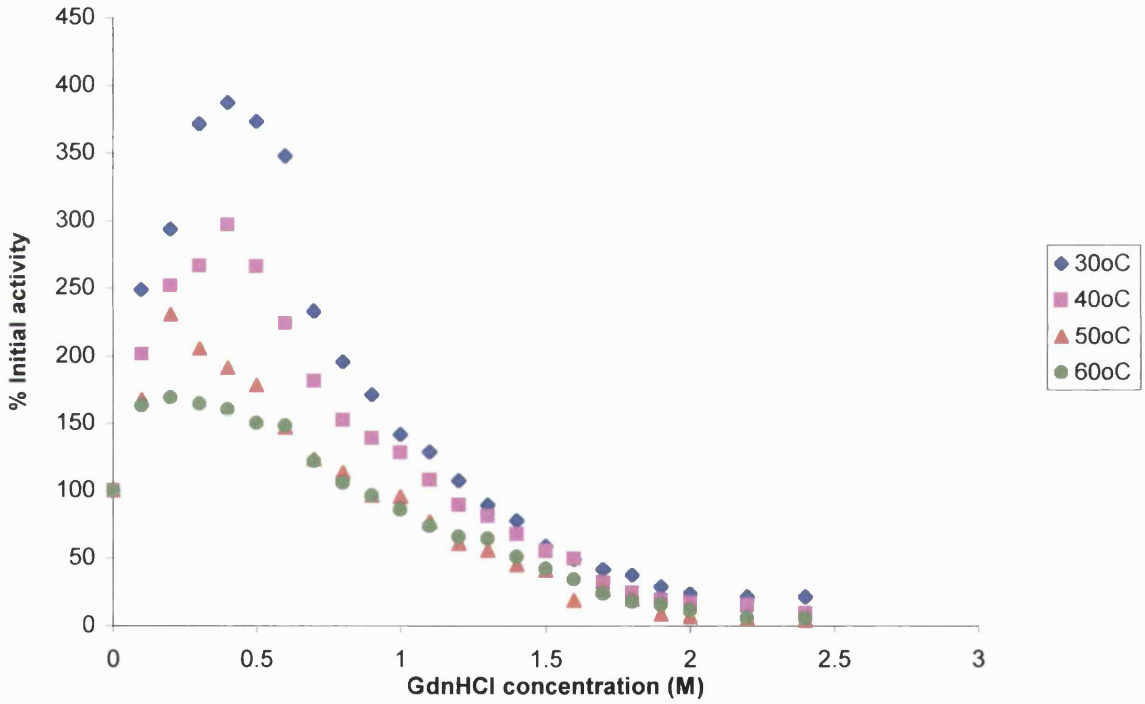

Figure 5.2: Activation of PfCS wt in the presence of low concentrations of GdnHCl at different temperatures (20-60°C).

The data show a decrease in the GdnHCl-induced activation of the enzyme as the temperature is increased. This suggests that as the temperature increases the need for the denaturant is reduced and that the enzyme is reaching its optimal flexibility.

These observations can be taken as an indication that the enzyme is activated by loosening of the structure either in the presence of denaturant or by heat and that the two produce a synergistic effect. The concentration at which the enzyme is fully denatured does not change, however, with the temperature increase.

A number of studies have shown that flexibility at the active site is essential for full expression of the enzyme activity. An enzyme will reach its optimal flexibility (and hence activity) around its physiological temperature. Therefore, at temepratures below this, the reduced flexibility limits the catalytic rate and that GdnHCl can overcome this rigidity and so activate the enzyme.

The results of an investigation of the GdnHCl-induced unfolding of the *P. furiosus* mutant citrate synthases are shown in **Figure 5.3**. In the case of PfCS (–2), PfCS (D113A) and PfCS (D113S) mutants, the relative activities increased in the same manner as that of the wildtype enzyme. There was, however, a more pronounced activation of the PfCS (-2) enzyme at 30°C. The PfCS (–13) enzyme was completely denatured at 0.5M GdnHCl with no activation effects at lower concentrations.

(a)

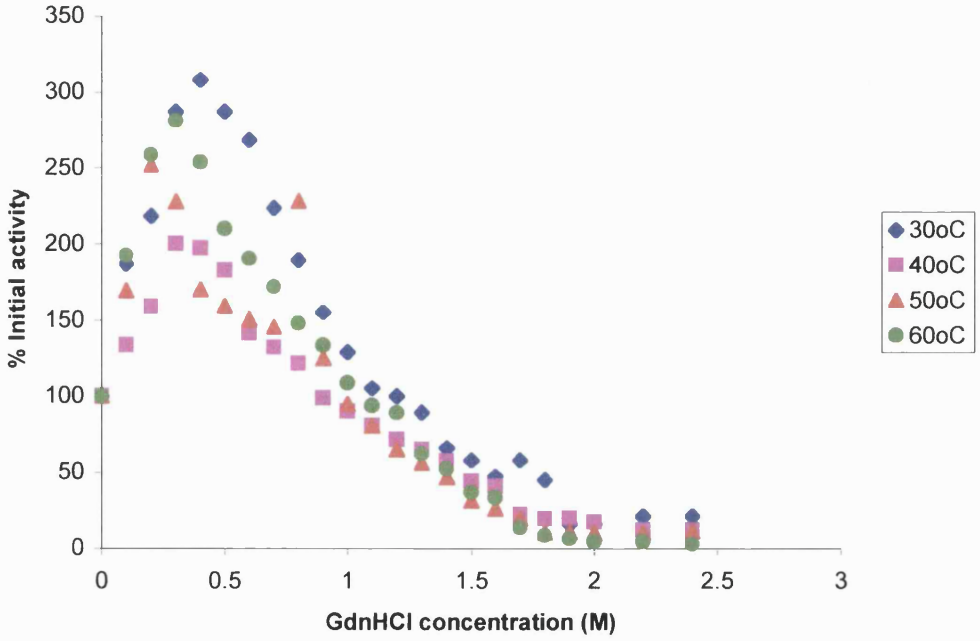
350
300
250
200
150
100
50
0
% Initial activity
0
0.5
1
1.5
2
2.5
3
GdnHCl concentration (M)
30oC
40oC
50oC
60oC

(b)

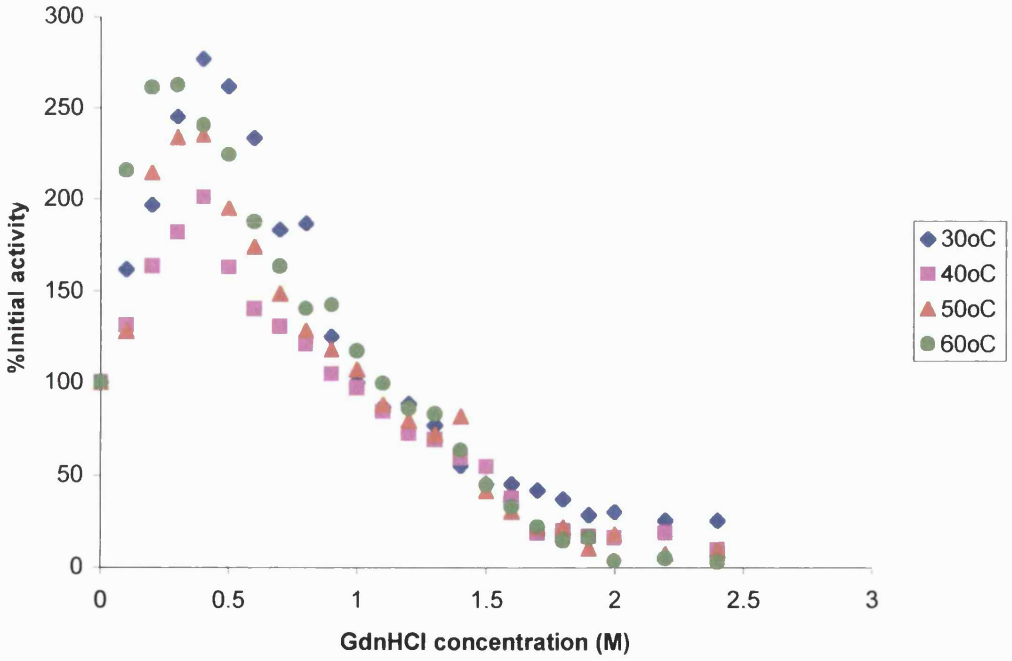
300
250
200
150
100
50
0
%Initial activity
0
0.5
1
1.5
2
2.5
3
GdnHCl concentration (M)
30oC
40oC
50oC
60oC

(c)

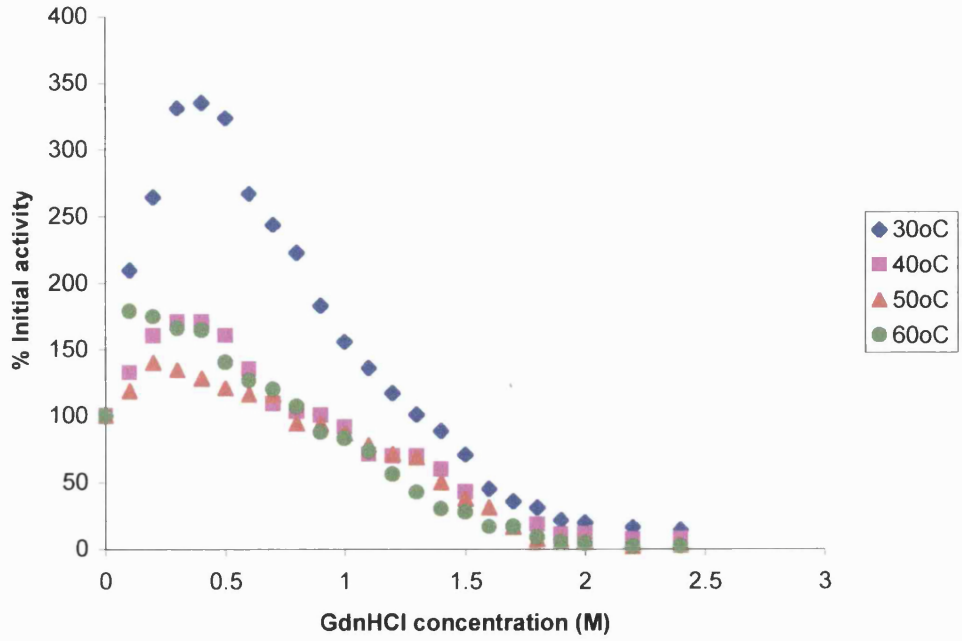
400
350
300
250
200
150
100
50
0
% Initial activity
0
0.5
1
1.5
2
2.5
3
GdnHCl concentration (M)
30oC
40oC
50oC
60oC

(d)

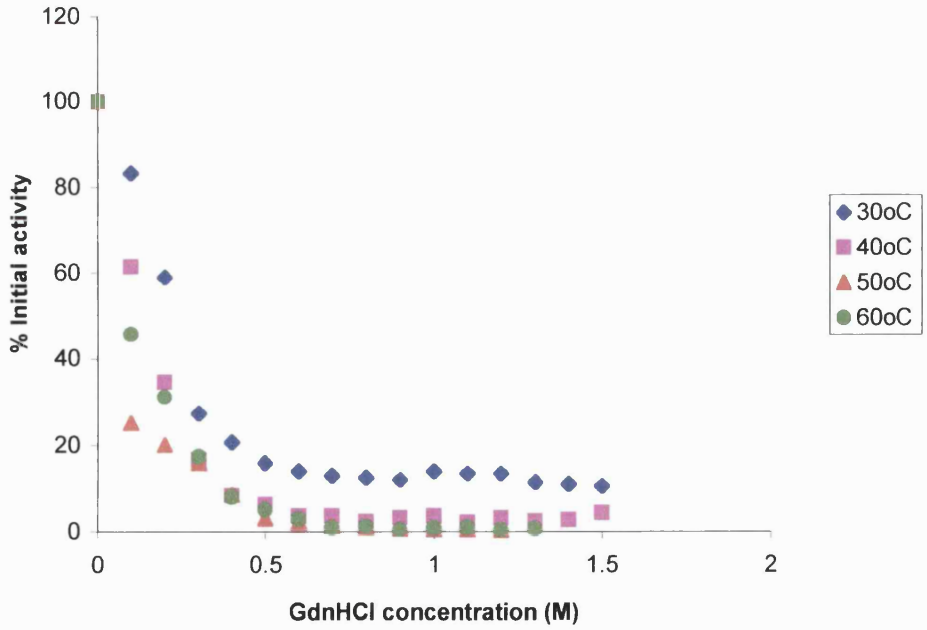
120
100
80
60
40
20
0
% Initial activity
0
0.5
1
1.5
2
GdnHCl concentration (M)
30oC
40oC
50oC
60oC

(e)

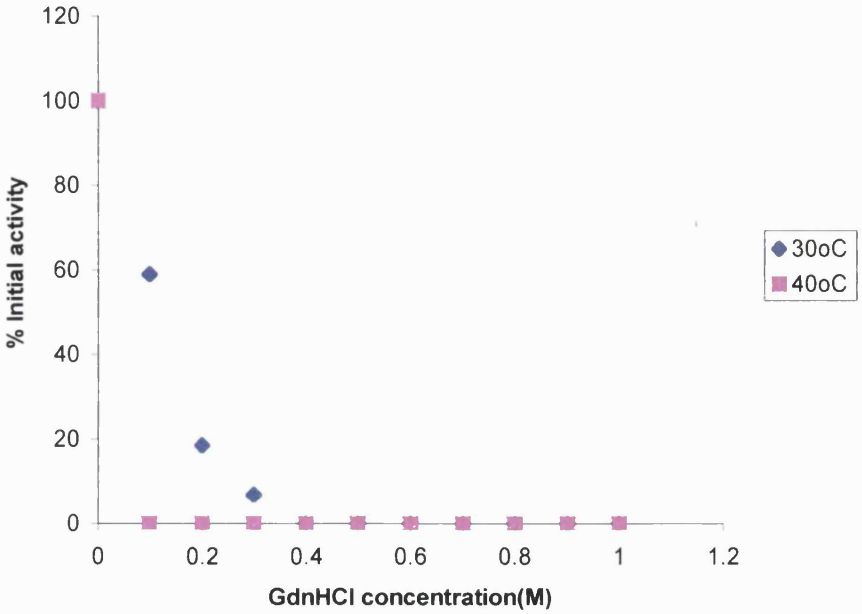

Figure 5.3: Activation of (a) PfCS (D113A), (b) PfCS (D113S), (c) PfCS –2, (d) PfCS –13, (e) *Arthrobacter* CS in the presence of low concentrations of GdnHCl at 30°C (◆), 40°C(■), 50°C(▲) and 60°C(●).

5.2.2. Thermal inactivation studies in the presence of GdnHCl

The aim of this set of experiments was to determine whether incubating citrate synthase in these low concentrations of GdnHCl would affect the enzyme's stability against thermal inactivation. Thermal inactivations were therefore carried out by incubating the enzyme in 50mM sodium phosphate, pH 7, 2mM EDTA, in the presence and absence of 0.5M GdnHCl, using an enzyme concentration of 100μg/ml. 100μl aliquots in 0.5ml PCR tubes were incubated at varying temperatures in an Eppendorf Mastercycler. Tubes were removed at timed intervals

and rapidly cooled in an ice/water bath. DTNB/412nm assays were carried out to determine residual enzyme activity (**Figure 5.4**).

(a)

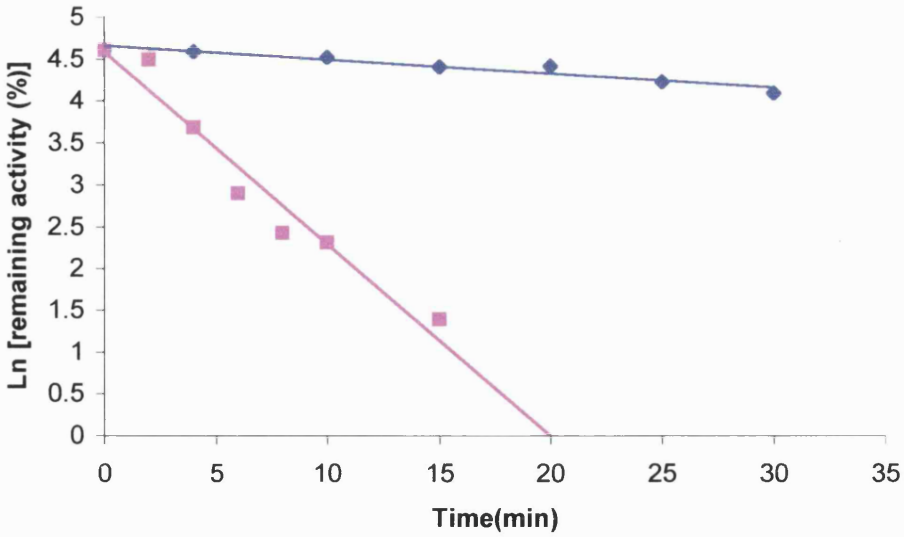

(b)

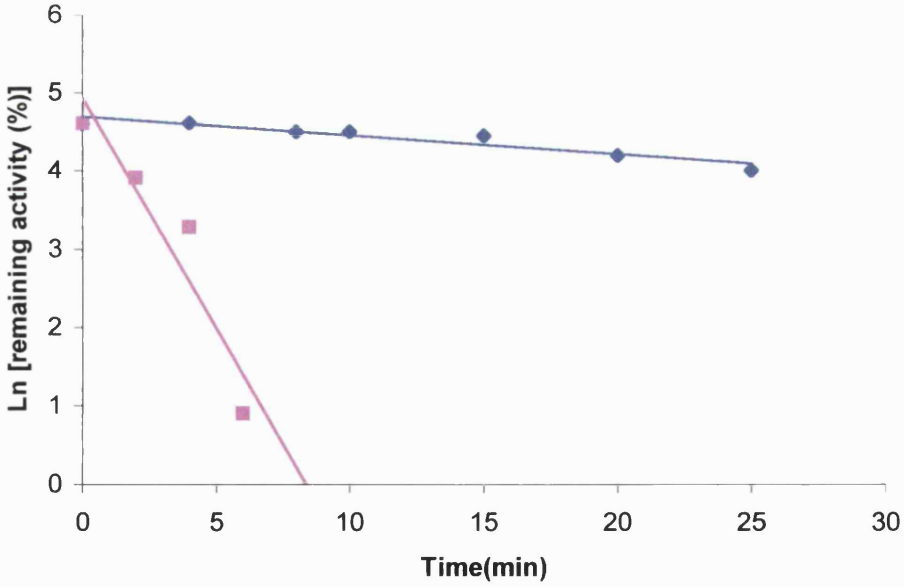

Figure 5.4: Thermal inactivation data of *P. furiosus* citrate synthase. The enzyme was incubated in buffer (◆) and in buffer containing 0.5M Gdn (■) at varying temperatures (a) 95°C and (b) 97°C.

The data show that in the presence of activating concentrations of GdnHCl the enzyme is more rapidly inactivated than in the absence of denaturant. This is therefore consistent with the proposal that low concentrations of GdnHCl activate the enzyme by increasing the flexibility of the enzyme active site.

5.2.3. Effect of GdnHCl on the kinetic parameters of PfCS wt

To determine the manner in which the presence of low concentrations of GdnHCl increase the activity of the enzyme, the K_M and V_{max} values of PfCS wt in the presence of 0.5M GdnHCl were determined. For the determination of kinetic parameters, assays were carried out in varying concentrations of one substrate whilst the other substrate was fixed at a high concentration (~20 x K_M).

The enzyme was incubated at 55°C for an hour in 50mM sodium phosphate buffer, pH7, 2mM EDTA, in the presence and absence of 0.5M GdnHCl, after which the kinetic analysis was carried out.

The concentration of OAA and AcCoA were determined enzymically using PigCS.

K_M and V_{max} values were calculated from the data by the direct linear plot of Eisenthal & Cornish Bowden (1974) using Enzpack 3 computer software (Biosoft, Cambridge UK). The kinetic data are summarised in Table 5.1. The Michaelis-Menten plots obtained are shown in **Appendix IV**.

Table 5.1: A summary of the kinetic data for PfCS wt in the absence and presence of 0.5M GdnHCl.

GdnHCl concentration	K_M AcCoA (μM)	K_M OAA (μM)	Vmax (μmol/min/mg)
0M	8 (± 0.7)	10 (± 0.3)	11 (±1)
0.5M	79 (± 4.1)	32 (± 1.3)	41 (±1.8)

The activation initially observed was approximately 2.5 fold (Figure 5.1). In this experiment, the data show that this is due to a 4-fold increase in the Vmax but a 3-10 fold increase in the K_M.

5.2.4. Fluorescence quenching of aromatic residues

Since the rate of quenching of tryptophan fluorescence in a globular protein is dependent upon the fluctuation of protein structure (Eftink & Ghiron, 1987), the ability of succinimide to quench the fluorescence of the tryptophans in *P. furiosus* citrate synthase incubated in 0.5M GdnHCl was measured. A comparative analysis of the flexibility of the *P.furiosus* enzyme and the psychrophilic *Arthrobacter* citrate synthase was also conducted.

10μg/ml of PfCS and DSCS were incubated separately in the presence and absence of 0.5M GdnHCl for one hour at 25°C. Fluorescence quenching experiments were then carried out with 30μg of each of these proteins. Experiments lasted thirty minutes in order to avoid any denaturation of the protein. It was found to be convenient to add 20μl aliquots of a 2M succinimide solution up to a final volume of 3.4ml of a single sample solution in a 3.6ml fluorimetric cuvette. Final concentrations of succinimide ranged from 0-235mM. The fluorescence of

succinimide was negligible and therefore there was no need to correct quenching values. An excitation wavelength of 295nm was used and the emission wavelength was 340nm. Measurements were carried out using a Perkin Elmer LS 50B with a 1cm pathlength cell, and the data obtained were then plotted in a Stern-Volmer fashion as shown in Figure 5.6.

(a)

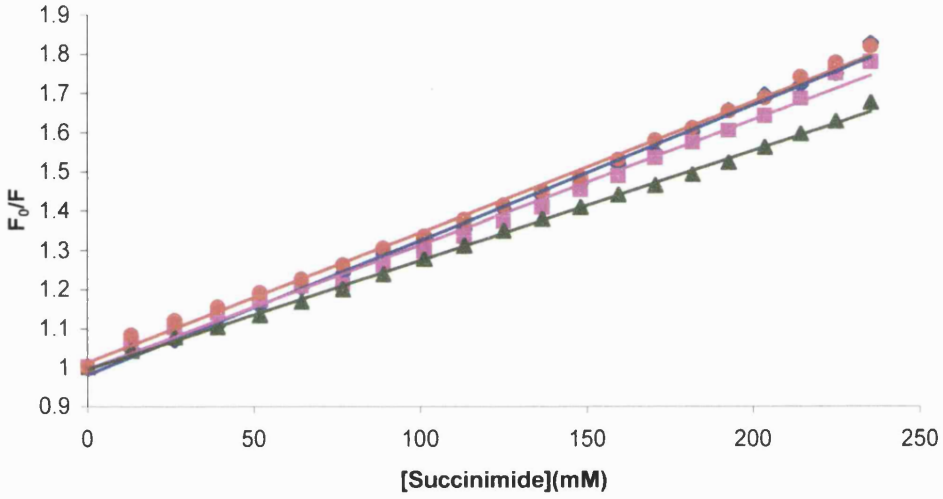

(b)

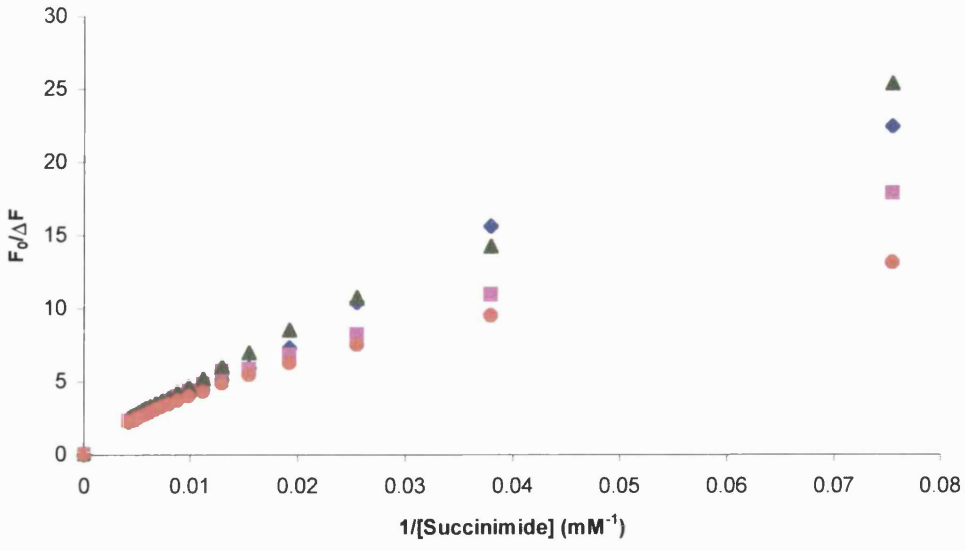

(c)

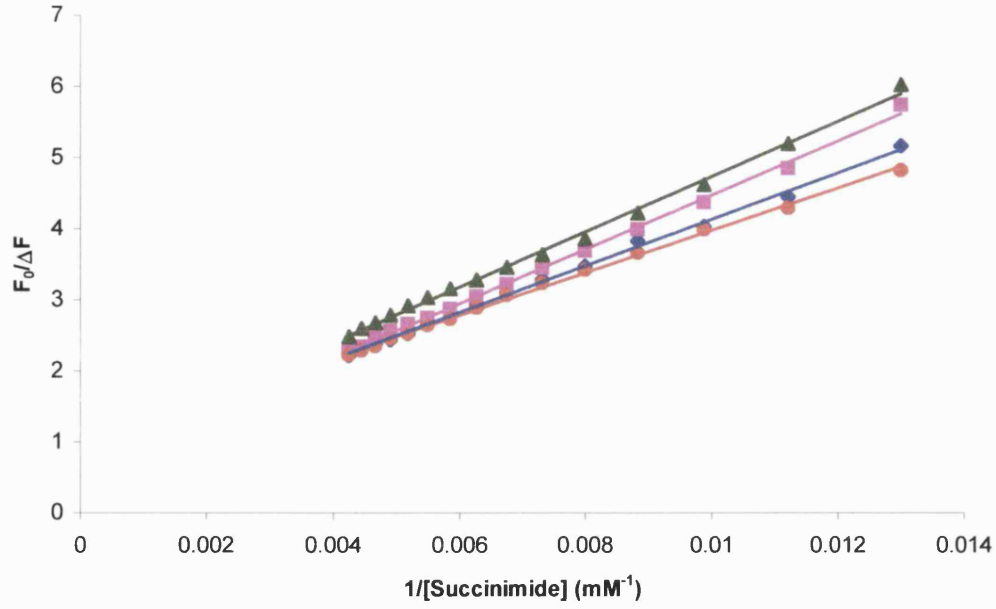

Figure 5.6: Stern-Volmer plots for the fluorescence quenching of accessible tryptophan residues in citrate synthase. The figure shows (a) the Stern-Volmer plot, (b) a modified Stern-Volmer plot and (c) the linear portion of the modified Stern-Volmer plot of PfCS in the absence of GdnHCl (◆) and in 0.5M GdnHCl (■), and also with *Arthrobacter* citrate synthase (DSCS) in the absence of GdnHCl (▲) and in 0.5M GdnHCl (●).

The Stern-Volmer plot shown in Figure 5.5a shows a linear plot. This is misleading as the replot of the data according to the modified Stern-Volmer equation of Lehrer Figure 5.5b shows a downward curvature. The downward curvature of this plot confirms that there are two populations of tryptophan residues in the protein – one accessible to the succinimide and the other buried within the protein structure and hence not accessible to the quencher. The modified form of the Stern-Volmer plot allows the fraction of accessible tryptophan residues (f_a) and the Stern-Volmer constant (K_{SV}) to be determined.

Table 5.2 shows the K_{SV} and f_a values obtained for both the thermophilic *P. furiosus* citrate synthase and the psychrophilic *Arthrobacter* citrate synthase in the presence and absence of GdnHCl. K_{SV1} were determined from F_0/F vs [Q] plots whereas K_{SV2} and f_a values were determined from the linear portions of their respective modified Stern-Volmer plots by linear regression.

Table 5.2: The quenching parameters of the succinimide quenching of citrate synthase at 25°C.

	Slope	Intercept	f_a	K_{SV1} (M^{-1})	K_{SV2} (M^{-1})
PfCS 0M Gdn	326.73	0.86	1.16	3.4	3.1
PfCS 0.5M Gdn	381.36	0.65	1.54	3.2	2.6
DSCS 0M Gdn	388.35	0.84	1.18	2.8	2.6
DSCS 0.5M Gdn	298.23	0.99	1.00	3.2	3.4

The values of f_a, the fraction of accessible residues obtained for both enzymes in the presence and absence of denaturant shows that nearly all the fluorophores are accessible. This is because only the linear portion of each plot was used in the calculations and hence a distorted picture is seen. This could be solved by using a non-linear least squares procedure which was not used in this case. The Stern-Volmer constants K_{SV}, determined are very similar in all cases. This suggests that either there is very little difference between the environments of the residues in both proteins or the quencher is not in physical contact with the tryptophan residues and therefore little quenching is occurring. All analyses assume the same fluorescence lifetime of the tryptophan residues (τ_0) in the presence and absence of GdnHCl.

5.3. Discussion

The effects of low concentrations of guanidine hydrochloride and of urea on the functional and structural properties of *P. furiosus* citrate synthase have been characterized. This is a novel finding that low denaturant concentrations (up to 0.5M GdnHCl and 3M urea) activates the thermophilic citrate synthase.

The results provide evidence that GdnHCl and urea produce dual effects – a stimulating effect and a denaturation effect (see Chapter 3 for urea activation of PfCS). When present at low concentrations, guanidine seems to increase the flexibility of PfCS, while at high concentrations it leads to unfolding of the protein. There seems to be a favourable interaction (for activity) of guanidine with the protein at low concentrations of the denaturant. The initial state of activation of the enzyme may involve conformational changes mostly at the active site region only; further unfolding is accompanied by changes of the enzyme molecule as a whole, which can then be detected by the commonly employed physical methods.

The increase in activity of citrate synthase at low concentrations of denaturant has been attributed to a decrease in the rigidity of the enzyme due to the denaturant present. It is thought that thermostable and mesophilic enzymes exhibit the same level of flexibility at their respective optimal temperatures (Daniel *et al*, 1996; Zavodsky *et al*, 1998; Fontana *et al*, 1998). It is often observed that the catalytic activity of an enzyme from a hyperthermophile, measured at its physiological temperature, is approximately the same as that for the mesophilic homologue measured at its temperature. Thermophilic and hyperthermophilic enzymes, therefore, are usually poor catalysts at room temperature and this is thought to be due to their rigidity at lower temperatures brought about by a variety of interactions and forces used to stabilise these proteins against heat denaturation. This rigidity

has an adverse effect on their catalytic efficiency since an appropriate degree of flexibility is required for enzyme catalysis.

The inverse correlation between enzyme activity and thermostability has been demonstrated in several cases. For example, Varley and Pain (1991) studied the relationships between stability, dynamics and enzyme activity in 3-phosphoglycerate kinase (PGK) from yeast, the moderate thermophile *B. stearothermophilus* and the hyperthermophile *Thermus thermophilius* HB8. The enzyme is a two-domain protein and operates a hinge bending mechanism and consequently its activity would be expected to be dependent upon large-scale dynamics due to domain movements. The thermophilic enzyme is more stable than the mesophilic enzyme but is less active at ambient temperature. Near the temperatures of their respective activity optima, flexibility differences disappear. Consequently, when thermophilic enzymes are assayed at temperatures lower than their optimum, there is a decrease in activity due to the loss of molecular flexibility that is essential for both substrate binding and catalytic action (Danson *et al*, 1996).

Comparison of the activities of natural series of homologous enzymes with different thermostabilities often shows that each member of any one series has approximately the same activity at its temperature optimum. **Table 5.4** shows the V_{max} values of four of the citrate synthases, where it can be seen that the activity achieved is fairly constant over a 60°C range. It is also worth stating that these enzyme possess almost identical active site residues and conformational positions.

Table 5.4: Catalytic activity of mesophilic and thermophilic citrate synthases (Danson & Hough, 2003).

Source organism	Assay temperature (°C)	Vmax (μmol/min/mg enzyme)
Pig	37	280
Thermoplasma acidophilum	60	170
Sulfolobus solfataricus	80	275
Pyrococcus furiosus	95	240

Enzyme flexibility is an essential requirement for catalysis. This flexibility is particularly important for citrate synthase whose active site occupies a cleft between the two subunits. As mentioned earlier, citrate synthase is a dimer and each monomer comprises a large domain containing 15 helices and a small domain containing 5 helices with the active site cleft between them (Gerstein *et al*, 1994). OAA binds first causing a major conformation change and the binding of the acetyl CoA is accompanied by the closing of the cleft over the substrates. The domain closure involves movement of the small domain over the large one burying the substrates (Remington, 1992). An extensive interface between the large and small domain prevents closure taking place through a hinge mechanism. Citrate synthase is thought to have a rigid-body hinge movement of the active site (Gerstein *et al*, 1994). There are considerable changes within the small domain/ large domain, which contributes to the observed closure of the cleft. The *P. furiosus* citrate synthase is thought to have a rigid structure at temperatures lower than physiological whereas the psychrophilic *Arthrobacter* enzyme shows adaptation consistent with its cold-active nature.

The hinge movement of the active sites of citrate synthase for catalysis requires overcoming an energy barrier, although this energy barrier is small. The evidence

currently available suggests that the open and closed states are only slightly different in energy (Gerstein *et al*, 1994). A slight loosening of the structure in the presence of low concentrations of GdnHCl may reduce this energy barrier and hence increases the efficiency of the enzyme. Activation of the some of these enzymes at low concentrations of GdnHCl results from the denaturant pushing the enzymes towards the more flexible form, which exists at the optimum temperature. Hence in the presence of 0.5M GdnHCl at low temperatures, PfCS wt probably assumes a flexible structure that is comparable to that achieved at ~100°C. However, the term flexibility encompasses a wide range of local and global dynamic properties of an enzyme.

This increase in activity in low concentrations of GdnHCl was not observed with *Arthrobacter* citrate synthase, the psychrophilic enzyme, and one of the C-terminus mutants, PfCS (–13). This may be attributed to the fact that at the assay temperature, these enzymes are close to their maximum flexibility. These enzymes would therefore be flexible even in the absence of GdnHCl and thus the addition of denaturant immediately begins the inactivation process. This strengthens the argument for the importance of structural flexibility in catalysis and an increase in flexibility with the addition of GdnHCl. It is generally accepted that psychrophilic enzymes are more flexible, in order to allow easy accommodation and transformation of substrates at low energy costs (Gerday *et al*, 2000). Another possibility is that in the case of the PfCS (–13) mutant, the whole C-terminal arm has been removed from where it emerges from inside the protein. The hinge of the active site could be close to this area, and therefore any attempts to increase the flexibility of this region results in the unfolding of the region.

There is much experimental evidence indicating that protein dynamics play an important role in enzyme catalysis. Flexibility believed to be essential for enzyme

activity can only be relative and limited to specific molecular regions. The conformational state of a protein can, therefore, have an influence on the exposure of its tryptophan residues to solvent and the study of the environment of these residues can yield data on the flexibility of the protein. Fluorescence quenching techniques have been used to obtain experimental data concerning protein dynamics. Quenching can be used to reveal certain details concerning the environment of tryptophan residues by comparing the profiles of a protein in different conditions (Eftink & Ghiron, 1987).

The dependence of the fluorescence intensity of the tryptophan residues upon the concentration of quencher is described by the Stern-Volmer equation. When the Stern-Volmer constant, K_{SV}, and the fluorescence lifetime of the fluorophore in the absence of quencher, τ_0, can be obtained for individual tryptophan residues in a protein, the k_q, the collisional quenching constant, can be determined. This provides information concerning the degree of exposure of the residues and, hence, information on protein dynamics.

Presented in Figure 5.6 are the results, plotted in Stern-Volmer fashion, of succinimide quenching studies of PfCS and DSCS in the presence and absence of 0.5M GdnHCl. The modified Stern-Volmer plot showed a downward curvature suggesting the presence of two fluorescing species - one accessible and the other buried within the protein and therefore inaccessible. The local flexibility around the active site could not, however, be observed by fluorescence quenching. K_{SV} values determined suggest either the quencher was inefficient or that any accessible residues were being quenched before the introduction of the target quencher. It is also possible that the quenching of the accessible residues was not being detected because the majority of the trytophan residues are within the protein structure and inaccessible to the quencher. An overall change in fluorescence intensity would

therefore be dependent on the majority of residues, which are inaccessible. Another possibility is that the equation used to calculate the K_{SV} was inappropriate - the quenching mechanism was assumed to be collisional and it is possible also that GdnHCl quenches the fluorescence of the trp residues before the addition of the succinimide.

Figure 5.7 shows the positions of tyrosine and tryptophan residues in the active sites of the PfCS and DSCS enzymes. Flexibility of the enzyme brought about by the presence of the denaturant is thought to affect this area. It was therefore thought that by quenching these active site residues the flexibility of the enzyme would be observed. These experiments to study the dynamics of *P. furiosus* citrate synthase in the presence of low GdnHCl were unsuccessful. The results did not indicate the accessibility of tryptophan residues or whether the incubation of the enzyme in 0.5M GdnHCl resulted in a change of conformation.

(a)

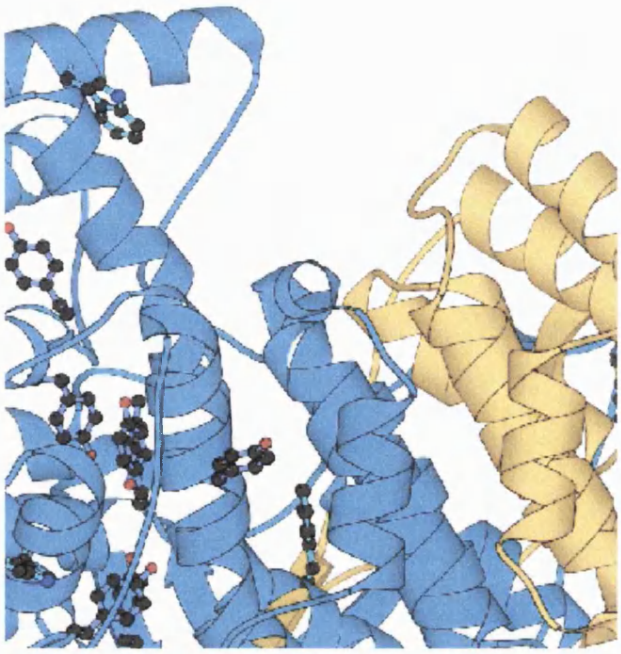

(b)

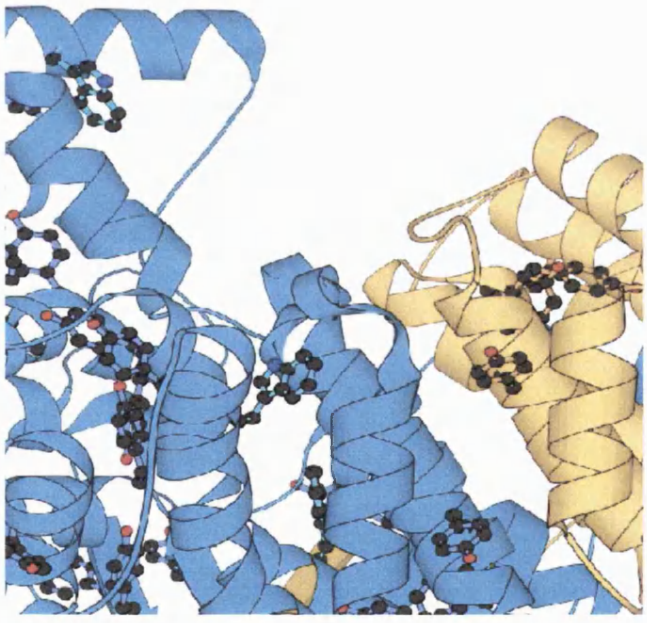

Figure 5.7: Tyrosines and tryptophan residues found in the active site of (a) *Arthrobacter* citrate synthase and (b) *P. furiosus* citrate synthase. The two polypeptides in each of the homdimeric structures are shown in blue and yellow respectively.

To study the activation of citrate synthase by fluorescence quenching, a fluorescent probe introduced at the active site of the molecule, which had a better sensitivity than the aromatic residues present in the protein, would be beneficial, as the aromatic residues in the active site seem to be quenched or perhaps overshadowed by the remaining aromatic residues within the protein. Fluorescence emission is an average of the emission of the aromatic residues present in the protein. As the majority of aromatic residues are buried within the protein, the accessible aromatic residues when quenched are perhaps not observed. A fluorescent probe in the active site would enable us to see any changes in the flexibility of the active site by studying the quenching of the probe in the presence and absence of low concentrations of denaturant.

This increase in activity in low concentrations of denaturants suggests the possibility of the use of thermophilic and hyperthermophilic enzymes in catalysing reactions at low and moderate temperatures with thermophilic enzymes. It would be interesting to examine whether this increase in enzyme activity is common in all thermophilic and hyperthermophilic enzymes as this would be very useful in creating mutant enzymes with properties that mimic the effect of low GdnHCl concentrations.

6. CHAPTER 6

CONCLUDING REMARKS

6.1. Three-state unfolding of *P. furiosus* citrate synthase

Crystal structures of members of the CS family show that the dimeric citrate synthases have similar three-dimensional structures. Although only the *P. furiosus* citrate synthase has been characterised in this study, it is thought that other citrate synthases are likely to follow a similar mechanism of denaturant-induced unfolding. Wu and Yang (1970) and Singh *et al* (1970) showed that pig heart citrate synthase can be dissociated into monomers and completely unfolded at 6M GdnHCl. It is therefore possible that the dissociation and unfolding proceed via a three-state mechanism.

This study has established conditions that allow a more extensive investigation of the conformational stability of citrate synthase. The existence of a stable, monomeric intermediate could allow direct investigations into the structural aspects of citrate synthase dimer formation and denaturation. Detailed information about other features at the subunit interface might be useful in engineering novel proteins with enhanced thermostability.

6.2. The role of ionic interactions in the increased stability of *P. furiosus* CS

There has been a growing interest in understanding the stabilization of proteins from hyperthermophiles. Such an understanding is not only essential for the theoretical description of the physico-chemical principles behind protein folding and stability, but it is also critical for designing efficient enzymes that work and are stable at high temperatures (Kumar *et al*, 2000). It is usual to compare the structure and sequence of mesophilic and thermophilic proteins in order to determine the factors involved in

protein thermostability. Ionic interactions and salt bridges show the most consistent trend, in that they appear to be more prevalent in hyperthermophilic proteins than in the mesophilic homologue. However, comparing the ΔG values of the unfolding of mesophilic and thermophilic proteins shows differences of approximately 30-70kJ/mol. This is equivalent to the energy required to break a few hydrogen bonds. The determination of the contribution of such interactions is difficult and mutations rarely show a difference in ΔG values, even though the mutants are less thermostable, as measured by the rate of thermal inactivation (R. Jaenicke, personal communication). This is thought to be because of entropy-enthalpy compensation effects. Entropy-enthalpy effects confer thermodynamic stability and buffering against environmental and mutational challenges that may be of a significant disadvantage in evolution and the function of biomolecular systems (Cooper *et al*, 2001). They indeed frustrate attempts to characterise protein-stabilising interactions.

The numerous studies carried out in the past on the molecular properties of thermophilic proteins have revealed that quite subtle structural differences between thermophilic and mesophilic proteins are sufficient to cause increased kinetic stability in the former (Jaenicke & Bohm, 1998; Arnott *et al*, 2001). The object of this project was to determine the role of ionic interactions in the thermostability of *P. furiosus* citrate synthase. The intention was to carry out the analysis with respect to the thermodynamic parameters such as ΔG, *m* and also the melting temperatures (T_m), thus measuring different aspects of thermostability from the previous studies.

The dimeric structure for citrate synthase is significant for the stabilization of the enzyme. As discussed previously, PfCS probably gains around 40% of its free energy of stabilization by forming a dimer. Ionic interactions are thought to be a major force in the association and stability of the dimer. However, ionic interactions

at the subunit interface and the C-terminal region do not seem to contribute as significantly toward stabilizing the structure of the enzyme as kinetic studies would suggest (Arnott *et al*, 2000). The thermodynamics of GdnHCl-induced unfolding of PfCS wt and mutants have also shown that within the margin of error there is no difference in the free energy values of these enzymes. Site-directed mutagenesis focused on these key ionic interactions. The substitution of the central residue in the ionic network at the subunit interface and the removal of amino acid residues at the C-terminal region have resulted in shifting the limit of stability to lower temperatures. These mutations have not changed the free energy of unfolding of PfCS but have affected the kinetic stability of the enzyme. The mutations have decreased the activation barrier against thermal inactivation at neutral pH (pH 7 & 8) and increased it at low pH (pH 5).

Without three-dimensional crystal structures of the disrupted ionic network and C-terminal arm in *P. furiosus* citrate synthase, it is imposible to tell whether the site-directed mutations are actually causing the intended disruption to the inter-subunit interactions or whether new and different stabilising interactions have been formed.

6.3. Activation in low denaturant concentrations

A novel finding of this work is that low concentrations of the denaturants GdnHCl and urea activate the hyperthermophilic *P. furiosus* citrate synthase. Data reported here show that these denaturants exert dual effects on the citrate synthase by stimulating activity at low concentrations and acting as chaotropic agents at higher concentrations disrupting the folded state. In the case of most of the enzymes studied, the relative activities increased markedly at low GdnHCl concentrations. The enzyme is activated about 2-fold in 0.5M GdnHCl and nearly 1.5-fold in 3M urea. The activated form has no significant conformational change that can be detected by intrinsic fluorescence measurements.

It is possible that subtle conformational changes occur at the active site of the enzyme concurrently with the activation of the enzyme in dilute GdnHCl. The activated enzyme shows greatly increased V_{max} and Michaelis constants compared to the enzyme in the absence of GdnHCl. This suggests that the activation may be due to a more open and flexible conformation of the enzyme in GdnHCl. These conformational changes could not be discerned by monitoring the tryptophan fluorescence quenching.

The GdnHCl-induced unfolding suggested that the denaturation of *P. furiosus* citrate synthase proceeds via a three-state model. The activation, dissociation of the dimer and the unfolding of the monomers occur at different GdnHCl concentrations. It is unclear whether the activated state of the enzyme with its subtle change in the active site can in any way be included as an intermediate state in the denaturant-induced unfolding of the enzyme.

Consistent with the established behaviour of thermophilic proteins, the activation of *P. furiosus* decreases with increasing temperature. The additive flexibility effects of temperature and chemical denaturants on thermophilic enzymes predicts that at higher temperatures lower concentration of GdnHCl should be required to reduce enzyme rigidity. The overall increase in activity in the presence of GdnHCl is therefore reduced. Although at higher temperatures the activation of the enzyme was reduced, 0.5M GdnHCl seemed to be the concentration at which the activation of the enzyme was maximum for all the enzymes studied. This is inconsistent with the lower denaturant concentration predicted to yield optimal enzyme flexibility at higher temperatures.

The global nature of interactions within a protein has made it difficult to explain some of the observations made during this study. An example is the increase thermal stability of the mutants at pH 5. It is difficult to understand why the substitution of an acidic amino acid residue (Asp) with a neutral-polar residue (Ser) and a hydrophobic residue (Ala) should increase the stability of the enzyme at pH 5. Crystal structures of the mutants may go some way to explaining some of these observations.

Taking all the data together, changes in ionic interactions may not be the strategy for increasing the free energy of stabilization of the protein. The intention had been to explore factors contributing to the stability of proteins from hyperthermophiles concentrating on the role of ionic interactions. This study indicates that the manipulation of ionic interactions is fraught with difficulties. This has also been shown with the attempt to increase the thermostability of the *Thermoplasma acidophilum* citrate synthase by introducing the five-membered ionic network present in *P. furiosus* citrate synthase (Michael, 2002). Thermal characterization showed that only one TaCS ionic network mutant with a single mutation had an increase in half-life compared to the wild-type enzyme. The majority of the mutations introduced caused a decrease in the half-life of the enzyme at the physiological temperature of *P. furiosus.* These studies suggest that not all differences in the structural features of thermophilic proteins we observe are due to thermostability. Menendez-Arias and Argos (1989) revealed that the enhanced thermostability of thermophilic proteins cannot be attributed to one determinant, but is a result of a variety of stabilizing effects brought by ionic interactions, hydrogen bonds, disulphide bonds etc. These effects are cumulative with each giving an extra free energy of stabilization of a few kJ/mol leading to a significant enhancement of a protein's stability.

These studies reported in this thesis also cast doubts on the benefits of rational design/site-directed mutagenesis. Even after carefully selecting residues for mutations on the basis of structural comparisons, the results are unpredictable. Each mutant exhibits new and unexpected properties. Given the fact that the overall stability of proteins is a marginal difference between large contributions of attractive and repulsive forces (Jaenicke & Bohm, 1998; Price, 2000) plus the corresponding entropy contributions (Cooper *et al*, 2001), this result is not surprising.

Finally, a quote from J.B.S. Haldane, from the preface to "What is Life?" Lindsay Drummond, 1949.

'**One cannot avoid making mistakes if one tries to produce a set of words, or of mathematical formulae, to describe nature. Nature is more complicated than language or mathematics. Nevertheless, one must do one's best to produce a set of symbols which are not too discordant with the facts.'**

7. REFERENCES

Aguilar, A. (1996) Extremophile reasearch in the European Union: from fundamental aspects to industrial expectations. *FEMS Microbiol. Rev.* **18**: 89-92.

Aguilar, C.F., Sanderson, I., Moracci, M., Ciaramella, M., Nucci, R., Rossi, M. & Pearl, L.H. (1997) Crystal structure of the beta-glycosidase from the hyperthermophilic archeon *Sulfolobus solfataricus*: Resilience as a key factor in thermostability. *J. Mol. Biol* **271**: 789-802.

Andersson, M. (1999) Protein stabilization: some methods and mechanisms. PhD thesis, University of Lund, Sweden.

Arnott, M.A., Michael, R.A., Thompson, C.R., Hough, D.W & Danson, M.J. (2000) Thermostability and thermoactivity of citrate synthases from the thermophilic and hyperthermophilic archaea, *Thermoplasma acidophilum* and *Pyrococcus furiosus*. *J. Mol. Biol.* **304**: 657-668.

Auerbach, G., Ostendorp, R., Prade, L. Korndorfer, I., Dams, T., Huber, R. & Jaenicke, R. (1998) Lactate dehydrogenase from the hyperthermophilic bacterium *Thermotoga maritima*: the crystal structure at 2.1 Å resolution reveals strategies for intrinsic protein stabilization. *Structure* **6**: 769-781.

Backmann, J., Schafer, G., Wyns, L. & Bonisch, H. (1998) Thermodynamics and kinetics of unfolding of the thermostable trimeric adenylate kinase from the Archaeon *Sulfolobus acidocaldirius*. *J. Mol. Biol.* **284**: 817-833.

Bastyns, K. & Engelborghs, Y. (1992) Acrylamide quenching of the fluorescence of glyceraldehyde-3-phosphate dehydrogenase – reversible and irreversible effects. *Photochem. Photobiol.* **55**: 9-16.

Bell, G.S. (1999) Crystallographic studies of central metabolic enzymes from hyperthermophilic Archaea. PhD thesis, University of Bath.

Bernstein, B.E., Michels, P.A.M. & Hol, W.G.J. (1997) Synergistic effects of substrate-induced conformational changes in phosphoglycerate kinase activation. *Nature* **385**: 275-278.

Bradford, M.M. (1976) A rapid sensitive method for the quantitation of microgram quantities of protein utilizing the principle of protein-dye binding. *Anal. Biochem.* **72**: 248-254.

Britton, K.L., Baker, P.J., Borges, K.M.M., Engel, P.C., Pasquo, A., Rice, O.W., Robb, F.T., Scandurra, R., Stillman, T.J. & Yip, K.S.P. (1995) Insights into thermal stability from a comparison of the glutamate dehydrogenases from *Pyrococcus furiosus* and *Thermococcus litoralis*. *Eur. J. Biochem.* **229**: 688-695.

Burley, S.K. & Petsko, G.A. (1985) Aromatic-aromatic interactions – a mechanism of protein structure stabilization. *Science* **229**: 23-29.

Cambillau, C. & Claverie, J.M. (2000) Structural and genomic correlates of hyperthermostability. *J. Biol. Chem.* **275**: 32383-32386.

Chi, Y-I., Martinez-Cruz, L.A., Jancarik, J., Swanson, R.V., Robertson, D.E. & Kim, S-H. (1999) Crystal structure of the β-glycosidase from the hyperthermophile *Thermospora aggregans*: insights into its activity and thermostability. *FEBS Lett.* **445**: 375-383.

Cooper, A., Johnson, C.M., Lakey, J.H. & Nollman, M. (2001) Heat does not come in different colours: entropy-enthalpy compensation, free energy windows, quantum confinement, pressure perturbation calorimetry, solvation and the multiple causes of heat capacity effects in biomolecular interactions. *Biophys. Chem.* **93**:215-230.

Daggett, V., & Levitt, M. (1993) Protein unfolding pathways explored through molecular dynamics simulations. *J. Mol. Biol.* **232**: 600-619.

Daniel, R.M., Dines, M. & Petach, H.H. (1996). The denaturation and degradation of stable enzymes at high temperatures. *Biochem. J.* **317**: 1-11.

Danson, M.J. & Hough, D.W. (1998) Structure, function and stability of enzymes from the Archaea. *Trends in Microbiol.* **6**:308-314.

Danson, M.J., Hough, D.W., Russell, R.J., Taylor, G.L. & Pearl, L. (1996) Enzyme thermostability and thermoactivity. *Protein Eng.* **9**: 629-630.

Danson, M.J. & Hough, D.W. (2003) Thermostability and thermoactivity of extremozymes. In Encyclopedia of Life Support Systems (Knowledge Foundations Area: Extremophiles). www.eolss.net. In Press.

Darby, N.J. & Creighton, T.E. (1993) Dissecting the disulphide-coupled folding pathway of bovine pancreatic trypsin-inhibitor – forming the first disulphide bonds in the analogs of the reduced protein. *J. Mol. Biol.* **232**: 873-896.

Dong, G., Vieille, C., Savchenko, A. & Zeikus, J.G. (1997) Cloning, sequencing, and expression of the gene encoding extracellular α-amylase from *Pyrococcus furiosus* and biochemical characterization of the recombinant enzyme. *Appl. Environ. Microbiol.* **63**: 3569-3576.

Duffy, T.H., Beckman, S.B., Peterson, S.M., Vitols, K.S., Huennekens, F.M. (1987) L1210 dihydrofolate reductase. Kinetics and mechanism of activation by various agents. *J Biol Chem* **262**:7028-33.

Eftink, M.R. & Ionescu, R.M. (1997) Thermodynamics of protein unfolding: Questions pertinent to testing the validity of the two-state model. *Biophys. Chem.* **64**:175-197.

Eftink, M.R. & Ghiron, C.A. (1976) Exposure of tryptophanyl residues and tryptophan dynamics. *Biochemistry* **16**: 5546-5551.

Eftink, M.R. & Ghiron, C.A. (1987) Does the fluorescence quencher acylamide bind to proteins? *Biochim. et Biophys. Acta* **916**: 343-349.

Eisenthal, R. & Cornish-Bowden, A. (1974) The direct linear plot. A new graphical procedure for estimating enzyme kinetic parameters. *Biochem. J.* **139**:715-720.

Elcock, A.H. (1998) The stability of salt bridges at high temperatures: implications for hyperthermophilic proteins. *J. Mol. Biol.* **284**: 489-502.

Evans, C.T., Kurz, L.C., Remington, S.J. & Srere, P.A. (1996) Active site mutants of pig citrate synthase: effects of mutations on the enzyme catalytic and structural properties. *Biochemistry* **35**: 10661-10672.

Fagain, C.O. & O'Kennedy, K. (1991) Functionally-stabilized proteins - a review. *Biotech Adv.* **9**: 351-409.

Fagain, C.O. (1995) Understanding and increasing protein stability. *Biochim. et Biophys. Acta* **1252**: 1-14.

Fan, Y.-X., Ju, M., Zhou, J.-M. & Tsou, C.-L. (1996) Activation of chicken liver dihydrofolate reductase by urea and guanidine hydrochloride is accompanied by conformational change at the active site. *Biochem J.* **315**: 97-102.

Fersht, A.R. (1997) Research: Protein structure – sieves in sequence. *Science* **280**:541-541.

Fontana, A., De Filippis, V., de Laureto, P.P., Scaramella, E. & Zambonin, M. (1998) Rigidity of thermophilic enzymes. In: stability and stabilization of biocatalysts. Eds. A. Ballesteros, F.J. Plou, J.L. Iborra and P.J. Halling. Pp. 277-291. Elsevier Science B.V.

Georis J., Esteves, F.D., Lamotte-Brasseur, J., Bougnet, V., Devreese, B., Giannotta, F., Granier, B. & Frere, J.M. (2000). An additional aromatic interaction improves the thermostability and thermophilicity of a mesophilic family 11 xylanase: Structural basis and molecular study. *Protein Sci.* **9**: 466-475.

Gerday, C., Aittaleb, M., Bentahir, M., Chessa, J.P., Claverie, P., Collins, T., D'Amico, S., Dumont, J., Garsoux, G., Georlette, D., Hoyoux, A., Lonhienne, T., Meuwis, M.A., Feller, G. (2000) Cold-adapted enzymes: from fundamentals to biotechnology. *Trends Biotechnol.* **18**:103-107.

Gerike, U., Danson, M.J., Russell, N.J. & Hough, D.W. (1997) Sequencing and expression of the gene encoding a cold-active citrate synthase from an Antartic bacterium, strain DS2-3R. *Eur. J. Biochem* **248**: 49-57.

Gerstein, M., Lesk, A.M. & Chothia, C. (1994) Structural mechanisms for domain movements in proteins. *Biochemistry* **33**: 6739-6749.

Grabarse, W., Vaupel, M., Vorholt, J.A., Shima, S., Thauer, R.K., Wittershagen, A., Bourenkov, G., Bartunik, H.D. & Ermler, U. (1999) The crystal structure of methenyltetrahydromethanopterin cyclohydrolase from the hyperthermophilic Archaeon *Methanopyrus kandleri. Structure* **7**: 1257-1268.

Grimsley, Janet K., Scholtz, J. Martin, Pace, C. N & Wild, J R. (1997) Organophosphorus hydrolase is a remarkably stable enzyme that unfolds through a homodimeric intermediate. *Biochemistry* **36**: 14366-1437.

Handford, P.A., Ner, S.S., Bloxham, D.P. & Wilton, D.C. (1988) Site-directed mutagenesis of citrate synthase; the role of the active-site aspartate in the binding of acetyl-CoA but not oxaloacetate. *Biochim. et Biophys. Acta* **953**: 232-240.

Haney, P.J., Stees, M. & Konisky, J. (1999) Analysis of thermal stabilizing interactions in mesophilic and thermophilic adenylate kinases from the genus *Methanococcus*. *J. Biol. Chem.* **272**: 28453-28458.

Hanslip, M. (2000) Solvent-induced unfolding of citrate synthase from *Pyrococcus furiosus*. MBiochem project report, University of Bath.

Hernandez, G., Jenney, Jr, F.E., Adams, M.W. & LeMaster, D.M. (2000) Millisecond time scale conformational stability in a hyperthermophile protein at ambient temperature. *Proc. Natl. Acad. Sci. USA* **97**: 3166-3170.

Honig, B. & Nicholls, A. (1995) Classical electrostatics in biology and chemistry. *Science* **265**: 1144-1149.

Hornby, J.A.T., Luo, J-K., Stevens, J.M, Wallace, L.A., Kaplan, W., Armstrong, R.N. and Dirr, H.W. (2000) Equilibrium folding of dimeric class μ glutathione transferases involves a stable monomeric intermediate. *Biochemistry* **39**: 12336-12344.

Hough, D.W. & Danson, M.J. (1999) Extremozymes. *Curr. Op. Chem. Biol.* **3**, 39-46.

Ichikawa, J.K & Clarke, S. (1998) A highly active protein repair enzyme from an extreme thermophile: the L-isoaspartyl methyltransferase from *Thermotoga maritima*. *Arch. Biochem. Biophys.* **358**: 222-231.

Ikeguchi,M , Nakamura, S & Shimizu K (2001) Molecular dynamics study on hydrophobic effects in aqueous urea solutions. *J. Amer. Chem. Soc.* **123**: 677-682.

Ishikawa, K., Okumura, M., Katayanagi, K., Kimura, S., Kanaya, S., Nakamura, H. & Morikawa, K. (1993) Crystal structure of ribonuclease H from *Thermus thermophilus* HB8 refined at 2.8A resolution. *J. Mol. Biol.* **230**: 529-542.

Isupov, M.N., Fleming, T.M, Dalby, A.R., Crowhurst, G.S., Bourne, P.C. & Littlechild, J.A. (1999) Crystal structure of the glyceraldehyde-3-phosphate dehydrogenase from the hyperthermophilic Archaeon *Sulfolobus solfataricus. J. Mol. Biol.* **291**: 651-660.

Jaenicke, R. & Bohme, G. (1998). The stability of proteins in extreme environments. *Curr. Opinion Struct. Biol.* **8**, 738-748.

Jaenicke, R. (1981) Enzymes under extremes of physical conditions. *Ann. Rev. Biophys. Bioeng.* **10**: 1-67.

James, K.D., Russell, R.J.D., Parker, L., Daniel, R.M., Hough, D.W. & Danson, M.J. (1994) Citrate synthases from the Archaea: development of a bio-specific, affinity chromatography purification procedure. *FEMS Micro Lett.* **119**: 181-185.

Jin, S.F. & Sonenshein, A.L. (1994) Identification of two distinct *Bacillus subtilis* citrate synthase genes. *J. Bacteriol.* **176**: 4669-4679.

John, D.M. & Weeks, K.M. (2000) van't Hoff enthalpies without baselines. *Protein Sci.* **9**:1416-1419.

John, J., Crennell, S.J. Hough, D.W., Danson, M.J. & Taylor, G.L. (1994) The crystal structure of glucose dehydrogenase from *Thermoplasma acidophilum. Structure* **2**: 385-393.

Johnson, C.M. & Fersht, A.R. (1995) Protein stability as a function of denaturant concentration: the thermal stability of barnase in the presence of urea. *Biochemistry*, **34**: 6795-6804.

Karshikoff, A. & Ladenstein, R. (1998) Proteins from thermophilic and mesophilic organisms essentially do not differ in packing. *Protein Eng.* **11**: 867-872.

Karshikoff, A. & Ladenstein, R. (2001) Ion pairs and the thermotolerance of proteins: a traffic rule for hot roads. *Trends Biochem. Sci.* **26**, 550-556.

Knapp, S., de Vos, W.M., Rice, D. & Ladenstein, R. (1997) Crystal structure of glutamate dehydrogenase from the hyperthermophilic eubacterium *Thermotoga maritima* at 3.0A resolution. *J. Mol Biol.* **267**: 916-932.

Knapp, S., Kardinahl, S., Hellgren, N., Tibbelin, G., Schafer, G. & Ladenstein, R. (1999) Refined crystal structure of a superoxide dimutase from the hyperthermophilic archaeon *Sulfolobus acidocaldarius* at 2.2 A resolution. *J. Mol. Biol.* **285**: 689-702.

Koshland, D.E., Jr. (1958) Application of a theory of enzyme specificity to protein synthesis. *Proc. Natl. Acad. Sci. USA* **44**: 98-104.

Kumar, S., Tsai, C-J. & Nussinov, R. (2001) Thermodynamic differences among homologous thermophilic and mesophilic proteins. *Biochemistry* **40**, 14152-14165.

Kurz, L.C., Nakra, T., Stein, R., Plungkhen, W. Riley, M., Hsu, F. & Drysdale, G.R. (1998) Effects of changes in three catalytic residues on the relative stabilities of some of the intermediates and transition states in the citrate synthase reaction. Biochemistry 37:9724-9737.

Kurz, L.C., Shah, S., Crane, B.R., Donald, L.J., Duckworth, H.W. & Drysdale, G.R. (1992) Proton uptake accompanies formation of the ternary complex of citrate synthase, oxaloacetate, and the transition-state analog inhibitor, carboxymethyl-CoA. Evidence that a neutral enol is the activated form of acetyl-CoA in the citrate synthase reaction. *Biochemistry* **31**:7899-7907.

Kurz, LC, Drysdale, GR, Riley, MC, Evans, CT & Srere, PA (1992) Catalytic strategy of citrate synthase: effects of amino acid changes in the acetyl-CoA binding site on transition-state analog inhibitor complexes. *Biochemistry* **31**: 7908-7914.

Kurz, LC, Shah, S, Frieden, C, Nakra, T, Stein, RE, Drysdale, GR, Evans, CT & Srere, PA (1995) Catalytic strategy of citrate synthase: subunit interactions revealed as a consequence of a single amino acid change in the oxaloacetate binding site. *Biochemistry* **34**: 13278-13288.

Kurz, L.C., Roble, J.H., Nakra, T., Drysdale, G.R., Buzan, J.M., Schwartz, B. & Drueckhammer, D.G. (1997) Ability of single-site mutants of citrate synthase to catalyze proton transfer from the methyl group of dethiaacetyl-coenzyme A, a non-thioester substrate analog. *Biochemistry* **36**:3981-3990.

Laemmli, U.K. (1970) Cleavage of structural proteins during the assembly of the head of bacteriophage T4. *Nature* **227**: 680-685.

Lakowicz, J.R. (1999) Principles of fluorescence spectroscopy. 2nd Ed. Plenum.

Laue, T. (2001) Biophysical studies by ultracentrifugation. *Curr. Opin. In Struct. Biol.* **11**:579-583.

Lazaridis, T., Lee, I., Karplus, M. (1997) Dynamics and unfolding pathways of a hyperthermophilic and a mesophilic rubredoxin. *Protein Sci.* **6**: 2589-2605.

Lebbink, J.H.G., Knapp, S., van der Oost, J., Rice, D., Ladenstein, R. & de Vos, W.M. (1999) Engineering activity and stability of *Thermotoga maritima* glutamate dehydrogenase II: construction of a 16-residue ion-pair network at the subunit interface. *J. Mol. Biol.* **289**: 357-369.

Lehrer, S.S. (1971) Solute perturbation of protein fluorescence. The quenching of the tryptophyl fluorescence of model compounds and of lysozyme by iodide ion. *Biochemistry* **10**: 3254-3263.

Liu, L.., Yang, C. & Guo, Q.X. (2000) A study on the enthalpy-entropy compensation in protein unfolding. *Biophys. Chem.* **84**: 239-251.

Macedo-Ribeiro, S., Martins, B.M., Pereira, P.J.B., Buse, G., Huber, R. & Soulimane, T. (2001) New insights into the thermostability of bacterial ferredoxins: high-resolution crystal structure of the seven-iron ferredoxin from *Thermus thermophilus*. *J. Biol. Inorg. Chem.* **6**: 663-674.

Matsumura, M., Signor, G. & Matthews, B.W. (1989) Substantial increase of protein stability by multiple disulphide. *Nature* **342**: 291-293.

Matthews, B.W. (1993) Structural and genetic analysis of protein folding and stability. *Curr. Opin. Struct. Biol.* **3**: 589-593.

Mayr, L.M. & Schmid, F.X. (1993) Stabilization of a protein by guanidinium chloride. *Biochemistry* **32**: 7994-7998.

McCary, B.S., Edmondson, S.P. & Shriver, J.W. (1996) Hyperthermophile protein folding thermodynamics: differential scanning calorimetry and chemical denaturation of *Sac*7d. *J. Mol. Biol.* **264**: 784-805.

Menendez-Arias, L. & Argos, P. (1989) Engineering protein thermal stability – sequence statistics point residue substitutions in alpha-helices. *J. Mol. Biol.* **206**: 397-405.

Meng, M., Lee, C., Bagdasarian, M. & Zeikus, J.G. (1991) Switching substrate preference of thermophilic xylose isomerase from D-xylose to D-glucose by redesigning the substrate binding pocket. *Proc. Natl. Acad. Sci. USA* **88**: 4015-4019.

Michael, R.A. (2002) Investigating the role of ionic networks in the thermostability of citrate synthase from the Archaea. PhD thesis, University of Bath.

Michels, P.C. & Clark, D.S. (1997) Pressure-enhanced activity and stability of a hyperthermophilic protease from a deep-sea methanogen. *Appl. Environ. Microbiol.* **63**: 3985-3991.

Miller, J.F., Nelson, C.M., Ludlow, J.M., Shah, N.N. & Clark, D.S. (1989) High pressure-temperature bioreactor: assays of thermostable hydrogenase with fiber optics. *Biotechnol. Bioeng.* **34**:1015-1021.

Monera, O.D., Kay, C.M. & Hodges, R.S. (1994) Electrostatic interactions control the parallel and antiparallel orientation of a-helical chains in 2 stranded α-helical coiled-coils. *Biochem*istry **33**: 3862-3871.

Monera, O.D., Zhou, N.E., Kay, C.M. & Hodges, R.S. (1993) Comparison of antiparallel and parallel 2-stranded α-helical coiled-coils – design, synthesis and characterization. *J. Biol. Chem.* **268**: 19218-19227.

Muir, J.M., Russell, R.J., Hough, D.W. and Danson, M.J. (1995) Citrate synthase from the hyperthermophilic archaeon, *Pyrococcus furiosus. Protein Eng.* **8**: 583-592.

Myers, J. Pace, C.N & Scholtz, J.M. (1995) Denaturant m values and heat capacity changes: relation to changes in accessible surface areas of protein unfolding. *Protein Sci.* **4**: 2138-2148.

Neet, K E & Timm, DE (1994) Conformational stability of dimeric proteins:quantitative studies by equilibrium denaturation. *Prot. Science* **3**: 2167-2174.

Nguyen, N.T., Maurus, R., Stokell, D.J., Ayed, A., Duckworth, H. & Brayer, G.D (2001) Comparative analysis of folding and substrate binding sites between regulated hexameric type II citrate synthase and unregulated dimeric type I enzymes. *Biochemistry* **40**: 13177-13187.

Pace C.N. (1992) Contribution of the hydrophobic effect to globular protein stability. *J. Mol. Biol.* **226**: 29-35.

Pace, C.N. & Scholtz, J.M. (1998) Measuring the conformational stability of a protein. In: Protein structure: a practical approach, 2nd ed, Ed. T.E. Creighton. Pp 299-321. IRL Press.

Pace, C.N. (1990) Measuring and increasing protein stability. *Trends.Biotech* **8**: 93-98.

Pace, C.N., Grimsley, G.R., Thomson, J.A. & Barnett, B.J. (1988) Conformational stability and activity of ribonuclease-T1 with zero, one and two intact disulphide bonds. *J. Biol. Chem.* **263**: 11820-11825.

Pace, C.N., Laurents, D.V. & Thomson, J.A. (1990) pH-dependence of the urea and guanindine hydrochloride denaturation of ribonuclease-A and ribonuclease-T1. *Biochem* **29**: 2564-2572.

Pace, C.N., Shirley, B.A., McNutt, M. & Gajiwala, K. (1996) Forces contributing to the conformational stability of proteins. *FASEB J.* **10**: 75-83.

Petsko, G.A. (2001) Structural basis of thermostability in hyperthermophilic proteins, or "there's more than one way to skin a cat". *Method Enzymol* **334**: 469-478.

Pfeil, W., Gesierich, U., Kleemann, G.R. & Sterner, R. (1997) Ferrodoxin from the hyperthermophile *Thermotoga maritima* is stable beyond the boiling point of water. *J. Mol. Biol.* **272**: 591-596.

Price, N.C. (2000) Conformational issues in the characterization of proteins. *Biotechnol. Appl. Biochem.* **31**: 29-40.

Rao, N.M. & Nagaraj, R. (1991) Anomalous stimulation of *Escherichia coli* alkaline phosphatase activity in guanidinium chloride – modulation of the rate-limiting step and negative cooperativity. J. Mol. Biol. 266: 5018-5024.

Rehaber, V. & Jaenicke, R. (1992) Stability and reconstitution of D-glyceraldehyde-3-phosphate dehydrogenase from the hyperthermophilic eubacterium *Thermotoga maritima*. *J. Biol. Chem.* **267**: 10999-11006.

Remington, S.J. (1992) Structure and mechanism of citrate synthase. *Curr. Top. Cell. Regul.* **33**: 209-229.

Rosenkrantz, M., Alam, T., Kim, K.S., Clark, B.J., Srere, P.A. & Guarente, L.P. (1986) Mitochondrial and nonmitochondrial citrate synthases in *Saccharomyces cerevisiae* are encoded by distinct homologous genes. *Mol. Cell. Biol.* **6**:4509-4515.

Rothschild, L.J. & Mancinelli, R.L. (2001) Life in extreme environments. *Nature* **409**: 1092-1101.

Russell, R.J., Hough, D.W., Danson, M.J. & Taylor, G.L. (1994) The crystal structure of citrate synthase from the thermophilic Archaeon, *Thermoplasma acidophilum*. *Structure* **2**: 1157-1167.

Russell, R.J.M. & Taylor, G.L. (1995) Engineering thermostability – lessons from thermophilic proteins. *Curr. Opin. Biotech.* **6**: 370-374.

Russell, R.J.M., Ferguson, M.C., Hough, D.W., Danson, M.J. & Taylor, G.L. (1997) The crystal structure of citrate synthase from the hyperthermophilic archaeon *Pyrococcus furiosus* at 1.9A resolution. *Biochemistry* **36**: 9983-9994.

Saiki, R.K., Gelfand, D.H., Stoffel, S., Scharf, S.J., Higuchi, R., Horn, G.T., Mullis, K.B. & Erlich, H.A. Primer-directed enzymatic amplification of DNA with a thermostable polymerase. *Science* **239**: 487-491.

Sanchez-Ruiz, J.M., Lopez-Lacomba, J.L., Cortijo, M. & Mateo, P.L. (1988) Differential scanning calorimetry of the irreversible thermal denaturation of thermolysin. *Biochemistry* **27**: 1648-1652.

Schellman, J.A. (1978) Solvent denaturation. *Biopolymers* **17**: 1305-1322.

Schmid, F.X. (1998) Optical spectroscopy to characterize protein conformation and conformational changes. In: Protein structure: a practical approach, 2nd ed, Ed. T.E. Creighton. Pp 261-297. IRL Press.

Serrano, L., Sancho, J., Hirshberg, M. & Fersht, A.R. (1992) Alpha-helix stability in proteins. 1. Empirical correlations corncerning substitution of side chains at the N and C-caps and the replacement of alanine by glycine or serine at solvent-exposed surfaces. *J. Mol. Biol.* **227**: 544-559.

Serrano, L., Neira, J.L., Sancho, J. & Fersht, A.R. (1992) Effect of alanine versus glycine in alpha-helices on protein stability. *Nature* **356**: 453-455.

Sharp, K. (2001) Entropy-enthalpy compensation: Fact or artifact? *Protein Sci.* **10**: 661-667.

Shima, S, Tziatzios, C, Schubert, D, Fukada, H, Takahashi, K, Ermler, U & Thauer, RK. (1998) Lyotropic-salt-induced changes in monomer/dimer/tetramer association equilibrium of formyltransferase from the hyperthermophilic *Methanopyrus kandleri* in relation to the activity and thermostability of the enzyme. *Eur. J. Biochem.* **258**: 85-92.

Shirley, B.A., Stanssens, P., Hahn, U. & Pace, C.N. (1992) Contribution of hydrogen bonding to the conformational stability of ribonuclease T1. *Biochemistry* **31**: 725-732.

Singleton, M., Isupov, M. & Littlechild, J. (1999) X-ray structure of pyrrolidone carboxyl peptidase from the hyperthermophilic archaeon Thermococcus litoralis. *Struct. Fold. Des.* **7**: 237-244.

Srere, P.A., Brazil, H. & Gonen, L. (1963) The citrate condensing enzyme of pigeon breast muscle and moth flight muscle. *Acta Chem. Scand.* **17**: 5129-5134.

Stadtman, E.R. (1957) Preparation of acyl coenzyme A and other thiol esters; use of hydroxylamine. *Methods Enzymol.* **3**: 931-932.

Stern, O. & Volmer, M. (1919) Decay of fluorescence. *Phys. Zeits.* **20**: 183-188.

Sterner, R., Kleeman, G.R., Szadkowski, H., Lustig, A., Henning, M & Kirschner, K. (1996) Phosphoribosyl anthranilate isomerase from *Thermotoga maritma* is an extremely stable and active homodimer. *Protein Sci.* **5**: 2000-2008.

Stetter, K.O. (1999) Extremophiles and their adaptation to hot environments. *FEBS Lett.* **452**: 22-25.

Tahirov, T.H., Oki, H., Tsukihara, T., Ogasahara, K., Yutani, K., Ogata, K., Izu, Y., Tsunasawa, S. & Kato, I. (1998) Crystal structure of methionine aminopeptidase from hyperthermophile, *Pyrococcus furiosus*. *J. Mol. Biol.* **284**: 101-124.

Tanner , J.J., Hecht, R.M. & Krause, K.L. (1996) Determinants of enzyme thermostability observed in the molecular structure of *Thermus aquaticus* D-glyceraldehye-3-phosphate dehydrogenase at 2.5Å resolution. *Biochemistry* **35**: 2597-2609.

Teplyakov, A.V., Kuranova, I.P., Harutyunyan, E.H., Vainshtein, B.K., Frommel, C., Hohne, W.E. & Wilson, K.S. (1990) Crystal structure of thermitase at 1.4A resolution. *J. Mol. Biol.* **214**: 261-279.

Thirumalai, D, Ashwin, V & Bhattacharjee. JK (1997) Dynamics of random hydrophobic-hydrophilic copolymers with implications for protein folding. *Phys. Rev. Lett.* **77**: 5385-5388.

Thoma, S., Hennig M., Sterner R. & Kirschner K. (2000) Structure and function of mutationally generated monomers of dimeric phosphoribosylanthranilate isomerase from *Thermotoga maritima*. *Structure* **8**: 265-276.

Thompson, M.J., Eisenberg, D. (1999) Transproteomic evidence of loop-deletion mechanism for enhancing protein thermostability. *J.Mol. Biol.* **290**: 595-604.

Tsou, C-L. (1998) The role of active site flexibility in enzyme catalysis. *Biochemistry (Moscow)* **63**:253-258.

Van den Burg, B., Vriend, G., Veltman, O.R., Venema, G. & Eijsink, V.G. (1998) Engineering an enzyme to resist boiling. *Proc. Natl. Acad. Sci.* USA **95**: 2056-2060.

Vanzi, F., Madan, B. & Sharp, K. (1998) Effect of the protein denaturants urea and guanidinium on water structure: A structural and thermodynamic study. *J. Amer. Chem. Soc.* **120**: 10748-10753.

Varley, P.G. & Pain, R.H. (1991) Relationship between stability, dynamics and enzyme-activity in 3-phosphoglycerate kinases from yeast and *Thermus thermophilus. J. Mol. Biol.* **220**: 531-538.

Vieille, C. & Zeikus, G.J. (2001) Hyperthermophilic enzymes: sources, uses, and molecular mechanisms of thermostability. *Microbiol. Mol. Biol. Rev.* **65**, 1-43.

Vihinen, M. (1987) Relationship of protein flexibility to thermostability. *Protein Eng.* **1**: 477-480.

Villafranca, J.E., Howell, E.E., Oatley, S.J., Xuong, N.H. & Kraut, J. (1987) An engineered disulphide bond in dihydrofolate-reductase. *Biochemistry* **26**: 2182-2189.

Vogt, G., Woell, S. & Argos, P. (1997) Protein thermal stability, hydrogen bonds and ion pairs. *J. Mol. Biol.* **269**: 631-643.

Volkin, D.B. & Klibanov, A.M. (1989) Minimizing protein inactivation. In Protein Function: a practical approach, T.E. Creighton, ed., pp 1-24.

Voorhorst, W.G.B., Warner, A., deVos, W.M. & Siezen, R.J. (1997) Homology modelling of two subtilisin-like serine proteases from the hyperthermophilic archaea *Pyrococcus furiosus* and *Thermococcus stetteri. Protein Eng.* **10**: 905-914.

Waldburger, C.D Schildbach, J.F. & Sauer R.T. (1995) Are buried salt bridges important for protein stability and conformational specificity? *Nat. Struct. Biol.* **2**:122-128.

Wallon, G., Kryger, G., Lovett, S.T., Oshima, T., Ringe, D. &. Petsko, G.A. (1997) Crystal Structures of *Escherichia coli* and *Salmonella typhimurium* 3-Isopropylmalate Dehydrogenase and Comparison with their Thermophilic Counterpart from *Thermus thermophilus*. *J. Mol. Biol.* **266**: 1016-1031.

Wallqvist, A, Covell, DG & Thirumalai, D (1998) Hydrophobic interactions in aqueous urea solutions with implications for the mechanism of protein denaturation. *J. Amer. Chem. Soc.* **120**: 427-428.

Weitzman, PD. (1966) Regulation of citrate synthase activity in *Escherichia coli*. *Biochim. et Biophys Acta* **128**: 213-215.

Wetzel, R., Perry, L.J., Baase, W.A. & Becktel, W.J. (1988) Disulfide bonds and thermal stability in T4 lysozyme. *Proc. Natl. Acad. Sci. USA* **85**: 401-405.

Wrba, A., Schweiger, A., Schultes, V., Jaenicke, R. & Zavodsky, P. (1990) Extremely thermostable D-glyceraldehyde-3-phosphate dehydrogenase from the eubacterium *Thermotoga maritima*. *Biochemistry* **29**: 7584-7592.

Yip, K.S.P., Stillman, T.J., Britton, K.L., Artymiuk, P.J., Baker, P.J., Sedelnikova, S.E., Engel, P.C., Pasquo, A., Chiaraluce, R., Consalvi, V., Scandurra, R. and Rice, D.W. (1995) The structure of *Pyrococcus furiosus* glutamate dehydrogenase reveals a key role for ionic networks in maintaining enzyme stability at extreme temperatures. *Structure* **3**: 1147-1158.

Zavodsky, P., Kardos, J., Svingov, A. & Petslav, G.A. (1998) Adjustment of conformational flexibility is a key event in thermal adaptation of proteins. *Proc. Natl. Acad. Sci.* USA **95**: 7406-7411.

Zhang, X.F., Meining, W., Fischer, M., Bacher, A. and Ladenstein, R. (2001) X-ray structure analysis and crystallographic refinement of lumazine synthase from the hyperthermophile

Aquifex aeolicus at 1.6 angstrom resolution: Determinants of thermostability revealed from structural comparisons. *J. Mol. Biol* **305**: 1099-1114.

8. APPENDIX

8.1. APPENDIX I PREPARATION OF REAGENTS

Luria-Bertani Medium (LB Broth)

10g of tryptone, 5g of yeast extract and 10g of sodium chloride were dissolved in 0.95L of water. The pH was adjusted to pH 7.0 with 5M NaoH (0.2ml). The volume was then adjusted to 1L with water and the solution autoclaved.

Terrific Broth (Tartof & Hobbs, 1987)

1L of Terrific broth is made up of 0.9L of Broth and 0.1L of salt solution

Broth – 12g of bacto tryptone and 24g of yeast extract were dissolved in 800ml of water. 4ml of glycerol was added to the solution as antifoam. The volume of the solution was then adjusted to 0.9L with water.

Salt solution – 12.54g of di potassium phosphate (K_2HPO_4) and 2.31g of potassium dihydrogen phosphate (KH_2PO_4) were dissolved in 0.09L of water. The volume of the solution was then adjusted to 0.1L with water.

Both solutions were sterilized by autoclaving. After autoclaving, the solutions were allowed to cool to below 60°C before mixing them together.

7mM Acetyl-CoA

Acetyl-CoA was prepared as described by Stadtman (1957). 10mg of CoA (lithium salt) was dissolved in 1ml of water and the solution cooled on ice (pH 5.0). 0.2ml of 1M $KHCO_3$ were added to bring the pH to 8.0. 50µl of acetic anhyride were added and the solution left on ice for at least ten minutes. This gives a solution of approximately 7mM acetyl-CoA.

Acetylation was tested by reaction with DTNB in 20mM Tris-HCl, pH 8.0, and monitoring the absorbance at 412nm. Aliquots of the solution were stored at –20°C until use.

10mM Oxaloacetate

6.6mg of Oxaloacetate powder was dissoled in 5ml of water. Solution used on day of preparation.

8.5mM 5.5'-dithio-bis(2-nitrobenzoic acid)(DTNB)

0.1M Tris-HCl, pH 8.0, was prepared by dissolving 1.21g of Tris powder in 100ml of water. The pH of the buffer was adjusted to pH 8.0 with concentrated HCl. 16.5mg of DTNB powder was dissolved in 5ml of the Tris buffer. Aliquots of the solution were frozen until use.

8M Guanidine hydrochloride solution and 10M Urea solution

Guanidine hydrochloride and urea stock solutions were prepared as described by Pace & Scholtz (1998). Stock solutions were prepared by weight and then the concentration checked by refractive index measurements. Stock solutions were only used if the concentrations agree within 1% of the required molarity.

8M GdnHCl = 1.816g of GdnHCl per gram of water.

10M Urea = 1.103g of urea per gram of water

8.2. APPENDIX II ANALYTICAL CENTRIFUGATION DATA

8.2.1. **Sedimentation equilibrium data** - The distribution data obtained from the equilibrium runs were fitted using a single ideal species model; the curve fits and the residual plots obtained are as follows.

Equilibrium Data - 18k rpm - single ideal model - PfCS

c:\176 **PfCS** **single ideal** **18k**

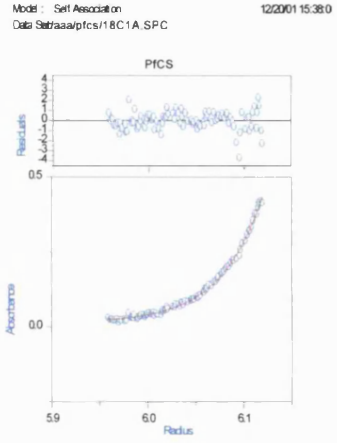

Mw, app **90.5** kDa **0.16** au

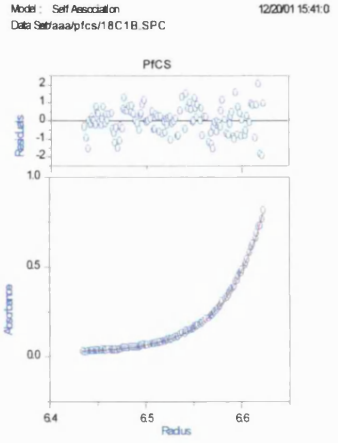

Mw, app **87.3** kDa **0.26** au

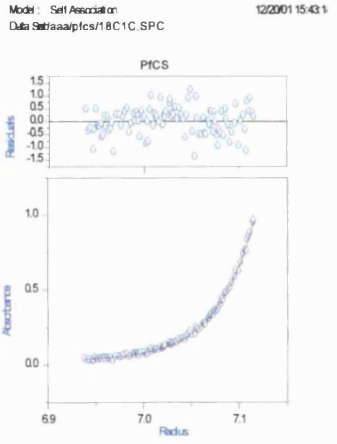

Mw, app **84.3** kDa **0.34** au

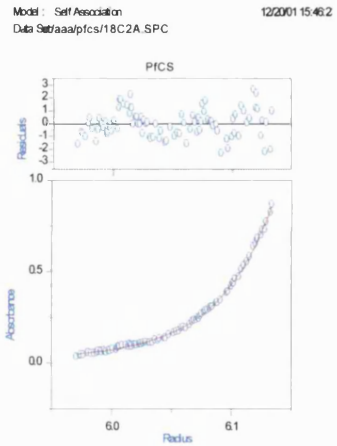

Mw, app **86.2** kDa **0.46** au

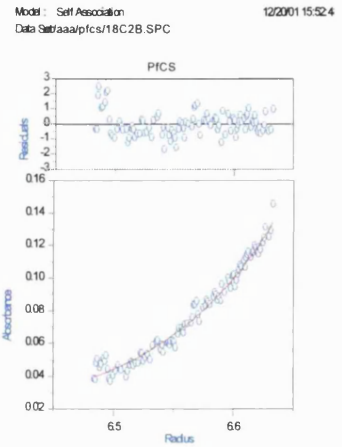

Mw, app **43.2** kDa **0.06** au

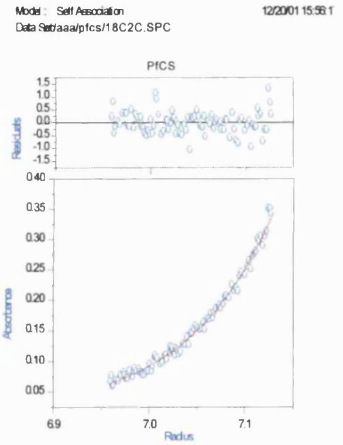

Mw, app **45.0** kDa **0.16** au

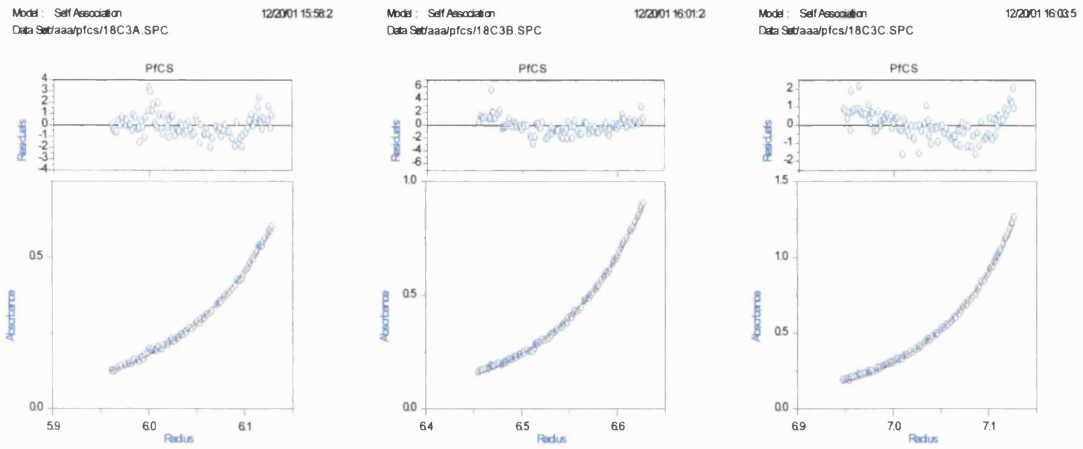

Mw, app **46.4** kDa **0.28** au Mw, app **46.2** kDa **0.40** au Mw, app **46.2** kDa **0.51** au

Equilibrium Data -24k rpm - single ideal model - PfCS

c:\176 **PfCS** **single ideal** **24k**

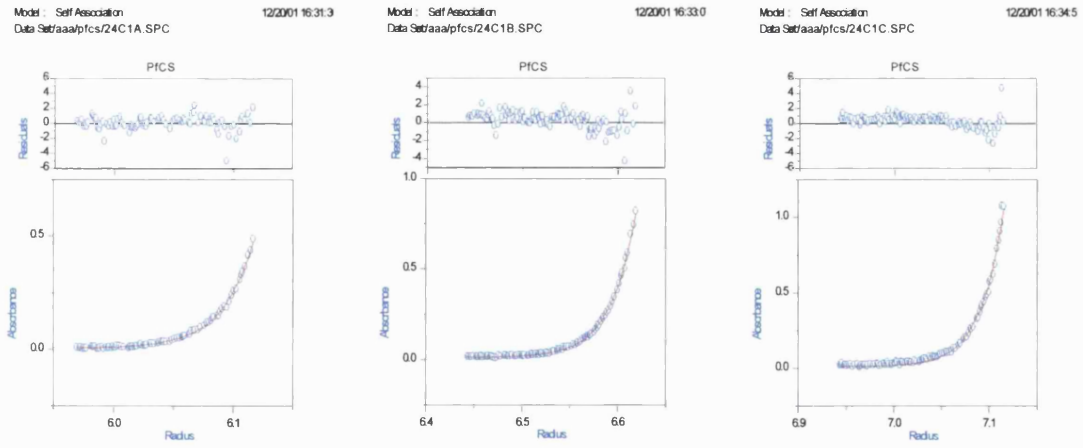

Mw, app **89.3** kDa **0.16** au Mw, app **83.5** kDa **0.26** au Mw, app **83.1** kDa **0.34** au

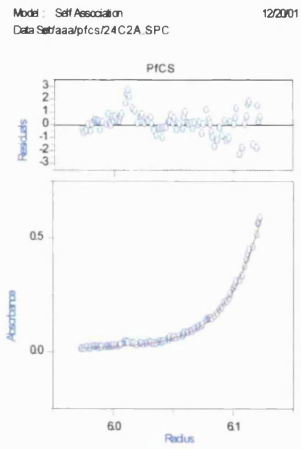

Mw, app **82.5** kDa **0.46** au

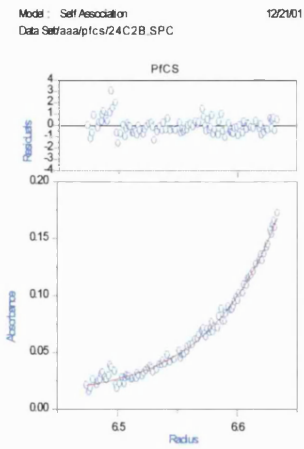

Mw, app **42.5** kDa **0.06** au

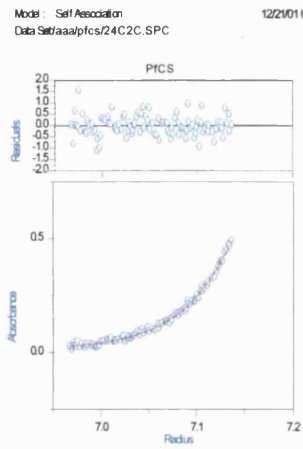

Mw, app **45.5** kDa **0.16** au

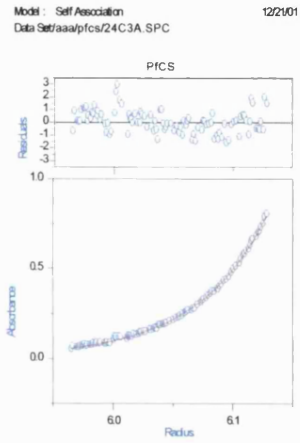

Mw, app **45.5** kDa **0.28** au

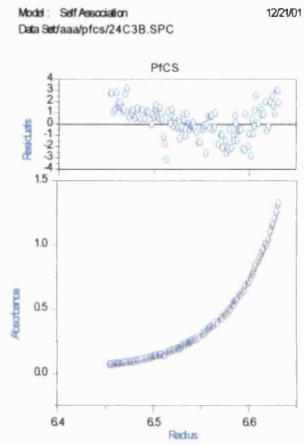

Mw, app **44.9** kDa **0.40** au

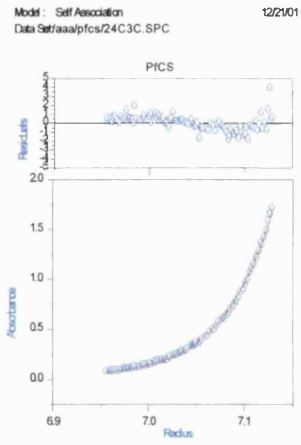

Mw, app **46.0** kDa **0.51** au

8.2.2. Sedimentation velocity data

CELL 1: Phosphate: conc = 1.6 fringes: files (164137)*.ip1 (1-200 every 2nd file)

	s app	**1.7**	**3.2**	**4.4**
	D app			
	C (%)	**1**	**82**	**17**
	s (20,w)			
	D (20,w)			
	MW from s (20,w)			
	Notes			
	Resolution 100 rmsd 0.0241			

CELL 2: Phosphate: conc = 0.8 fringes: files (164137)*.ip2 (1-200 every 2nd file)

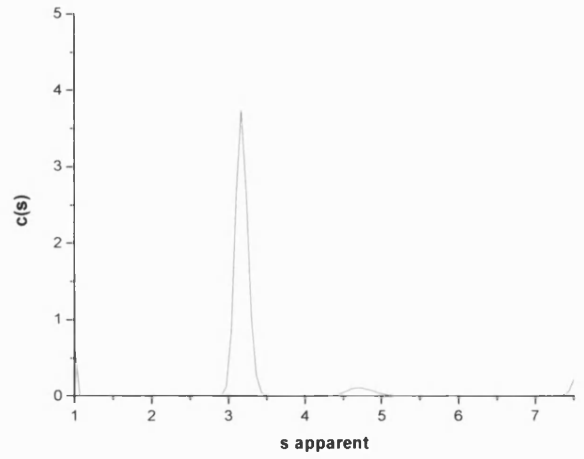

s app	**3.2**	**4.8**
D app		
C (%)	**91**	**9**
s (20,w)		
D (20,w)		
MW from s (20,w)		

Notes

Resolution 100
rmsd 0.0120

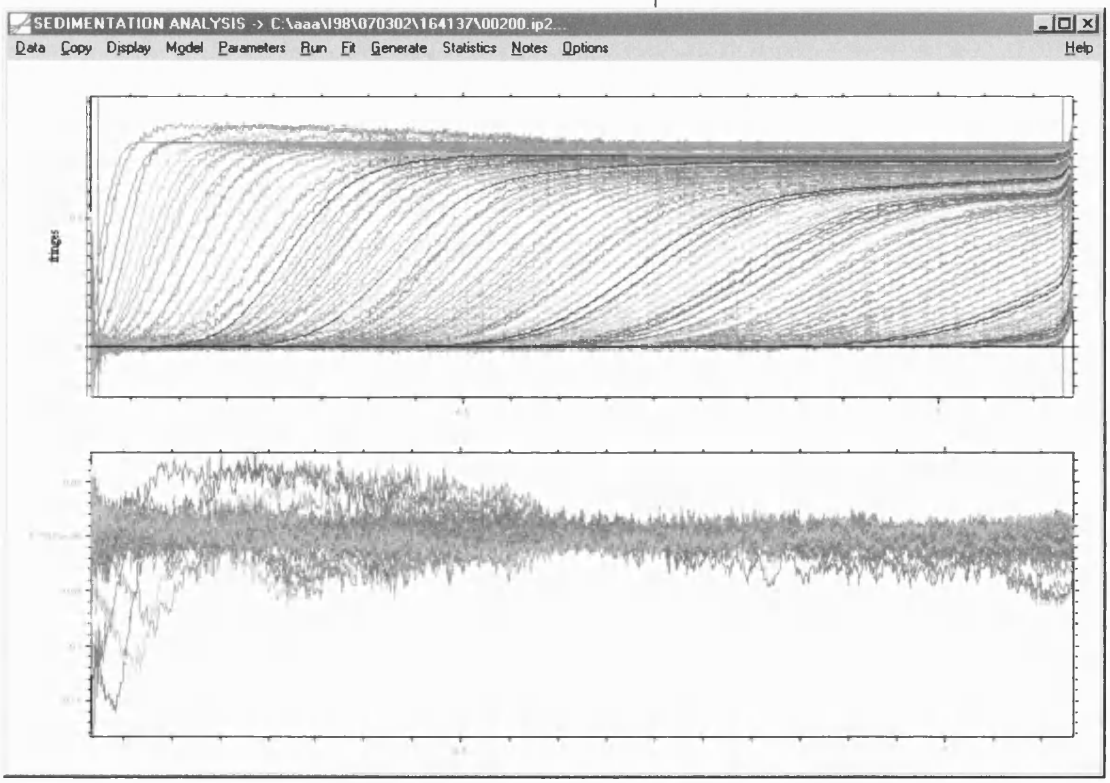

CELL 3: Phosphate: conc = 0.5 fringes: files (164137)*.ip3 (1-200 every 2nd file)

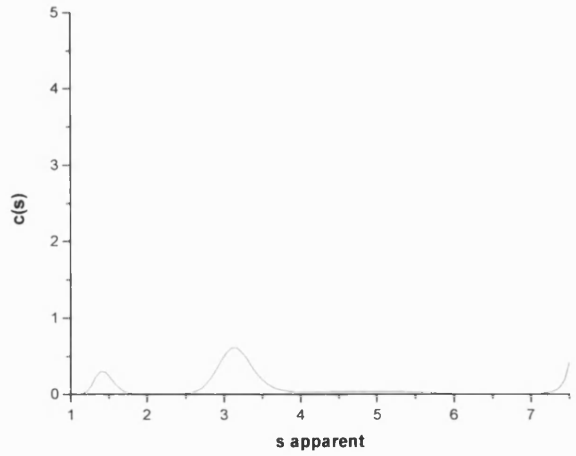

s app	**1.4**	**3.2**
D app		
C (%)	**10**	**90**

s
(20,w)
D
(20,w)
MW
from s
(20,w)

Notes

Resolution 100
rmsd 0.020

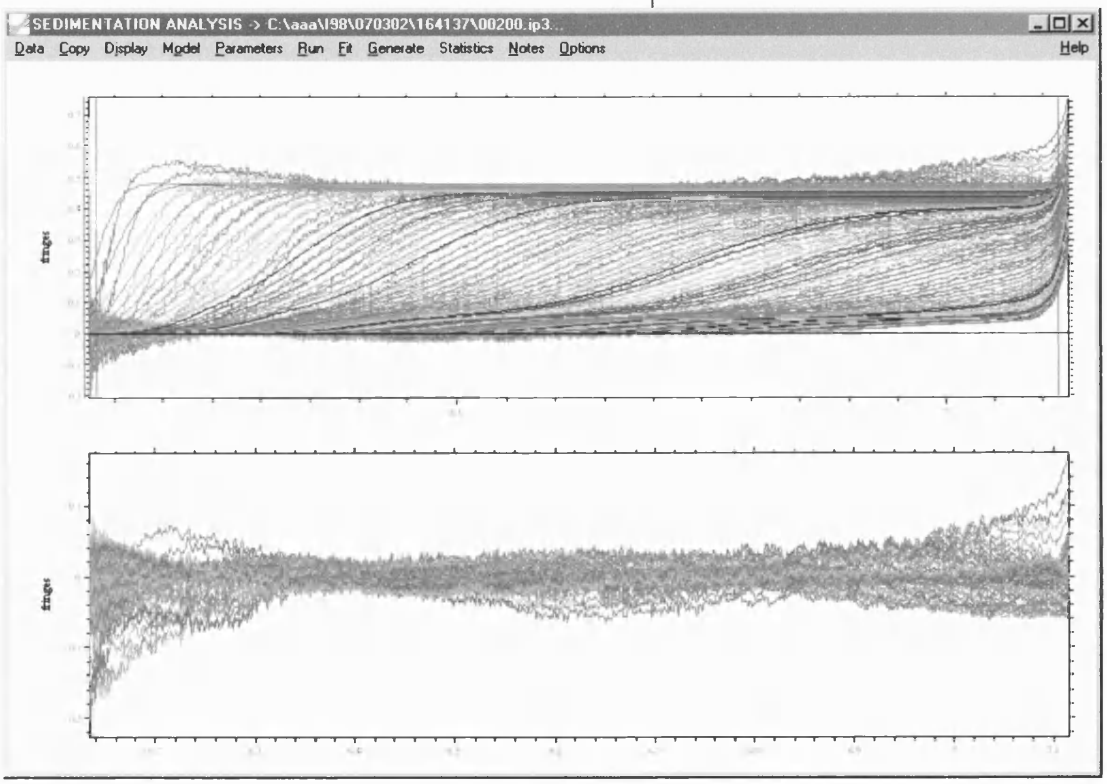

CELL 4: Guanidine: conc = 2.5 fringes: files (164137)*.ip4 (1-200 every 2nd file)

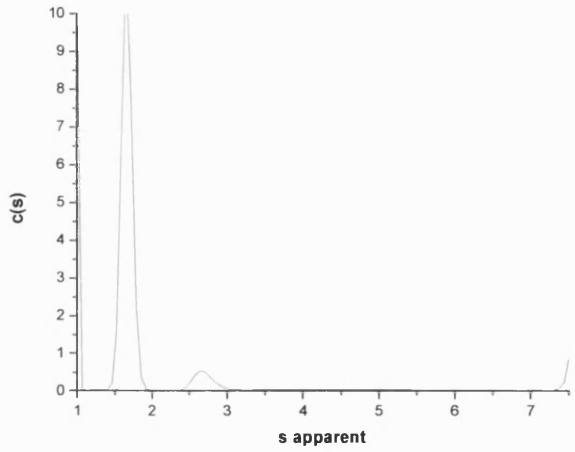

s app	**1.6**	**2.6**
D app		
C (%)	**84**	**16**
s (20,w)		
D (20,w)		
MW from s (20,w)		

Notes

Resolution 100
rmsd 0.047

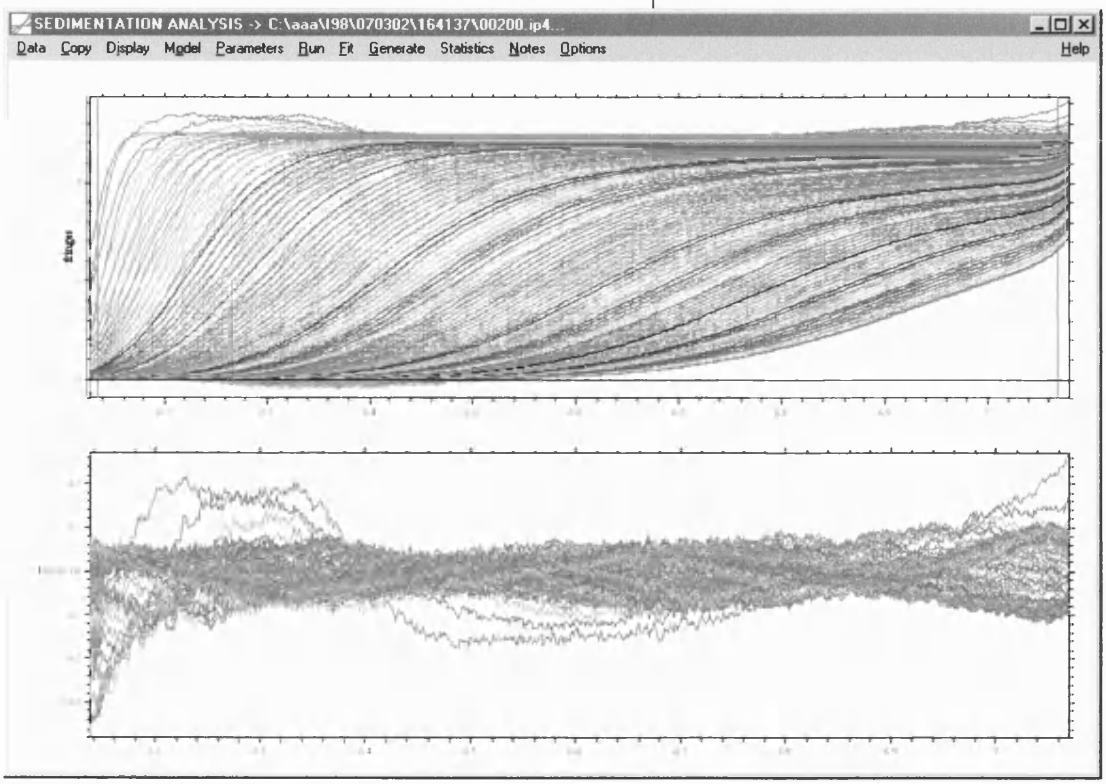

CELL 5: Guanidine: conc = 1.5 fringes: files (164137)*.ip5 (1-200 every 2nd file)

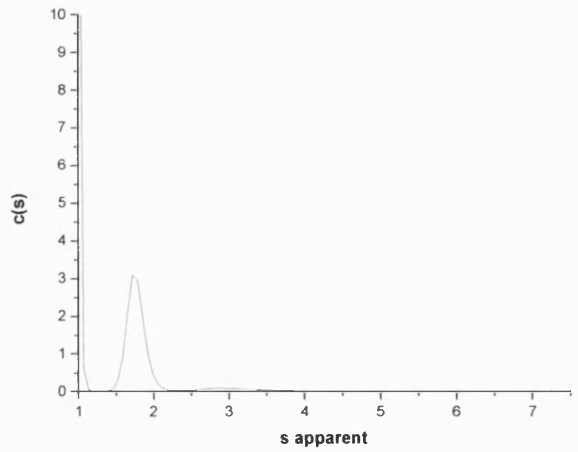

s app **1.5**

D app

C (%) **100**

s
(20,w)
D
(20,w)
MW
from s
(20,w)

Notes

Resolution 100
rmsd 0.062

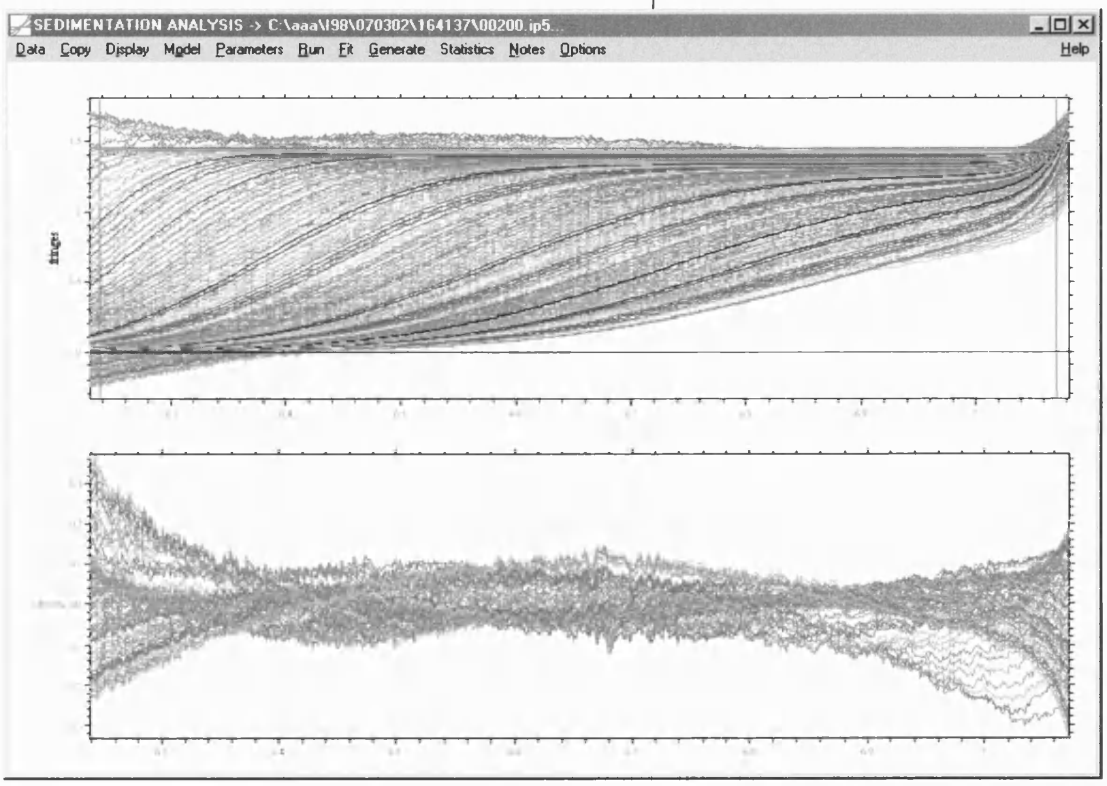

CELL 6: Guanidine: conc = 1.26 fringes: files (164137)*.ip6 (1-200 every 2nd file)

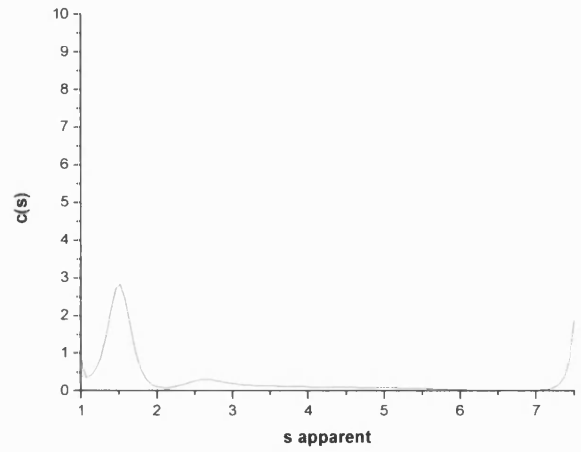

s app	**1.5**	**2.7**
D app		
C (%)	**70**	**30**
s (20,w)		
D (20,w)		
MW from s (20,w)		

Notes

Resolution 100
rmsd 0.085

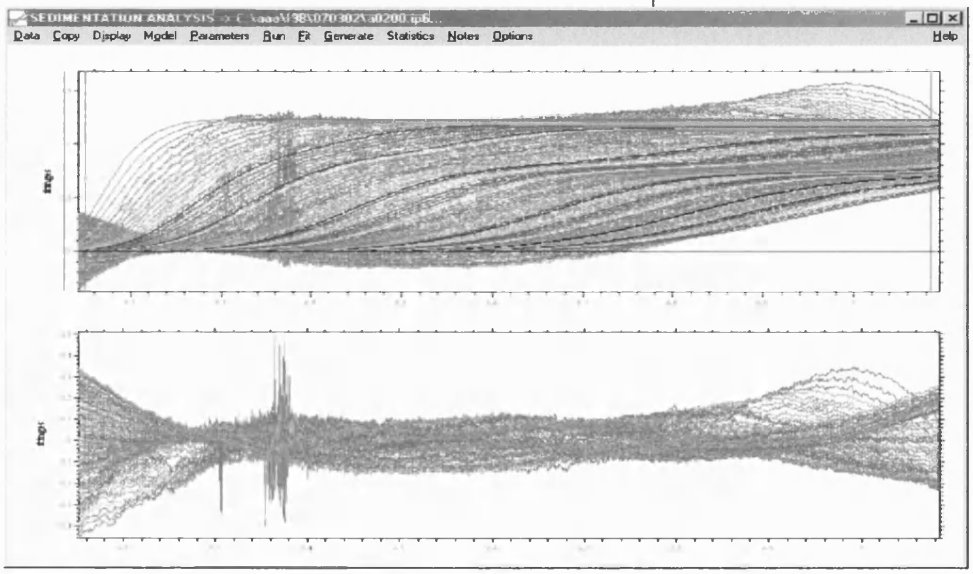

CELL 7: Guanidine: conc = 1.07 fringes: files (164137)*.ip7 (11-200 every 2nd file)

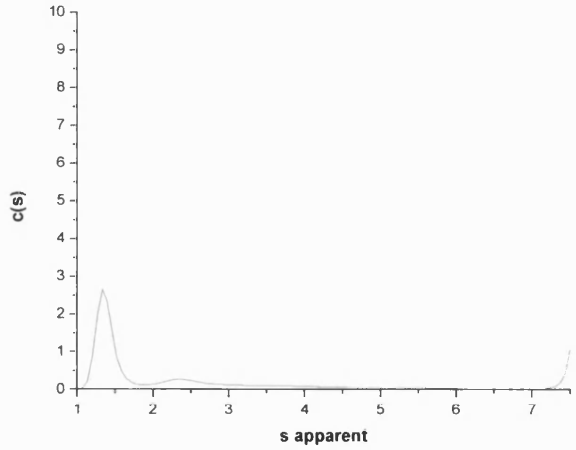

s app	**1.5**	**3.4**
D app		
C (%)	**70**	**30**
s (20,w)		
D (20,w)		
MW from s (20,w)		

Notes

Resolution 100
rmsd 0.041

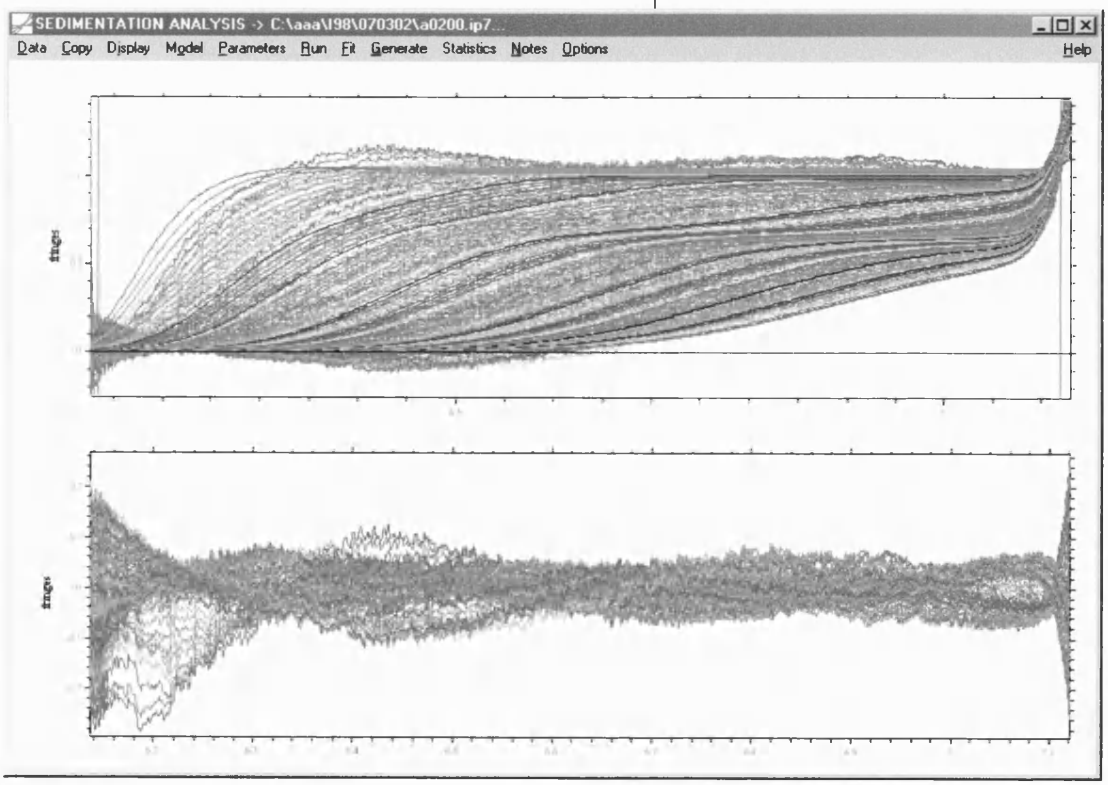

8.3. APPENDIX III ANALYSIS OF ΔG AND CALCULATION PROCEDURE

UNFOLDING MODEL - MONOMER UNFOLDING ($N \leftrightharpoons U$)

Number of parameters = 8

Independent variable: D

Dependent variable:Y

Parameters fitted: $Y_F, M_F, Y_U, M_U, G_W, M, R, T$

Formula

PAR=(GW+M*D)/(R*T)

K=EXP(-PAR)

$Y_{FOLD}=Y_F+M_F$x D

$Y_{UNF}=Y_U+M_U$ x D

$Y=(Y_{FOLD}+Y_{UNF}$ x K)/(1+K)

UNFOLDING MODEL - DIMER UNFOLDING ($N_2 \leftrightharpoons 2N$)

Number of parameters = 9

Independent variable: D

Dependent variable: Y

Parameters fitted: $Y_F, M_F, Y_U, M_U, G_W, M, R, T, P$

Formula

PAR=(G_W+M*D)/(R*T)

K=EXP(-PAR)

$Y_{FOLD}=Y_F+M_F$*D

$Y_{UNF}=Y_U+M_U$*D

F_U=((EXP(-PAR)^2+8*P*K)^0.5-K)/(4*P)

$F_F=1-F_U$

$Y=Y_{FOLD}$ x F_F+Y_{UNF} x F_U

Key to symbols:

Symbol	Definition
D	Denaturant concentration
F_F	Fraction of protein in folded state
F_U	Fraction of protein in unfolded state
G_W	ΔG of unfolding in the absence of denaturant
K	Equilibrium constant
M	Slope of transition region
M_F	Slope of pre-transition baseline
M_U	Slope of post-transition baseline
P	Protein concentration in monomer quantities
PAR	ΔG determined by Linear Extrapolation Method
R	Gas constant
T	Temperature
Y	Fluorescence intensity / Enzyme activity measurements
Y_{FOLD}	Y of pre-transition baseline determined by linear regression
Y_{UNF}	Y of post-transition baseline determined by linear regression

8.4. APPENDIX IV – MICHAELIS MENTEN PLOTS OF *P. FURIOSUS* CS

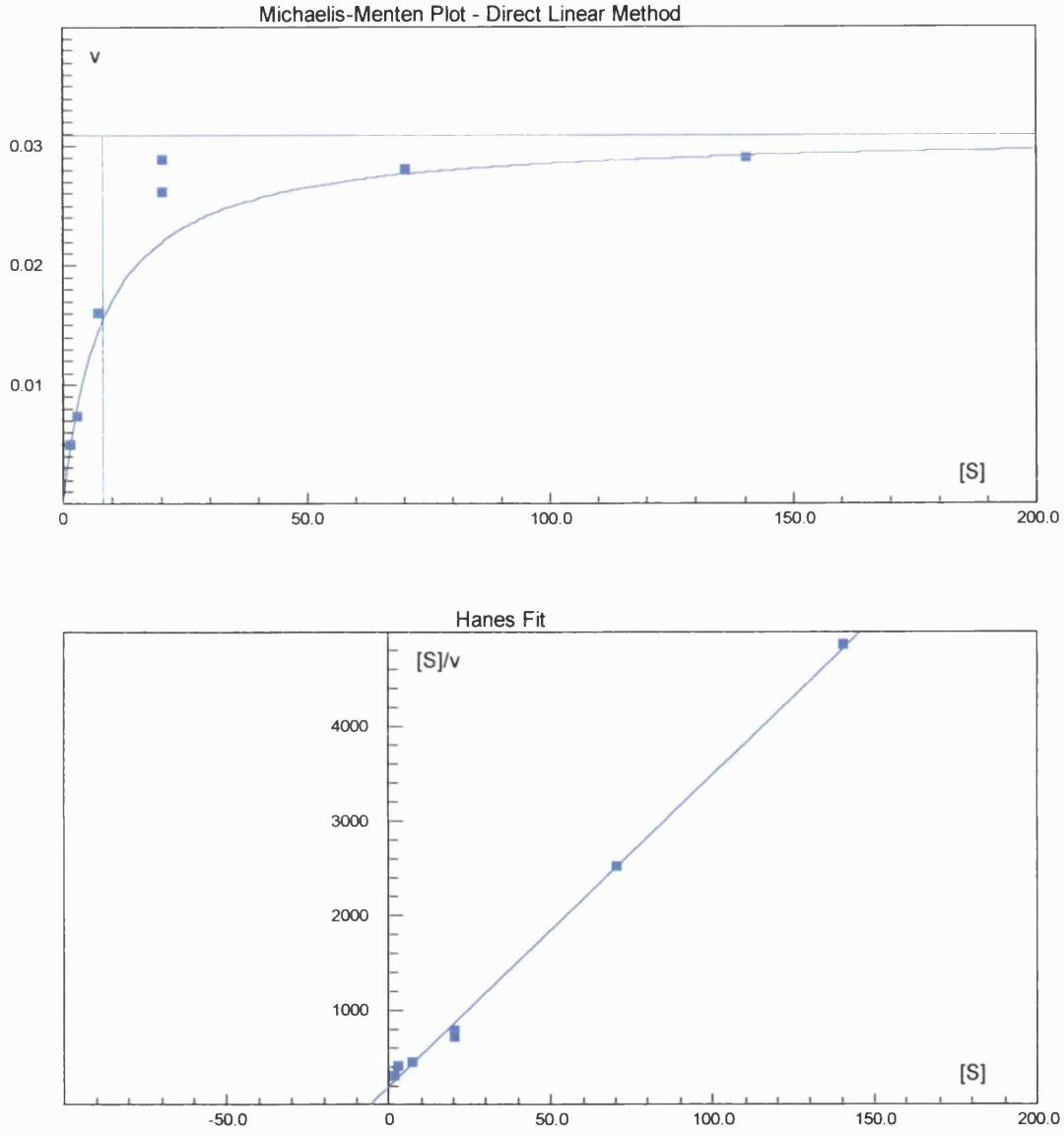

Figure 8.4a: Shows the **v** (U/mg) against **[S]**(mM) plot and the Hanes plot (**[S]/V** against **[S]**) plot when PfCS is assayed in phosphate buffer and the concentration of OAA is fixed to determine the K_M of AcCoA. The values of K_M and Vmax have been determined from the V/S data by Direct Linear Plot.

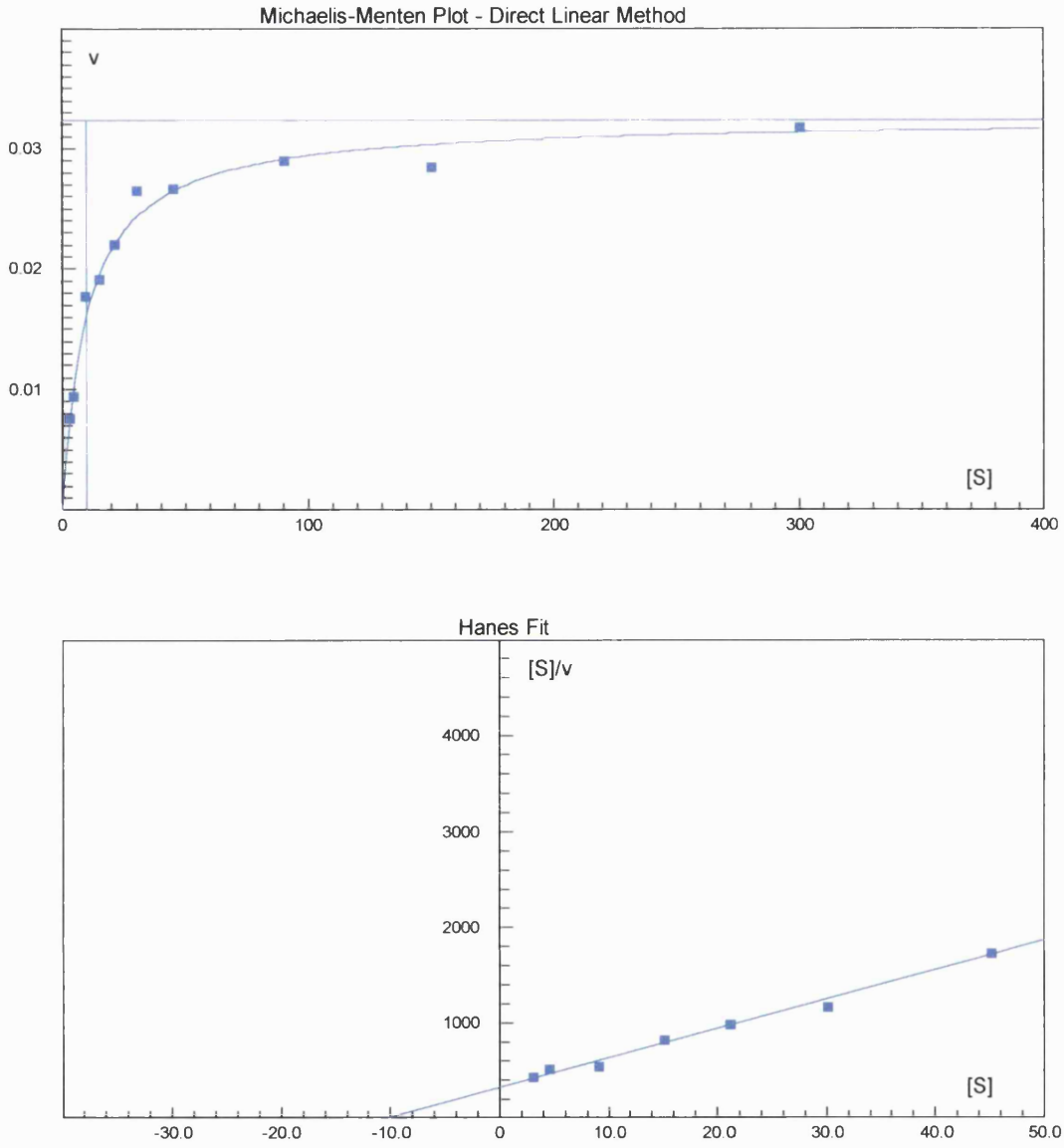

Figure 8.4b: Shows the **v** (U/mg) against **[S]**(mM) plot and the Hanes plot (**[S]/V** against **[S]**) plot when PfCS is assayed in phosphate buffer and the concentration of AcCoA is fixed to determine the K_M of OAA. The values of K_M and Vmax have been determined from the V/S data by Direct Linear Plot.

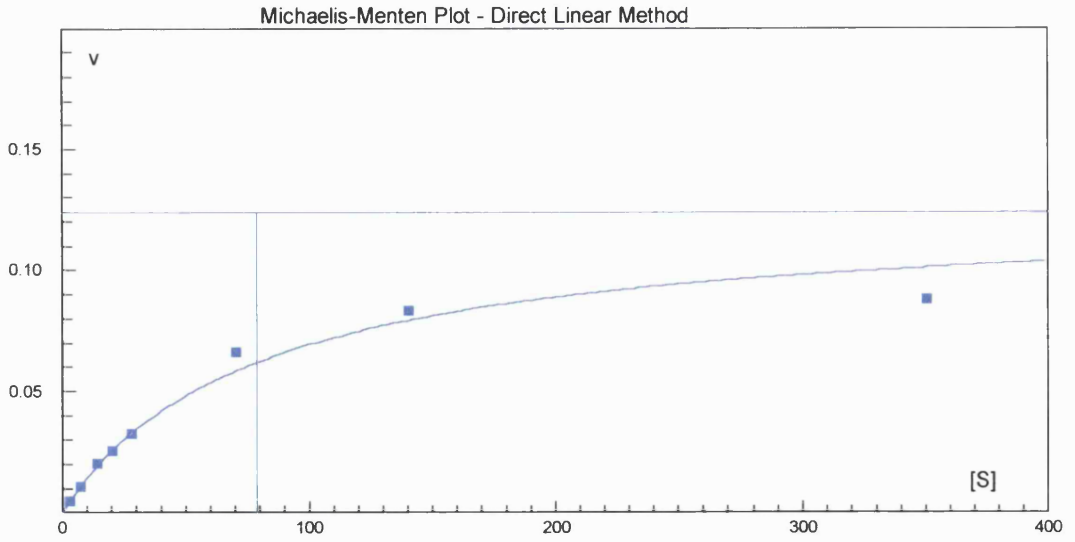

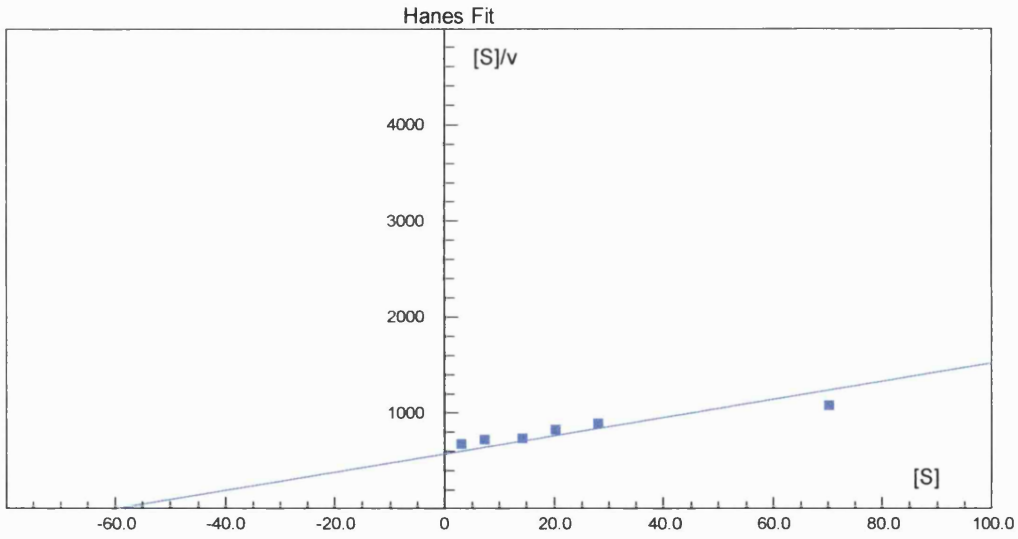

Figure 8.4c: Shows the **v** (U/mg) against **[S]**(mM) plot and the Hanes plot (**[S]/V** against **[S]**) plot when PfCS is assayed in 0.5M GdnHCl and the concentration of OAA is fixed to determine the K_M of AcCoA. The values of K_M and Vmax have been determined from the V/S data by Direct Linear Plot.

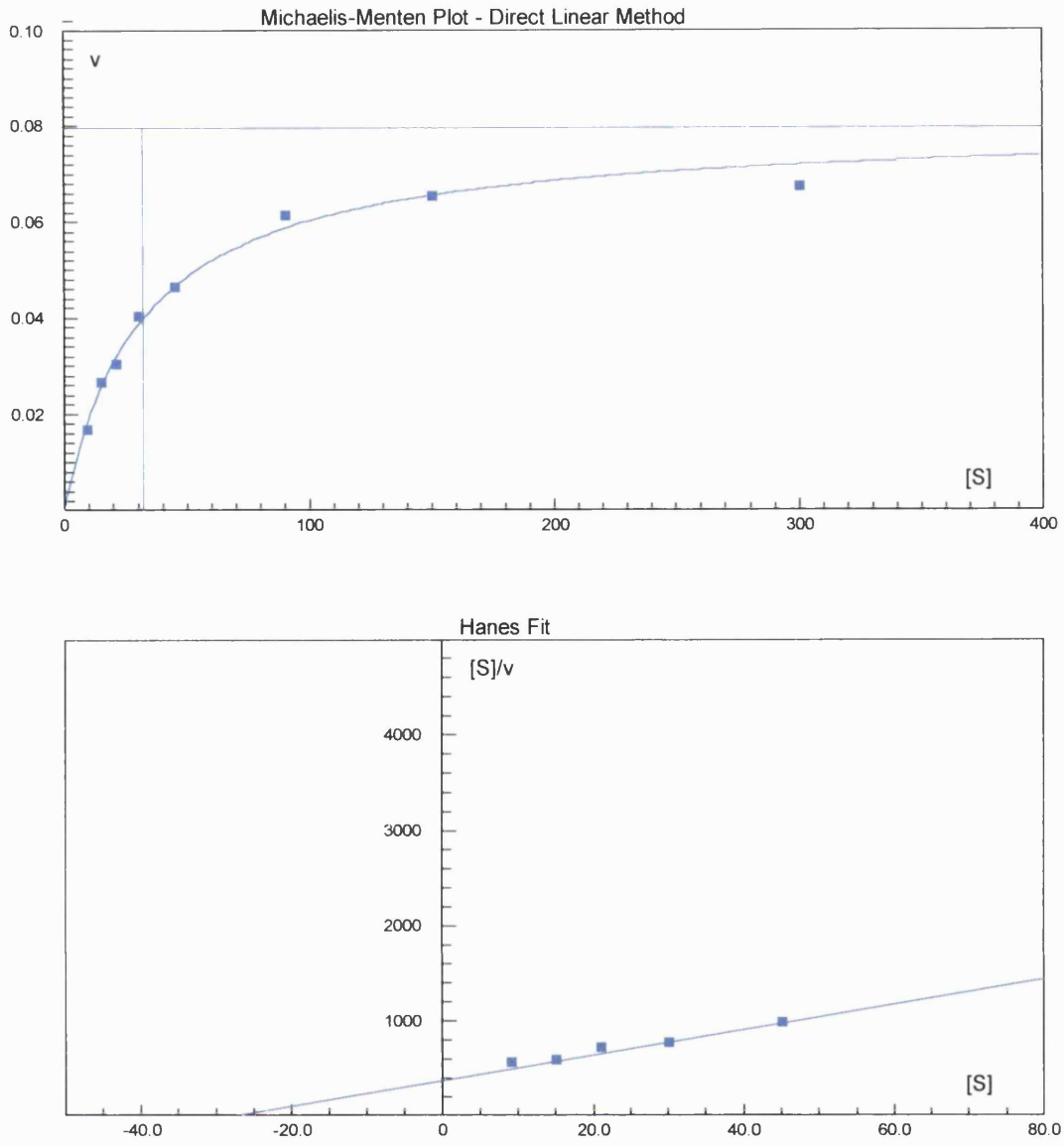

Figure 8.4d: Shows the **v** (U/mg) against **[S]**(mM) plot and the Hanes plot (**[S]/V** against **[S]**) plot when PfCS is assayed in 0.5M GdnHCl and the concentration of AcCoA is fixed to determine the K_M of OAA. The values of K_M and Vmax have been determined from the V/S data by Direct Linear Plot.

8.5. APPENDIX V – GDNHCL-INDUCED UNFOLDING OF PFCS AS MONITORED BY CD

(a)

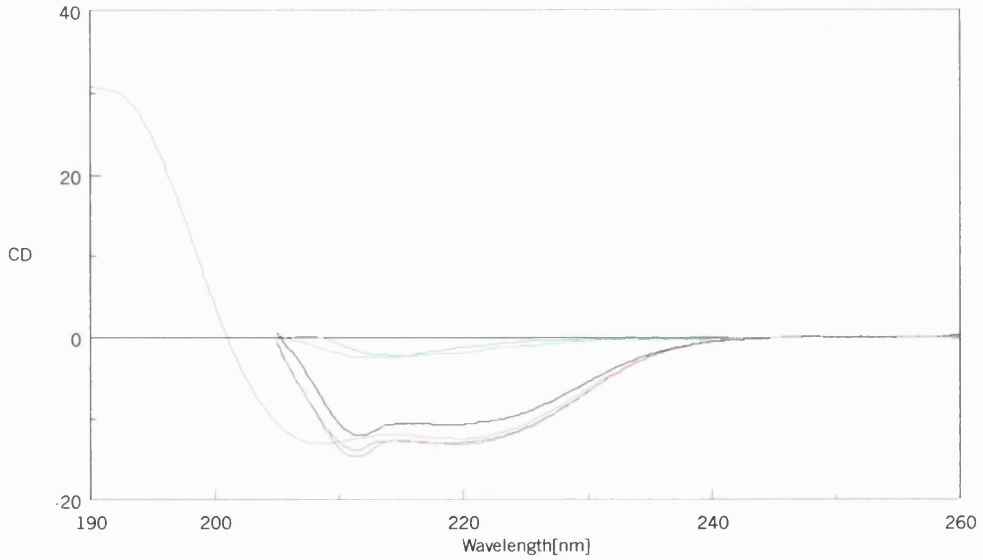

(b)

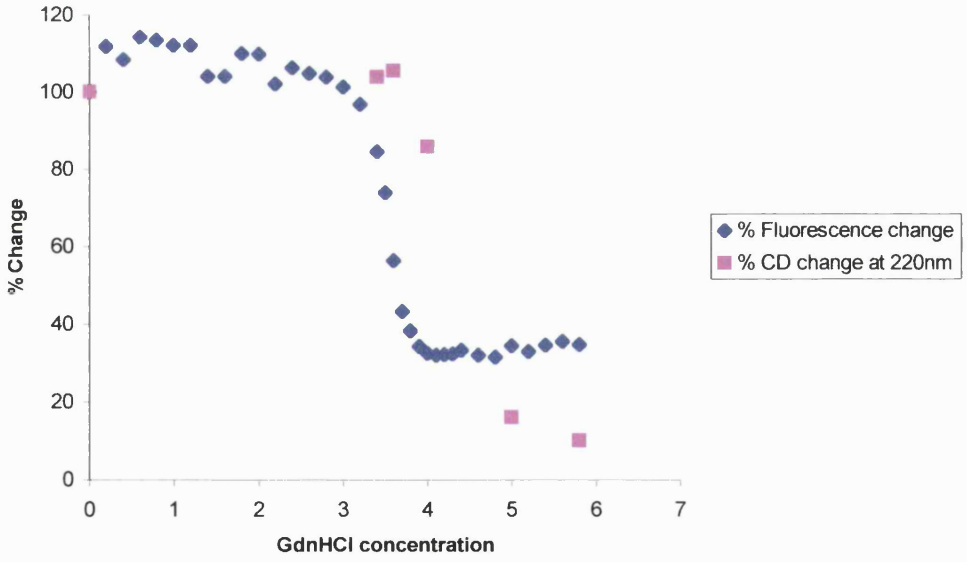

Figure 8.5: GdnHCl-induced unfolding as followed by circular dichroism. (a) shows the CD spectra of PfCS wt in 0M, 3.4M, 3.6M, 4M, 5M and 6M GdnHCl. (b) shows a plot of the change in ellipticity values at 220nm. Protein concentration was 0.2mg/ml.